BIOGEOCHEMICAL CONTROLS AND SPATIAL MODELING OF CO_2 AND CH_4 FLUXES IN A COMPLEX FOREST LANDSCAPE

by

Daniel L Warner

A dissertation submitted to the faculty of University of Delaware in partial fulfillment of the requirements for the degree of Doctor of Philosophy in Water Science and Policy

Summer 2018

BIOGEOCHEMICAL CONTROLS AND SPATIAL MODELING OF CO_2 AND CH_4 FLUXES IN A COMPLEX FOREST LANDSCAPE

by

Daniel L. Warner

Approved: _____
Erik H. Ervin, Ph.D.
Chair of the Department of Plant and Soil Sciences

Approved: _____
Mark Rieger, Ph.D.
Dean of the College of Agriculture and Natural Resources

Approved: _____
Ann L. Ardis, Ph.D.
Senior Vice Provost of Graduate and Professional Education

I certify that I have read this dissertation and that in my opinion it meets the academic and professional standard required by the University as a dissertation for the degree of Doctor of Philosophy.

Signed: _____

Shreeram Inamdar, Ph.D.
Professor in charge of dissertation (Adviser)

I certify that I have read this dissertation and that in my opinion it meets the academic and professional standard required by the University as a dissertation for the degree of Doctor of Philosophy.

Signed: _____

Rodrigo Vargas, Ph.D.
Professor in charge of dissertation (Co-adviser)

I certify that I have read this dissertation and that in my opinion it meets the academic and professional standard required by the University as a dissertation for the degree of Doctor of Philosophy.

Signed: _____

Angelia Seyfferth, Ph.D.
Member of dissertation committee

I certify that I have read this dissertation and that in my opinion it meets the academic and professional standard required by the University as a dissertation for the degree of Doctor of Philosophy.

Signed: _____

JinJun Kan, Ph.D.
Member of dissertation committee

ACKNOWLEDGEMENTS

This work would not have been possible without financial support from the US Department of Agriculture (USDA-AFRI 2013-02758), and support in the field and laboratory from the UD Soil Testing Lab, Jillian Warner, Shawn Del Percio, Catherine Winters, John Dougherty, Samuel Villarreal, and Margaret Orr. I would also like to thank the staff at Fair Hill Natural Resources Management Area for generously allowing us to conduct this research on their land.

TABLE OF CONTENTS

Appendices

LIST OF TABLES

LIST OF FIGURES

ABSTRACT

Forest ecosystems store massive quantities of carbon in the form of living biomass, dead wood, and soils. Additionally, large quantities of carbon are exchanged between these carbon pools and the atmosphere in the form of greenhouse gases, CO_2 and CH_4. Small changes in the amounts of carbon storage and exchange may have major consequences for global CO_2 and CH_4 dynamics. This dissertation consists of three original studies that investigate the spatiotemporal variability of CO_2 and CH_4 fluxes from multiple carbon pools within a temperate forested watershed in the Maryland Piedmont. Chamber techniques were employed for measuring fluxes, coupled with measurements of soil chemical and physical properties, tree species and coarse woody debris surveys, and GIS analyses.

The first study focused on CO_2 and CH_4 fluxes across soils, coarse woody debris, and living tree stems within a forest plot, with the goal of identifying the relative contributions of these ecosystem components to plot scale fluxes. Soils acted as the dominant component of both CO_2 and CH_4 fluxes, and were the focus of subsequent chapters. This study also documented some of the first *in situ* observations of CH_4 emissions from living tree stems and coarse woody debris in existing literature. Emissions varied with tree species and with the level of decay in coarse woody debris, suggesting potential implications of forest management strategies for ecosystem scale CO_2 and CH_4 exchange.

The second study expanded the scope of soil CO_2 and CH_4 fluxes from a plot to the entire watershed, with the goal of identifying the relationships of fluxes to the biogeochemical characteristics of the soil. Sampling locations were distributed across hillslope gradients to include flat upland areas, steep transitional slopes, and valley bottom flats. Fluxes were measured across seasons for two years, along with an array of soil biogeochemical properties such as carbon content, sorption capacity, porewater chemistry, and soil structure. Although soils on transitional slopes had been documented to act as landscape hotspots of CO_2 emission, this study found them to act as consistent hotspots of CH_4 uptake as well. The well-drained, carbon and clay-rich soil environment supported high rates of CH_4 uptake relative to other landscape positions across all seasons.

The third study built upon the finding of topographic influence on spatial distributions of soil CO_2 and CH_4 fluxes, with the goal of developing a modeling framework for upscaling chamber measurements across complex landscapes. Digital terrain analysis and soil mapping techniques were employed to upscale point observations of fluxes to a high resolution continuous distribution across the landscape. This novel modeling approach provided reliable, transparent estimates of seasonal mean soil CO_2 and CH_4 fluxes across the topographically complex landscape. Unlike conventional upscaling techniques, this approach preserved the inherent spatial variability of fluxes across the watershed, which revealed shifting spatial distributions of fluxes in response to seasonal changes in temperature and precipitation. Findings suggested that steeply sloping areas may act as greater sources of CO_2 but also greater sinks of CH_4

under warmer future climates, while valley bottom areas may have complex responses to changing precipitation patterns.

This dissertation provides novel insights into CO_2 and CH_4 dynamics within temperate forest ecosystems, the biogeochemical controls on these gas fluxes, and modeling techniques for making large-scale estimates of soil CO_2 and CH_4 fluxes in complex terrain. The findings will be of interest to climate scientists, land managers, and the biogeosciences community at large.

Chapter 1

INTRODUCTION

1.1 Temperate forests and CO_2 and CH_4 dynamics

Over the past two centuries, anthropogenic emissions of potent greenhouse gases such as carbon dioxide (CO_2) and methane (CH_4) have significantly altered the composition of earth's atmosphere (Forster et al. 2007). These two potent greenhouse gases are of great concern for climate change, as global increases of both gases in the atmosphere are tied to human activities (Rodhe 1990; IPCC 2014). However, natural carbon cycling processes are inherently tied to global dynamics of both gases, and disruptions to these processes may serve as major climate change feedbacks. Thus, understanding the spatiotemporal variability and biogeochemical controls of CO_2 and CH_4 exchange within natural ecosystems is critical for forecasting future ecosystem function and climate patterns.

At the global scale, temperate forests store large quantities of carbon and generally act as net sinks of atmospheric CO_2 (Pan et al. 2011). However, a large portion of CO_2 taken up by forest canopies is offset by emissions from below-canopy carbon pools including living trees, coarse woody debris (CWD), and soils (Raich and Potter 1995; Gough et al. 2007). Temperate forests are estimated to store 150 to 500 Mg C ha^{-1} (Dixon et al. 1994; Pregitzer and Euskirchen 2004), and relatively small disturbances to this stored C may have major impacts on net ecosystem CO_2 fluxes (Harmon et al. 2011).

In addition to CO_2, temperate forests play an important role in global CH_4 budgets. Forested wetlands may act as large net sources of CH_4, while upland forest soils act as net sinks of CH_4 (Ambus and Christensen 1995; Smith et al. 2000). Recently, there has been increasing interest in the roles of CWD and living tree stems in forest CH_4 fluxes. There is strong evidence that living tree stems act as net sources of CH_4, and that CWD may act as both a net source and sink of CH_4 (Terazawa and others 2015; Wang and others 2016). Mechanisms behind CH_4 fluxes from soils, stems, and CWD are discussed in the Literature Review. These recent findings highlight the need for inclusion of tree stems and coarse woody debris in global CH_4 models (Butenhoff and Khalil 2007; Carmichael et al. 2014).

Although the importance of temperate forests to regional and global CO_2 and CH_4 dynamics is well recognized, also recognized is the immense spatiotemporal variability of these greenhouse gas fluxes across the different carbon pools present in forested landscapes. Such variability represents a major challenge to researchers attempting to accurately estimate and forecast large-scale greenhouse gas fluxes for downstream application in budgets and policy decisions. In addition to investigations into the relative contributions of different ecosystem components to greenhouse gas budgets, understanding the variability of these fluxes within components (i.e., between soil types, tree species, decay classes) is necessary for making these estimates. For example, soil CO_2 and CH_4 fluxes can vary significantly in magnitude and in sensitivity to temperature or precipitation across small distances, yet how this is related to the biogeochemical properties of the soil environment is poorly understood, particularly with regards to CH_4 fluxes. Furthermore, although researchers are aware of

the large spatiotemporal variability in fluxes, techniques for large scale estimation of fluxes often assume an unrealistic level of homogeneity in the environment. There is a need for a framework for estimating fluxes across complex landscapes in a way that preserves their heterogeneity, which will allow estimates to incorporate the differential responses of fluxes from different landscape features to environmental changes.

1.2 Overview of research

The research presented in this dissertation was conducted within a small forested watershed in the hilly landscape of the Maryland piedmont, and investigates the heterogeneity and environmental drivers of CO_2 and CH_4 fluxes across different ecosystem carbon pools (Chapter 3, published in 2017 in *Ecosystems*), the effects of landscape position on soil CO_2 and CH_4 fluxes and their relationships to soil biogeochemical properties (Chapter 4; published 2018 in *Biogeochemistry*), and the potential for using terrain features to upscale measurements of soil CO_2 and CH_4 fluxes from individual point measurements to the entire landscape (Chapter 5; in review for publication in *Agricultural and Forest Meteorology*).

Chapter 3 presents a study conducted in a 25 by 100 meter plot in the study watershed over the 2014 growing season. This chapter investigates the relative contribution of different ecosystem components (soils, coarse woody debris, and living tree stems) to plot scale CO_2 and CH_4, as well as the factors that control the variability of fluxes within each component group. Chamber flux measurements were taken from late spring to late fall 2014 in sampling clusters capturing living stems, dead wood, and adjacent soils. Plot scale flux estimates were made by surveying tree species, diameter,

and height, along with CWD size and decay class, and then upscaling observed fluxes based on surface areas of these categorical groups. Specifically, this study addressed the question: How do CO_2 and CH_4 fluxes vary across and within different ecosystem components?

Chapter 4 presents a study conducted across the entire 12 hectare study watershed from fall 2014 to fall 2016. This chapter focuses on soil fluxes, and investigates the variability of soil CO_2 and CH_4 fluxes across different landscape positions and seasons, as well as the relationships of these fluxes to soil biogeochemical properties. Chamber flux measurements were taken across hillslope transects roughly every two weeks over the study period, along with measurements of soil temperature, moisture, porewater chemistry, mineral sorption capacity, total carbon content, and soil structure. Principal components analysis was employed to examine the overall relationships between fluxes and seasonally changing soil biogeochemical properties across the landscape. This study addressed the central question: How do soil CO_2 and CH_4 fluxes vary across the landscape and seasons in relation to soil biogeochemical properties?

Chapter 5 presents a study that builds on the findings from Chapter 4, that soil CO_2 and CH_4 fluxes show consistent spatial variability between topographic features within the landscape. This study investigates the application of digital soil mapping techniques for upscaling seasonal mean fluxes from point measurements, as well as the seasonal relationships between fluxes and seasonal temperature and precipitation patterns. Using the flux data from Chapter 4, a high resolution DEM, and meteorological data from a nearby weather station, this study employed an ensemble learning model (quantile regression forests) to predict spatially continuous distributions of fluxes and

evaluate the uncertainty of these predictions. This study specifically asks: Can chamber measurements be reliably upscaled based on terrain attributes, and how do soil fluxes vary spatially in response to seasonal environmental change?

Taken together, the three studies in this dissertation provide a detailed picture of CO_2 and CH_4 dynamics below the canopy in a temperate forest, and address several key knowledge gaps that have not yet been adequately addressed in scientific literature. The running theme of this work is that large scale ecological questions (such as greenhouse gas budgets) cannot be adequately addressed if the heterogeneity within natural systems is ignored. Each part of the landscape, or component of the ecosystem, contributes to the whole picture, but responses to environmental changes may not be consistent across each of these parts. This novel research will be of interest to several scientific communities, including plant physiologists, carbon cycle and soil biogeochemists, ecological modelers, and the digital soil mapping community.

REFERENCES

Ambus P, Christensen S (1995) Spatial and Seasonal Nitrous Oxide and Methane Fluxes in Danish Forest-, Grassland-, and Agroecosystems. J. Environ. Qual. 24:993

Butenhoff CL, Khalil MAK (2007) Global methane emissions from terrestrial plants. Environ Sci Technol 41:4032–4037. doi: 10.1021/es062404i

Carmichael MJ, Bernhardt ES, Bräuer SL, Smith WK (2014) The role of vegetation in methane flux to the atmosphere: Should vegetation be included as a distinct category in the global methane budget? Biogeochemistry. doi: 10.1007/s10533-014-9974-1

Dixon R, Solomon A, Brown S, et al (1994) Carbon pools and flux of global forest ecosystems. Science (80-) 263:185–90. doi: 10.1126/science.263.5144.185

Forster P, Ramaswamy V, Artaxo P, et al (2007) Changes in Atmospheric Constituents and in Radiative Forcing. In: Nakajima T, Ramanathan V (eds) Climate Change 2007: The Physical Science Basis. Contri- bution of Working Group I to the Fourth Assessment Report of the Intergovernmental Panel on Climate Change. Cambridge University Press, Cambridge, United Kingdom and New York, NY, USA, pp 129–234

Gough CM, Vogel CS, Kazanski C, et al (2007) Coarse woody debris and the carbon balance of a north temperate forest. For Ecol Manage. doi: 10.1016/j.foreco.2007.03.039

Harmon ME, Bond-Lamberty B, Tang J, Vargas R (2011) Heterotrophic respiration in disturbed forests: A review with examples from North America. J Geophys Res Biogeosciences 116:1–17. doi: 10.1029/2010JG001495

Pachauri RK, Allen MR, Barros VR, et al (2014) IPCC Climate Change 2014: Synthesis

Report

Pan Y, Birdsey RA, Fang J, et al (2011) A Large and Persistent Carbon Sink in the World's Forests. Science (80-). doi: 10.1126/science.1201609

Pregitzer KS, Euskirchen ES (2004) Carbon cycling and storage in world forests: Biome patterns related to forest age. Glob Chang Biol 10:2052–2077. doi: 10.1111/j.1365-2486.2004.00866.x

Raich JW, Potter CS (1995) Global patterns of carbon dioxide emissions from soils. Global Biogeochem Cycles 9:23–36

Rodhe H (1990) A comparison of the contribution of various gases to the greenhouse effect. Science (80-) 248:1217–9. doi: 10.1126/science.248.4960.1217

Smith KA, Dobbie KE, Ball BC, et al (2000) Oxidation of atmospheric methane in Northern European soils, comparison with other ecosystems, and uncertainties in the global terrestrial sink. Glob Chang Biol. doi: 10.1046/j.1365-2486.2000.00356.x

Terazawa K, Yamada K, Ohno Y, et al (2015) Spatial and temporal variability in methane emissions from tree stems of Fraxinus mandshurica in a cool-temperate floodplain forest. Biogeochemistry. doi: 10.1007/s10533-015-0070-y

Wang ZP, Gu Q, Deng FD, et al (2016) Methane emissions from the trunks of living trees on upland soils. New Phytol. doi: 10.1111/nph.13909

Chapter 2

LITERATURE REVIEW

The following chapter provides information on the sources, mechanisms, and controlling environmental factors behind below-canopy CO_2 and CH_4 fluxes within forest ecosystems. The influence of topography, climate, and weather on the spatial and temporal variability of CO_2 and CH_4 fluxes and their controlling factors is also discussed.

2.1 Mechanisms and drivers of below-canopy CO_2 and CH_4 fluxes

Soil respiration is the sum of CO_2 released from plant roots (autotrophic) and during the decomposition of organic substrates by microorganisms (heterotrophic). The ratio of autotrophic to heterotrophic respiration varies between and within systems (Hanson et al. 2000; Bond-Lamberty et al. 2004; Takahashi et al. 2011), and has been observed to decrease with increasing stand age (Saiz et al. 2006). Diel variation in heterotrophic respiration tends to be much greater than that of autotrophic respiration, while the relative contribution of autotrophic respiration varies substantially from growing season to non-growing season (Tang et al. 2005). As they each employ different mechanisms for CO_2 emission, rates of autotrophic and heterotrophic respiration may respond to changing environmental factors such as soil moisture and temperature in distinctly different ways (Wang et al. 2014).

While rates of soil respiration are primarily driven by soil temperature and moisture (Skopp et al. 1990; Lloyd and Taylor 1994; Raich and Tufekcioglu 2000), the

relative importance of these two primary drivers varies between arid and wet systems, as well as tropical and temperate climates (Kim et al. 2012). Soil respiration generally follows a positive exponential relationship to soil temperature, and is often modeled with Arrhenius equations (Lloyd and Taylor 1994). The relationship between soil respiration and moisture is more bell-shaped, with the greatest fluxes occurring in moist, but not saturated soils (Skopp et al. 1990; Davidson et al. 1998). Saturated soils limit oxygen diffusion into the soil, inhibiting aerobic processes which generate much more CO_2 than anaerobic pathways. Excessively dry soils reduce CO_2 fluxes by limiting organic carbon availability to microorganisms and, in extreme circumstances, may desiccate and kill microbial populations (Borken and Matzner 2009). Soil structure, vegetation cover, and organic matter content and quality also exert some degree of control on soil respiration, and soil respiration is generally greatest in soils that are loose and well-aerated, with an abundance of labile organic substrates (Raich and Tufekcioglu 2000; Ball 2013; Kirschbaum 2013).

Methane fluxes from soils are a net balance of two opposing microbial processes called methanogenesis (CH_4 production) and methanotrophy (CH_4 consumption). Methanogenesis is an anaerobic process that may exceed methanotrophy in frequently saturated wetland soils, while methanotrophy generally exceeds methanogenesis in drier, aerobic upland soils (Le Mer and Roger 2001). Though wetland soils are the largest natural source of global CH_4, upland soils are the second largest sink of atmospheric CH_4 (Smith et al. 2000; Le Mer and Roger 2001; Dlugokencky et al. 2011). However, large uncertainties exist in quantifying these sources and sinks at global scales, as CH_4

processes are highly spatially heterogeneous both between and within systems (Curry 2007; Frei et al. 2012; Bridgham et al. 2013).

Several physical and chemical factors influence soil CH_4 fluxes, including the quality of organic substrates, soil moisture, soil temperature, physical soil properties, and redox conditions (Le Mer and Roger 2001; Serrano-Silva et al. 2014). In methanogenic soils, CH_4 is released to the atmosphere via diffusion, ebullition, and vertical transport through plant aerenchyma (Le Mer and Roger 2001). Methanogens produce CH_4 through either acetate reduction or hydrogenotrophy (Thauer et al. 2008). The former is generally dominant in forested wetlands and requires labile organic substrates (ultimately acetate), while the latter reduces CO_2 in the presence of H_2 and requires highly reducing conditions to occur (Thauer et al. 2008). CH_4 production may be inhibited in the presence of NO_3^- and SO_4^{2-} due to increases in redox potential and competition with sulfate-reducing bacteria for H_2 and acetate (Serrano-Silva et al. 2014). Rates of CH_4 consumption by methanotrophs depends on the availability of oxygen and CH_4 diffusion in the soil, which is lowered by high moisture conditions, thick organic layers, and dense soils (Curry 2007), and enhanced by wind (Wang et al. 2013). Soils comprised of a mix of both coarse and fine particles have been suggested to support high rates of methanotrophy as the promote drainage and gas diffusion while also providing abundant surface area for microbial colonization (Saari et al. 1997). Methanotrophs are very closely related to ammonia-oxidizing bacteria (Holmes et al. 1999), and there is evidence that methanotrophy is influenced by ammonium fertilization, though both positive and negative effects have been observed (Serrano-Silva et al. 2014). Methanotrophs primarily utilize carbon from atmospheric and soil CH_4, however recent studies suggest that the

metabolisms of some species may utilize more complex carbon substrates to supplement their carbon intake in a process termed “facultative methanotrophy” (Semrau et al. 2011).CO_2 fluxes from coarse woody debris (CWD) are the result of the slow decay of woody biomass by fungal and bacterial communities (Harmon et al. 2004). CO_2 fluxes from stems are the combined result of growth and maintenance respiration within the living tissues of the tree as well as lateral diffusion of xylem-transported CO_2 originating from the rhizosphere (Amthor 1984; Teskey et al. 2008). The magnitudes of these fluxes may vary substantially due to differences in microbial community assemblages, stand age, disturbance history, and forest species composition (Edwards and Hanson 1996; Gough et al. 2007; Ryan et al. 2009; Fukami et al. 2010; Russell et al. 2014).

Pathways of CH_4 production within living and dead woody biomass include photodegradation of woody compounds (Keppler et al. 2008; Vigano et al. 2008), fungal production of CH_4 in CWD (Mukhin and Voronin 2008; Lenhart et al. 2012), and fermentation within living stems (Mukhin and Voronin 2011; Covey et al. 2012). Other studies have found living tree stems and leaves to function as major conduits for CH_4 emissions from CH_4-producing soils (Terazawa et al. 2007; Rice et al. 2010; Pangala et al. 2013; Maier et al. 2017; Pitz et al. 2018). The magnitudes of CH_4 fluxes from stems and CWD range widely, and may vary between species, decay status, seasons, and subsurface soil processes (Terazawa et al. 2015; Wang et al. 2016; Maier et al. 2017). In some upland forest ecosystems, stem CH_4 emissions may offset net soil CH_4 uptake by well over 50% (Wang et al. 2016).

2.2 Spatial variability of soil CO_2 and CH_4 fluxes and controlling environmental factors

A wide array of soil properties influence soil CO_2 and CH_4 fluxes. However, the spatial distributions of these drivers are in turn controlled by relatively static soil-forming factors such as parent material, vegetation, time, and, of greatest interest to this dissertation, topography and climate.

Climate is clearly a driver of seasonal soil temperature patterns in temperate ecosystems, but topographic features may also influence soil temperature. Soil temperature varies slightly, but predictably, within a catchment due differences in hillslope aspect, elevation, and soil moisture content, allowing soil temperature to be reliably estimated based on air temperature measurements corrected with topographic data (Liang et al. 2014; Kunkel et al. 2016). It should be noted, however, that spatial differences in soil temperature are generally small relative to temperature variability in time.

Topography and climate are closely linked to hydrologic processes. Climate determines the frequency, timing, and total amount of precipitation an ecosystem receives, while also influencing the amount of moisture loss via evapotranspiration. Topography controls the lateral redistribution of precipitation. Several quantitative topographic metrics have been established to explain spatial distributions of moisture throughout a given landscape (Beven and Kirkby 1979a; Kang et al. 2004; Creed and Sass 2011; Gala et al. 2011). The topographic wetness index (TWI) was introduced by Beven and Kirkby (1979), and is simply derived as the natural logarithm of upslope accumulation area divided by the tangent of local slope angle for a given point on a

landscape. Though very useful in many applications, the TWI does not consider heterogeneity of soil textures, soil profile depth, vegetation cover, and aspect, all of which may confound estimates of spatial soil moisture patterns (Wang et al. 2003; Bennie et al. 2008; Zhu et al. 2014; Yang et al. 2015). The TWI has been modified by several methods to improve its representativeness of soil moisture across a landscape, but still is not a perfect method for predicting soil moisture conditions (Boehner et al. 2001; Buchanan et al. 2014).

In addition to soil moisture, topography and climate influence soil organic matter (SOM) and texture. In general, ecosystems with wetter, cooler climates feature larger stores of SOM than warm and dry ecosystems. Several studies have observed topographic influence on both the quantity and quality of SOM, with generally greater SOM content and lower C:N ratios in lower topographic positions in many arid or moist ecosystems (Garten et al. 1994; Hirobe et al. 1999; Chen and Chiu 2000; Hishi et al. 2004; Yoo et al. 2006; Webster et al. 2008b; Pacific et al. 2011). This is because organic materials from upland soils are gradually eroded, transported downslope, and eventually deposited along transition slopes and valley bottoms. However, other factors such as vegetation cover, soil texture, and hydrology may alter these patterns (Epron et al., 2006; Takahashi et al., 2011; Yuan et al., 2013). As many forms of SOM adsorb tightly on fine clay particles, wet ecosystems with frequent flushing of fine particles from valley bottom soils may actually have less SOM than nearby upland soils (Luizao et al. 2004; Epron et al. 2006).

Given the influence of topography on distributions of many of the soil properties that influence soil CO_2 and CH_4 fluxes, it is not surprising that topographic variation in fluxes has been observed in several temperate ecosystems. In temperate grasslands, rates of soil respiration generally increase from upland to lowland sites due to increasing soil moisture and substrate availability (Pacific et al. 2008, 2011; Braun et al. 2013). However, this generalization is complicated in wetter temperate forests with valley-bottom wetlands or depressions, where soil respiration is suppressed due to limited oxygen diffusion into the soil (Webster et al. 2008b; Creed et al. 2013; Gomez et al. 2016). In these systems, soil respiration may be greatest along valley bottom-upland "transition zones", where organic substrates accumulate due to the deposition of eroded upland topsoil, and soil moisture is within an optimal range (Webster et al. 2008a, b; Creed et al. 2013). Soil respiration in topographic positions above and below these transition zones is thus limited by opposite mechanisms of deficient and excess soil moisture, as well as smaller SOM pools. The morphology of a hillslope may also play a role in rates of soil respiration. In grasslands, riparian (lowland) soil respiration may be greater in a U-shaped valley than in a V-shaped valley due to the increased SOM deposition and slower drainage (Pacific et al. 2011). Slope aspect may or may not influence rates of soil respiration. Kang et al. (2003) found rates of soil respiration to limited by moisture deficiency on south-facing slopes and by excess moisture on north-facing slopes in a temperate hardwood forest. However, other studies in temperate systems did not observe such a relationship (Webster et al. 2008b; Pacific et al. 2011; Creed et al. 2013). As temperate systems are strongly influenced by seasonal changes,

these spatial patterns may vary over annual timescales, which will be discussed in following sections.

When compared to soil respiration, the relationships between soil methane processes and topography remain largely unstudied. There have been few observations of CH_4 fluxes following specific patterns along topographic sequences. In temperate grassland ecosystems, methanotrophy may be reduced in lowland topographic positions with soil moisture beyond optimal levels (Mosier et al. 1996), and these positions may shift to CH_4 sources at near-saturated conditions (Ambus and Christensen 1995; Liu et al. 2009; Wang et al. 2013). Above the wet lowland positions, rates of methanotrophy may be independent of topographic position, and relatively homogeneous (Ambus and Christensen 1995; Liu et al. 2009; Wang et al. 2013). However, Mosier et al. (1996) found greater rates of methanotrophy along middle-slopes than upland crest positions during a particularly dry period. Similarly, Liu et al. (2009) found reduced rates of methanotrophy at a crest position relative to the hillslope, but attributed this to extensive erosion of the topsoil at this position rather than moisture deficiency. Observations of topographic influence on soil CH_4 fluxes from temperate forests are scarce in the literature and represent a major knowledge gap in CH_4 processes.

2.3 Temporal variability of soil CO_2 and CH_4 fluxes and controlling environmental factors

Soil CO_2 and CH_4 fluxes vary significantly at multiple time scales, including diel cycles, responses to meteorological events, seasonal climate changes, and inter-annual variability. The research presented in this dissertation did not include investigations into

diel patterns of fluxes or inter-annual variability, and for this reason this review of temporal variability will be limited to meteorological events and seasonal variability.

Drought and rewetting cycles have been shown by many studies to significantly alter rates of soil respiration in short timescales (Borken and Matzner 2009; Kim et al. 2012). The degree of this response is greatest in water-limited ecosystems, where soil respiration has been observed to increase by orders of magnitude following rewetting events (Sponseller and Fisher 2008; Kim et al. 2012; Gallo et al. 2014). The duration of rewetting effects may vary due to soil drainage and evapotranspiration rates of a system, with effects ranging from only 24 hours to several weeks (Sponseller and Fisher 2008; Berryman et al. 2015). While the response to rewetting may account for a sizeable fraction of annual soil CO_2 emissions, it may not compensate for the suppression of soil respiration during a preceding drought period (Joos et al. 2010; Hagedorn and Joos 2014).

The influence of drying and rewetting cycles on soil CH_4 processes remains unclear, and what few studies exist on the topic have found mixed results (Kim et al. 2012). Rewetting can inhibit CH_4 and oxygen diffusion into the soil, conversely, it may enhance methanotrophy in extremely dry systems due the relief of osmotic stress on methanotrophic microbes (Kim et al. 2012). Drying and rewetting effects may vary substantially across topographic gradients. During drought periods, normally wet areas may dry down and change from CH_4 sources to sinks, while opposite processes may occur following storm events (Ambus and Christensen 1995; Purbopuspito et al. 2006; Itoh et al. 2007; Wang et al. 2013). Similarly, as both excess and deficient soil moisture inhibit soil respiration, upland and lowland soils may respond oppositely to drying and

rewetting (Riveros-Iregui et al. 2012). These different responses of topographic positions to drought and rewetting are both an interesting and complicating factor for identifying hotspots and hot moments of soil CO_2 and CH_4 fluxes across a watershed.

In temperate and boreal systems, snowmelt and cycles of freezing and thawing also influence soil CO_2 and CH_4 fluxes. Studies have found mixed results when investigating these effects, as they occur on short timescales that may be missed by measurement strategies with coarse temporal resolution, or during periods where site access is limited (Kim et al. 2012; Blankinship and Hart 2014). In aerobic soils, frozen surface layers may create diffusion barriers under which CO_2 accumulates and CH_4 is depleted, causing rapid CO_2 efflux and CH_4 uptake upon thawing (Crill 1991; Goldberg et al. 2008; Kim et al. 2012). Conversely, rapid CH_4 efflux may be observed when frozen surface layers thaw in wet soils (Kim et al. 2012), as methanogenic processes may occur in deeper soil layers leading to CH_4 accumulation (Yu et al. 2007). Freeze-thaw cycles disrupt soil aggregates and lyse microbes, releasing organic substrates upon thawing (Schlesinger 1977) and potentially stimulating C mineralization as temperatures warm.

Seasonal changes in temperature and precipitation, as well as seasonal inputs of organic matter (i.e., autumn leaf fall, root exudates, and pollen release) represent a more long-term temporal variation in the environmental drivers of soil CO_2 and CH_4 fluxes. Seasonal changes are most obvious in temperate ecosystems, where they significantly alter prevailing soil conditions which influence soil CO_2 and CH_4 fluxes. In temperate biomes, seasonal changes dictate both soil temperature and moisture, with soil temperature being the dominant seasonal control on soil respiration (Raich and Potter 1995; Hibbard et al. 2005). Seasonal inputs of carbon substrates (i.e. litter fall) may

complicate temperature controls on soil respiration, as the gradual depletion of these inputs may shift microbial processes from temperature to substrate limitation from the early to late growing season (Kirschbaum 2013). As root respiration constitutes a large portion of soil respiration in some systems, seasonal changes in plant phenology also control rates of soil respiration, following a similar temporal pattern to temperature (Epron et al. 2001). Seasonal patterns in soil respiration may be further complicated in ecosystems receiving a large portion of annual precipitation as snow, with peak CO_2 emissions in spring followed by a gradual decline due to increasing moisture limitation through the growing season (Pacific et al. 2008; Blankinship and Hart 2012).

Soil moisture may be a greater seasonal control for CH_4 processes relative to soil respiration (Wang et al. 2013), though extremely cold temperatures may shut down CH_4 processes entirely (Wang and Han 2005). In perennially saturated soils, methanogenesis tends to be driven by temperature (Simpson et al. 1999), while particularly wet seasons in dryer areas may shift soils from CH_4 sinks to sources (Wang et al. 2013). In soils that are annual net CH_4 sinks, winter may represent a rare period of CH_4 emission, though the amount may be insignificant to regional and global budgets (Mosier et al. 1996).

Seasonal change in soil CO_2 and CH_4 fluxes across topographic gradients may present itself as shifts in the relative contribution of different topographic positions to total fluxes. This effect may be most prominent in seasonally wet and dry ecosystems, as moisture distributions are so closely linked to topography (Pacific et al. 2008; Takahashi et al. 2011; Zanchi et al. 2014). Pacific et al. (2008) found that while lowland soils respired more CO_2 on an annual scale, upland soil respiration was substantially higher immediately following spring snow melt, when soils held an optimum moisture content.

As the growing season progressed and upland soils dried down, riparian soil respiration rates surpassed the uplands. Similar patterns have been observed in forests with seasonal rainfall differences between early and late summer (Webster et al. 2008b). Thus, lowland soils tend to contribute a greater fraction of total soil respiration than uplands in dry seasons, and a smaller fraction in wet seasons. Similarly, seasonal dry down of ephemerally-inundated wetlands may function as an on-off switch for CH_4 emissions throughout the year, with high emissions during inundation and early dry down, and virtually no net CH_4 fluxes during other seasons (Pennock et al. 2010). However, CH_4 efflux from perennial wetlands may increase substantially during warm summer months, and greatly exceed rates of upland net CH_4 uptake, causing source and sink status of a forested catchment to vary seasonally as well (Itoh et al. 2005). Methanotrophy generally increases in upland and transition zone soils during dry seasons due to enhanced diffusion of CH_4 into active soil layers (Ambus and Christensen 1995), though particularly dry conditions may reduce methanotrophy in upland soils due to microbial osmotic stress (Mosier et al., 1996).

REFERENCES

Ambus P, Christensen S (1995) Spatial and Seasonal Nitrous Oxide and Methane Fluxes in Danish Forest-, Grassland-, and Agroecosystems. J. Environ. Qual. 24:993

Amthor JS (1984) The role of maintenance respiration in plant growth. Plant, Cell Environ 7:561–569. doi: 10.1111/j.1365-3040.1984.tb01856.x

Ball BC (2013) Soil structure and greenhouse gas emissions: A synthesis of 20 years of experimentation. Eur J Soil Sci. doi: 10.1111/ejss.12013

Bennie J, Huntley B, Wiltshire A, et al (2008) Slope, aspect and climate: Spatially explicit and implicit models of topographic microclimate in chalk grassland. Ecol Modell. doi: 10.1016/j.ecolmodel.2008.04.010

Berryman EM, Barnard HR, Adams HR, et al (2015) Complex terrain alters temperature and moisture limitations of forest soil respiration across a semiarid to subalpine gradient. J Geophys Res Biogeosciences. doi: 10.1002/2014JG002802

Beven KJ, Kirkby MJ (1979) A physically based, variable contributing area model of basin hydrology / Un modèle à base physique de zone d'appel variable de l'hydrologie du bassin versant. Hydrol Sci Bull 24:43–69. doi: 10.1080/02626667909491834

Blankinship JC, Hart SC (2012) Consequences of manipulated snow cover on soil gaseous emission and N retention in the growing season: a meta-analysis. Ecosphere 3:1. doi: 10.1890/ES11-00225.1

Blankinship JC, Hart SC (2014) Hydrological Control of Greenhouse Gas Fluxes in a Sierra Nevada Subalpine Meadow Hydrological Control of Greenhouse Gas Fluxes in a Sierra Nevada Subalpine Meadow. 46:355–364

Boehner J, Koeth R, Conrad O, et al (2001) Soil regionalisation by means of terrain analysis and process parameterisation. In: Soil Classification 2001 - Europa. pp 213–222

Bond-Lamberty B, Wang C, Gower ST (2004) A global relationship between the heterotrophic and autotrophic components of soil respiration? Glob Chang Biol 10:1756–1766. doi:

10.1111/j.1365-2486.2004.00816.x

Borken W, Matzner E (2009) Reappraisal of drying and wetting effects on C and N mineralization and fluxes in soils. Glob Chang Biol. doi: 10.1111/j.1365-2486.2008.01681.x

Braun M, Bai Y, McConkey B, et al (2013) Greenhouse gas flux in a temperate grassland as affected by landform and disturbance. Landsc Ecol. doi: 10.1007/s10980-013-9878-9

Bridgham SD, Cadillo-Quiroz H, Keller JK, Zhuang Q (2013) Methane emissions from wetlands: Biogeochemical, microbial, and modeling perspectives from local to global scales. Glob Chang Biol. doi: 10.1111/gcb.12131

Buchanan BP, Fleming M, Schneider RL, et al (2014) Evaluating topographic wetness indices across central New York agricultural landscapes. Hydrol Earth Syst Sci 18:3279–3299. doi: 10.5194/hess-18-3279-2014

Chen JS, Chiu CY (2000) Effect of topography on the composition of soil organic substances in a perhumid sub-tropical montane forest ecosystem in Taiwan. Geoderma. doi: 10.1016/S0016-7061(99)00092-0

Covey KR, Wood SA, Warren RJ, et al (2012) Elevated methane concentrations in trees of an upland forest. Geophys Res Lett. doi: 10.1029/2012GL052361

Creed IF, Sass GZ (2011) Digital Terrain Analysis Approaches for Tracking Hydrological and Biogeochemical Pathways and Processes in Forested Landscapes. In: Forest Hydrology and Biogeochemistry. pp 69–100

Creed IF, Webster KL, Braun GL, et al (2013) Topographically regulated traps of dissolved organic carbon create hotspots of soil carbon dioxide efflux in forests. Biogeochemistry. doi: 10.1007/s10533-012-9713-4

Crill PM (1991) Seasonal patterns of methane uptake and carbon dioxide release by a temperate woodland soil. Global Biogeochem Cycles 5:319–334. doi: 10.1029/91GB02466

Curry CL (2007) Modeling the soil consumption at atmospheric methane at the global scale. Global Biogeochem Cycles. doi: 10.1029/2006GB002818

Davidson EA, Belk E, Boone RD (1998) Soil water content and temperature as independent or confounded factors controlling soil respiration in a temperate mixed hardwood forest. Glob Chang Biol. doi: 10.1046/j.1365-2486.1998.00128.x

Dlugokencky EJ, Nisbet EG, Fisher R, Lowry D (2011) Global atmospheric methane: budget, changes and dangers. Philos Trans A Math Phys Eng Sci 369:2058–2072. doi: 10.1098/rsta.2010.0341

Edwards NT, Hanson PJ (1996) Stem respiration in a closed-canopy upland oak forest. Tree Physiol 16:433–439. doi: 10.1093/treephys/16.4.433

Epron D, Bosc A, Bonal D, Freycon V (2006) Spatial variation of soil respiration across a topographic gradient in a tropical rain forest in French Guiana. J Trop Ecol. doi: 10.1017/S0266467406003415

Epron D, Le Dantec V, Dufrene E, Granier A (2001) Seasonal dynamics of soil carbon dioxide efflux and simulated rhizosphere respiration in a beech forest. Tree Physiol 21:145–152. doi: 10.1093/treephys/21.2-3.145

Frei S, Knorr KH, Peiffer S, Fleckenstein JH (2012) Surface micro-topography causes hot spots of biogeochemical activity in wetland systems: A virtual modeling experiment. J Geophys Res Biogeosciences. doi: 10.1029/2012JG002012

Fukami T, Dickie IA, Paula Wilkie J, et al (2010) Assembly history dictates ecosystem functioning: Evidence from wood decomposer communities. Ecol Lett 13:675–684. doi: 10.1111/j.1461-0248.2010.01465.x

Gala TS, Aldred DA, Carlyle S, Creed IF (2011) Topographically based spatially averaging of SAR data improves performance of soil moisture models. Remote Sens Environ. doi: 10.1016/j.rse.2011.08.013

Gallo EL, Lohse KA, Ferlin CM, et al (2014) Physical and biological controls on trace gas fluxes in semi-arid urban ephemeral waterways. Biogeochemistry. doi: 10.1007/s10533-013-9927-0

Garten CT, Huston MA, Thoms CA (1994) Topographic variation of soil nitrogen dynamics at Walker Branch Watershed, Tennessee. Forest Science

Goldberg SD, Muhr J, Borken W, Gebauer G (2008) Fluxes of climate-relevant trace gases between a Norway spruce forest soil and atmosphere during repeated freeze-thaw cycles in mesocosms. J Plant Nutr Soil Sci 171:729–739. doi: 10.1002/jpln.200700317

Gomez J, Vidon P, Gross J, et al (2016) Estimating greenhouse gas emissions at the soil–atmosphere interface in forested watersheds of the US Northeast. Environ Monit Assess 188:295. doi: 10.1007/s10661-016-5297-0

Gough CM, Vogel CS, Kazanski C, et al (2007) Coarse woody debris and the carbon balance of a north temperate forest. For Ecol Manage. doi: 10.1016/j.foreco.2007.03.039

Hagedorn F, Joos O (2014) Experimental summer drought reduces soil CO_2 effluxes and DOC leaching in Swiss grassland soils along an elevational gradient. Biogeochemistry. doi: 10.1007/s10533-013-9881-x

Hanson PJ, Edwards NT, Garten CT, Andrews JA (2000) Separating root and soil microbial contributions to soil respiration: A review of methods and observations. Biogeochemistry. doi: 10.1023/A:1006244819642

Harmon ME, Franklin JF, Swanson FJ, et al (2004) Ecology of Coarse Woody Debris in Temperate Ecosystems. Adv Ecol Res 15:133–276. doi: 10.1016/S0065-2504(03)34002-4

Hibbard KA, Law BE, Reichstein M, Sulzman J (2005) An Analysis of Soil Respiration across Northern Hemisphere Temperate Ecosystems. Source Biogeochem Soil Respir 73:29–70

Hirobe M, Tokuchi N, Iwatsubo G (1999) Spatial variability of soil nitrogen transformation patterns along a forest slope in a Cryptomeria japonica plantation. Eur J Soil Biol 34:123–131. doi: 10.1016/S1164-5563(00)88649-5

Hishi T, Hirobe M, Tateno R, Takeda H (2004) Spatial and temporal patterns of water-extractable organic carbon (WEOC) of surface mineral soil in a cool temperate forest ecosystem. Soil Biol Biochem. doi: 10.1016/j.soilbio.2004.04.030

Holmes AJ, Roslev P, McDonald IR, et al (1999) Characterization of methanotrophic bacterial populations in soils showing atmospheric methane uptake. Appl Environ Microbiol 65:3312–3318

Itoh M, Ohte N, Katsuyama M, et al (2005) Temporal and spatial variability of methane flux in a temperate forest watershed. J Japan Soc Hydrol Water Resour. 18:244–256

Itoh M, Ohte N, Koba K, et al (2007) Hydrologic effects on methane dynamics in riparian wetlands in a temperate forest catchment. J Geophys Res Biogeosciences. doi: 10.1029/2006JG000240

Joos O, Hagedorn F, Heim A, et al (2010) Summer drought reduces total and litter-derived soil CO_2 effluxes in temperate grassland – clues from a 13 C litter addition experiment. Biogeosciences 7:1031–1041

Kang S, Doh S, Lee D, et al (2003) Topographic and climatic controls on soil respiration in six temperate mixed-hardwood forest slopes, Korea. Glob Chang Biol 9:1427–1437. doi: 10.1046/j.1365-2486.2003.00668.x

Kang S, Lee D, Kimball JS (2004) The effects of spatial aggregation of complex topography on hydroecological process simulations within a rugged forest landscape: development and application of a satellite-based topoclimatic model. Can J For Res 34:519–530. doi: 10.1139/x03-213

Keppler F, Hamilton JTG, McRoberts WC, et al (2008) Methoxyl groups of plant pectin as a precursor of atmospheric methane: Evidence from deuterium labelling studies. New Phytol. doi: 10.1111/j.1469-8137.2008.02411.x

Kim DG, Vargas R, Bond-Lamberty B, Turetsky MR (2012) Effects of soil rewetting and thawing on soil gas fluxes: A review of current literature and suggestions for future research. Biogeosciences. doi: 10.5194/bg-9-2459-2012

Kirschbaum MF (2013) Seasonal variations in the availability of labile substrate confound the temperature dependence of organic matter decomposition. Soil Biol Biochem. doi:

10.1016/j.soilbio.2012.10.012

Kunkel V, Wells T, Hancock GR (2016) Soil temperature dynamics at the catchment scale. Geoderma 273:32–44. doi: 10.1016/j.geoderma.2016.03.011

Le Mer J, Roger P (2001) Production, oxidation, emission and consumption of methane by soils: A review. Eur J Soil Biol. doi: 10.1016/S1164-5563(01)01067-6

Lenhart K, Bunge M, Ratering S, et al (2012) Evidence for methane production by saprotrophic fungi. Nat Commun 3:1046. doi: 10.1038/ncomms2049

Liang LL, Riveros-Iregui DA, Emanuel RE, McGlynn BL (2014) A simple framework to estimate distributed soil temperature from discrete air temperature measurements in data-scarce regions. J Geophys Res Atmos 119:407–417. doi: 10.1002/2013JD020597

Liu C, Holst J, Yao Z, et al (2009) Growing season methane budget of an Inner Mongolian steppe. Atmos Environ 43:3086–3095. doi: 10.1016/j.atmosenv.2009.03.014

Lloyd J, Taylor JA (1994) On the Temperature Dependence of Soil Respiration. Funct Ecol 8:315–323

Luizao RCC, Luizao FJ, Paiva RQ, et al (2004) Variation of carbon and nitrogen cycling processes along a topographic gradient in a central Amazonian forest. Glob Chang Biol 10:592–600. doi: 10.1111/j.1529-8817.2003.00757.x

Maier M, Paulus S, Nicolai C, et al (2017) Drivers of Plot-Scale Variability of CH_4 Consumption in a Well-Aerated Pine Forest Soil. Forests 8:193. doi: 10.3390/f8060193

Mosier AR, Parton WJ, Valentine DW, Schimel DS (1996) CH_4 and N_2O fluxes in the Colorado shortgrass steppe : 1 . Impact of landscape and nitrogen addition. Global Biogeochem Cycles 10:387–399

Mukhin VA, Voronin PY (2011) Methane emission from living tree wood. Russ J Plant Physiol. doi: 10.1134/S1021443711020117

Mukhin VA, Voronin PY (2008) A new source of methane in boreal forests. Prikl Biokhim Mikrobiol 44:330–332. doi: 10.1134/S0003683808030125

Ngao J, Epron D, Delpierre N, et al (2012) Spatial variability of soil CO_2 efflux linked to soil parameters and ecosystem characteristics in a temperate beech forest. Agric For Meteorol. doi: 10.1016/j.agrformet.2011.11.003

Pacific VJ, McGlynn BL, Riveros-Iregui DA, et al (2011) Landscape structure, groundwater dynamics, and soil water content influence soil respiration across riparian-hillslope transitions in the Tenderfoot Creek Experimental Forest, Montana. Hydrol Process. doi: 10.1002/hyp.7870

Pacific VJ, McGlynn BL, Riveros-Iregui DA, et al (2008) Variability in soil respiration across riparian-hillslope transitions. Biogeochemistry. doi: 10.1007/s10533-008-9258-8

Pangala SR, Moore S, Hornibrook ERC, Gauci V (2013) Trees are major conduits for methane egress from tropical forested wetlands. New Phytol 197:524–531. doi: 10.1111/nph.12031

Pennock D, Yates T, Bedard-Haughn A, et al (2010) Landscape controls on N_2O and CH_4 emissions from freshwater mineral soil wetlands of the Canadian Prairie Pothole region. Geoderma 155:308–319. doi: 10.1016/j.geoderma.2009.12.015

Pitz SL, Megonigal JP, Chang CH, Szlavecz K (2018) Methane fluxes from tree stems and soils along a habitat gradient. Biogeochemistry 1–14. doi: 10.1007/s10533-017-0400-3

Purbopuspito J, Veldkamp E, Brumme R, Murdiyarso D (2006) Trace gas fluxes and nitrogen cycling along an elevation sequence of tropical montane forests in Central Sulawesi, Indonesia. Global Biogeochem Cycles 20:1–11. doi: 10.1029/2005GB002516

Raich JW, Potter CS (1995) Global patterns of carbon dioxide emissions from soils. Global Biogeochem Cycles 9:23–36

Raich JW, Tufekcioglu A (2000) Vegetation and soil respiration: Correlations and controls. Biogeochemistry 48:71–90

Rice AL, Butenhoff CL, Shearer MJ, et al (2010) Emissions of anaerobically produced methane by trees. Geophys Res Lett 37:1–6. doi: 10.1029/2009GL041565

Riveros-Iregui DA, Mcglynn BL, Emanuel RE, Epstein HE (2012) Complex terrain leads to

bidirectional responses of soil respiration to inter-annual water availability. Glob Chang Biol. doi: 10.1111/j.1365-2486.2011.02556.x

Russell MB, Woodall CW, Fraver S, et al (2014) Residence Times and Decay Rates of Downed Woody Debris Biomass/Carbon in Eastern US Forests. Ecosystems 17:765–777. doi: 10.1007/s10021-014-9757-5

Ryan MG, Cavaleri MA, Almeida AC, et al (2009) Wood CO_2 efflux and foliar respiration for Eucalyptus in Hawaii and Brazil. Tree Physiol. doi: 10.1093/treephys/tpp059

Saari A, Martikainen PJ, Ferm A, et al (1997) Methane oxidation in soil profiles of dutch and finnish coniferous forests with different soil texture and atmospheric nitrogen deposition. Soil. Biol. Biochem. 29:1625–1632

Saiz G, Green C, Butterbach-Bahl K, et al (2006) Seasonal and spatial variability of soil respiration in four Sitka spruce stands. Plant Soil. doi: 10.1007/s11104-006-9052-0

Schlesinger WH (1977) Carbon Balance in Terrestrial Detritus. Annu Rev Ecol Syst 8:51–81. doi: 10.1146/annurev.es.08.110177.000411

Semrau JD, DiSpirito AA, Vuilleumier S (2011) Facultative methanotrophy: False leads, true results, and suggestions for future research. FEMS Microbiol. Lett.

Serrano-Silva N, Sarria-Guzmán Y, Dendooven L, Luna-Guido M (2014) Methanogenesis and Methanotrophy in Soil: A Review. Pedosphere. doi: 10.1016/S1002-0160(14)60016-3

Simpson IJ, Edwards GC, Thurtell GW (1999) Variations in methane and nitrous oxide mixing ratios at the southern boundary of a Canadian boreal forest. Atmos Environ. doi: 10.1016/S1352-2310(98)00235-0

Skopp J, Jawson MD, Doran JW (1990) Steady-State Aerobic Microbial Activity as a Function of Soil Water Content. Soil Sci. Soc. Am. J. 54:1619

Smith KA, Dobbie KE, Ball BC, et al (2000) Oxidation of atmospheric methane in Northern European soils, comparison with other ecosystems, and uncertainties in the global terrestrial sink. Glob Chang Biol. doi: 10.1046/j.1365-2486.2000.00356.x

Sponseller RA, Fisher SG (2008) The influence of drainage networks on patterns of soil respiration in a desert catchment. Ecology. doi: 10.1890/06-1933.1

Takahashi M, Hirai K, Limtong P, et al (2011) Topographic variation in heterotrophic and autotrophic soil respiration in a tropical seasonal forest in Thailand. Soil Sci Plant Nutr. doi: 10.1080/00380768.2011.589363

Tang J, Misson L, Gershenson A, et al (2005) Continuous measurements of soil respiration with and without roots in a ponderosa pine plantation in the Sierra Nevada Mountains. Agric For Meteorol. doi: 10.1016/j.agrformet.2005.07.011

Terazawa K, Ishizuka S, Sakata T, et al (2007) Methane emissions from stems of Fraxinus mandshurica var. japonica trees in a floodplain forest. Soil Biol Biochem 39:2689–2692. doi: 10.1016/j.soilbio.2007.05.013

Terazawa K, Yamada K, Ohno Y, et al (2015) Spatial and temporal variability in methane emissions from tree stems of Fraxinus mandshurica in a cool-temperate floodplain forest. Biogeochemistry. doi: 10.1007/s10533-015-0070-y

Teskey RO, Saveyn A, Steppe K, McGuire MA (2008) Origin, fate and significance of CO_2 in tree stems. New Phytol 177:17–32. doi: 10.1111/j.1469-8137.2007.02286.x

Thauer RK, Kaster A, Seedorf H, et al (2008) Methanogenic archaea: ecologically relevant differences in energy conservation. Nat Rev Microbiol 6:579–91. doi: 10.1038/nrmicro1931

Vigano I, van Weelden H, Holzinger R, et al (2008) Effect of UV radiation and temperature on the emission of methane from plant biomass and structural components. Biogeosciences 5:. doi: 10.5194/bgd-5-243-2008

Wang H, Hall CAS, Cornell JD, Hall MHP (2003) Spatial dependence and the relationship of soil organic carbon and soil moisture in the Luquillo Experimental Forest, Puerto Rico. Landsc Ecol 17:671–684

Wang JM, Murphy JG, Geddes JA, et al (2013) Methane fluxes measured by eddy covariance and static chamber techniques at a temperate forest in central Ontario, Canada. Biogeosciences.

doi: 10.5194/bg-10-4371-2013

Wang X, Liu L, Piao S, et al (2014) Soil respiration under climate warming: Differential response of heterotrophic and autotrophic respiration. Glob Chang Biol. doi: 10.1111/gcb.12620

Wang ZP, Gu Q, Deng FD, et al (2016) Methane emissions from the trunks of living trees on upland soils. New Phytol. doi: 10.1111/nph.13909

Wang ZP, Han XG (2005) Diurnal variation in methane emissions in relation to plants and environmental variables in the Inner Mongolia marshes. Atmos Environ. doi: 10.1016/j.atmosenv.2005.07.010

Webster KL, Creed IF, Beall FD, Bourbonnière RA (2008a) Sensitivity of catchment-aggregated estimates of soil carbon dioxide efflux to topography under different climatic conditions. J Geophys Res Biogeosciences. doi: 10.1029/2008JG000707

Webster KL, Creed IF, Bourbonnière RA, Beall FD (2008b) Controls on the heterogeneity of soil respiration in a tolerant hardwood forest. J Geophys Res Biogeosciences. doi: 10.1029/2008JG000706

Yang L, Chen L, Wei W (2015) Effects of vegetation restoration on the spatial distribution of soil moisture at the hillslope scale in semi-arid regions. Catena. doi: 10.1016/j.catena.2014.09.014

Yoo K, Amundson R, Heimsath AM, Dietrich WE (2006) Spatial patterns of soil organic carbon on hillslopes: Integrating geomorphic processes and the biological C cycle. Geoderma. doi: 10.1016/j.geoderma.2005.01.008

Yu J, Sun W, Liu J, et al (2007) Enhanced net formations of nitrous oxide and methane underneath the frozen soil in Sanjiang wetland, northeastern China. J Geophys Res Atmos 112:2–9. doi: 10.1029/2006JD008025

Yuan Z, Gazol A, Lin F, et al (2013) Soil organic carbon in an old-growth temperate forest: Spatial pattern, determinants and bias in its quantification. Geoderma. doi: 10.1016/j.geoderma.2012.11.008

Zanchi FB, Meesters AGCA, Waterloo MJ, et al (2014) Soil CO_2 exchange in seven pristine Amazonian rain forest sites in relation to soil temperature. Agric For Meteorol. doi: 10.1016/j.agrformet.2014.03.009

Zhu Q, Nie X, Zhou X, et al (2014) Soil moisture response to rainfall at different topographic positions along a mixed land-use hillslope. Catena. doi: 10.1016/j.catena.2014.03.010

Chapter 3

CARBON DIOXIDE AND METHANE FLUXES FROM TREE STEMS, COARSE WOODY DEBRIS, AND SOILS IN AN UPLAND TEMPERATE FOREST

As published in Ecosystems, 2017. DOI: 10.1007/s10021-016-0106-8

Authors:

Daniel L. Warner[1], Samuel Villarreal[1], Kelsey McWilliams[2], Shreeram Inamdar[1], Rodrigo Vargas[1]

Affiliations:

[1]University of Delaware, Department of Plant and Soil Sciences, DE, USA

[2]University of Delaware, Department of Civil and Environmental Engineering, DE, USA

Abstract

Forest soils and canopies are major components of ecosystem CO_2 and CH_4 fluxes. In contrast, less is known about coarse woody debris and living tree stems, both of which function as active surfaces for CO_2 and CH_4 fluxes. We measured CO_2 and CH_4 fluxes from soils, coarse woody debris, and tree stems (22-78 cm diameter at breast height) over the growing season in an upland temperate forest. Soils were CO_2 sources (4.58 ± 2.46 µmol m^{-2} s^{-1}, mean ± 1 S.D.) and net sinks of CH_4 (-2.17 ± 1.60 nmol m^{-2} s^{-}

^{1}). Coarse woody debris were a CO_2 source (4.23 ± 3.42 µmol m^{-2} s^{-1}) and net CH_4 sink, but with large uncertainty (-0.27 ± 1.04 nmol m^{-2} s^{-1}) and with substantial differences depending on wood decay status. Stems were CO_2 sources (1.93 ± 1.63 µmol m^{-2} s^{-1}), but also net CH_4 sources (up to 0.98 nmol m^{-2} s^{-1}), with a mean of (0.11 ± 0.21 nmol m^{-2} s^{-1}) and significant differences depending on tree species. Stems of *N. sylvatica*, *F. grandifolia*, and *L. tulipifera* consistently emitted CH_4, while stems of *A. rubrum*, *B. lenta*, and *Q. spp* were intermittent sources. Coarse woody debris and stems accounted for 35% of total measured CO_2 fluxes, while CH_4 emissions from living stems offset net soil and CWD CH_4 uptake by 3.5%. Our results demonstrate the importance of CH_4 emissions from living stems in upland forests, and the need to consider multiple forest components to understand and interpret ecosystem CO_2 and CH_4 dynamics.

Keywords: carbon cycle, forested watershed, biogeochemistry, methane, carbon dioxide

3.1 Introduction

Carbon dioxide (CO_2) and methane (CH_4) are the two greenhouse gases of greatest concern for climate change on our planet (Rodhe 1990). While increasing atmospheric concentrations of CO_2 and CH_4 are tied to human activities (IPCC 2014), natural processes are inherently tied to global dynamics of both gases. Unfortunately, the influences of many natural processes on present and future CO_2 and CH_4 dynamics remain unclear (Raich and Potter 1995; Dlugokencky et al. 2011). At the ecosystem scale, forests are generally net sinks of CO_2, and store large quantities of carbon in their soils (Pan et al. 2011). However, forest soils also emit large quantities of CO_2, and may be a major source (in wetlands) or sink (in uplands) of CH_4 depending on the net balance of CH_4 production and oxidation by specialized microbial communities (Raich and Potter 1995; Smith et al. 2000; Dlugokencky et al. 2011). The roles of living tree stems and coarse woody debris (CWD) in ecosystem CO_2 and CH_4 budgets have been less studied than soils and forest canopies, but are a subject of increasing interest (Harmon et al. 2011; Carmichael et al. 2014).

Emissions of CO_2 from CWD are a product of the gradual decay of dead wood by decomposer communities (Harmon et al. 2004), and stem CO_2 emissions are a result of growth and maintenance respiration (i.e. stem respiration) from living tissues within a tree, as well as lateral diffusion of xylem-transported CO_2 originating from the rhizosphere (Amthor 1984; Teskey et al. 2008). The magnitudes of these fluxes may vary substantially due to differences in microbial community assemblages, stand age, and forest species composition (Edwards and Hanson 1996; Gough et al. 2007; Ryan et al. 2009; Fukami et al. 2010; Russell et al. 2014). Many previous studies have overlooked

the contributions of these important forest carbon pools to sub-canopy CO_2 emissions, either by considering them negligible or by using large-scale measurement techniques such as eddy covariance that are unable to distinguish fluxes from different ecosystem carbon pools (Harmon et al. 2011). However, it is unlikely that CO_2 fluxes from soils, CWD, and living stems respond to environmental variability in the same manner, and understanding the function and responses of these sources is necessary for understanding present and future carbon dynamics in forests.

Upland forest soils primarily act as net sinks of CH_4 (Steudler et al. 1989; Smith et al. 2000), but the role of CWD and stems in CH_4 processes remains poorly understood. Recent studies have identified several pathways of CH_4 production within living and dead woody biomass, including photodegradation of wood compounds (Keppler et al. 2008; Vigano et al. 2008), fungal production of CH_4 in CWD (Mukhin and Voronin 2008; Lenhart et al. 2012), and fermentation within living stems (Mukhin and Voronin 2011; Covey et al. 2012; Wang et al. 2016). Other studies have found living tree stems and leaves to function as major conduits for CH_4 emissions from wetlands and other CH_4-producing soils (Terazawa et al. 2007; Rice et al. 2010; Pangala et al. 2013). These findings highlight the need for inclusion of tree stems and coarse woody biomass in global CH_4 models (Butenhoff and Khalil 2007; Carmichael et al. 2014). However, *in situ* studies of CH_4 fluxes from these sources are scarce, thus limiting our ability to assess the role of CWD and stems in CH_4 fluxes across broad spatial scales and ecosystem types.

In this study, we measured CO_2 and CH_4 fluxes from soils, CWD, and living tree stems over one growing season within an upland temperate forest. Specifically we sought to answer the following questions:

- How do CO_2 and CH_4 fluxes vary between soils, CWD, and stems in a temperate forest?
- Which environmental factors control these fluxes?

Our study integrates multiple components of CO_2 and CH_4 fluxes in an upland temperate forest, and we provide evidence that living tree stems act as net sources of CH_4.

3.2 Methods

Site Description

This study was conducted in a 12 hectare forested headwater catchment at Fair Hill Natural Resources Management Area, Cecil County, Maryland, USA (39° 42' N, 75° 50' W). Vegetation is primarily *Fagus grandifolia*, *Quercus spp.*, *Lirodendron tulipifera*, and *Acer spp*. Soils within the study area are coarse-loamy, mixed, mesic Lithic Dystrucepts belonging to the Manor and Glenelg series loams, which overlay peltic gneiss and schist bedrock. Annual precipitation is approximately 1231 mm. Annual snowfall is approximately 350 mm, but snowpack does not last through the entire winter. Annual mean temperature is 12.2 ^{o}C, reaching a maximum mean of 24.6 ^{o}C in July, and a minimum mean of -0.6 ^{o}C in January (Inamdar et al. 2012).

All measurements were taken within a representative forested area of 100-by-30 meters in size. The selected area had similar topography and vegetation throughout. We established 16 sampling clusters within the study area. Each cluster contained a sampling

point on a stem at breast height, a nearby piece of CWD, and the adjacent soil, for a total of 48 sampling points.

CO_2 and CH_4 flux measurements

At each sampling point, 2 mm thick PVC rings with a 10 cm internal diameter were inserted 5 cm into the soil with 3 cm exposed. For CWD and stems, 3 cm-deep rings were affixed to the surface with a neutral sealant. CO_2 and CH_4 concentrations were measured using an Ultra-Portable Greenhouse Gas Analyzer (Los Gatos Research, Mountain View, California, USA) connected to a 10 cm diameter chamber that fit snugly over the rings. The chamber was allowed to equilibrate with ambient air until a stable baseline was observed before each measurement. Once the chamber was sealed, gas was allowed to accumulate for 3 minutes while being circulated through the instrument via an internal vacuum pump, and gas concentrations were measured at 1 Hz with a range and error of 1 to 20,000 ± 0.3 ppm for CO_2 and 0.01 to 100 ± 0.002 ppm for CH_4 (Pearson et al. 2016). Gas fluxes were calculated using 180 measurements and fitting the following equation (Pumpanen et al. 2004):

$$F = \left(\frac{dC}{dt}\right)\left(\frac{V_c}{A_c}\right)\frac{P}{(R*(T+273.15))} \quad (1)$$

where F is the flux of a gas, dC/dt is the change in concentration over time as measured by the instrument (ppm s^{-1}), V_c is the closed system volume (0.00119 m^3), A_c is the chamber area (0.0081 m^2), P is the atmospheric pressure (101.325 kg m^{-1} s^{-2}), R is the ideal gas law constant (0.00831447 kg m^2 µmol^{-1} K^{-1} s^{-2}), T is measured soil temperature (^{o}C), and 273.15 is the conversion factor from Celsius to Kelvin. Slopes (i.e., dC/dt in Eq. 1) with a p-value greater than 0.1 were deemed as not significant and were therefore set to zero. Slopes with non-linear trends due to poor seals or ring disturbance during measurement were removed from this study.

Volumetric water content (VWC) and temperature were measured concurrently with fluxes at all sites from 0-4 cm depth for soils (WET Sensor, Delta-T Devices, Cambridge, UK), and at the surface for CWD and stems using a Mini Ligno DX (Lignomat, Portland, Oregon, USA) for moisture and a non-contact infrared thermometer (Nubee NUB8500H) for surface temperature. Gas flux, moisture, and temperature measurements were taken 1-2 times monthly from April to December 2014.

Soil and wood samples

Soil and CWD samples were collected in late 2014 for C and N analysis and wood density estimation. Soil samples were collected in triplicate to a depth of 10 cm adjacent to each soil ring and homogenized (O-horizon was carefully removed prior to collection). Samples were sieved to remove roots and stones (>2 mm), dried, and ground prior to analysis. Wood samples were collected in triplicate from the upper 5-10 cm of CWD with a trowel or saw (if necessary) adjacent to each CWD ring. Each block was carefully shaved with a razor to create a smooth, angular shape from which volume could

be easily estimated. Samples were then dried and weighed to estimate wood density and ground prior to C and N analysis. Total C and N analysis were performed on a Vario-Max CN Analyzer (Elementar, Mt. Laurel, New Jersey, USA).

Surface area estimation and spatiotemporal upscaling

To estimate the abundance of CWD and stems in our study site we surveyed the entirety of two 25-by-25 meter areas to calculate the total surface area of soils, CWD, and stems contained in each. Within each area, CWD of diameter greater than 10 cm was measured in length and width, and all tree stems were measured in diameter at breast height (DBH) and height using a clinometer. CWD surface area was estimated as a half cylinder. Stem surface area was estimated as a cone with DBH as the basal width and clinometer-measured height. This information allowed us to estimate the total surface area and footprint of CWD and stems per hectare. Soil surface area per hectare was estimated as one hectare minus the total footprint of CWD and stems.

CO_2 and CH_4 fluxes were estimated though the 2014 growing season using categorical and temporal data presented in Table 3.1. First, we identified categorical groups for CWD decay status ("fresh" and "decayed") and tree species (*A. rubrum, B. lenta, F. grandifolia, L. tulipifera, N. sylvatica,* and *Q. spp*), both of which showed influence on growing season mean fluxes (Table 3.1). CWD was classified as "fresh" or "decayed" based on a distinct separation in our wood density ("fresh" > 0.5 mg cm^{-3}, "decayed" < 0.5 mg cm^{-3}) and C:N data, as well as visual and tactile inspection of the wood. Second, we fit empirical models to explain the temporal variability of the datasets using daily meteorological data from a nearby (~1 km) weather station (DEOS 2014). Temperature was assumed as the primary driver of both gas fluxes, and temperature

dependency functions were fit to flux data from each categorical group of the form (Lloyd and Taylor 1994):

$$F_{gas} = Ae^{BT} \tag{2}$$

where F_{gas} is the flux of CO_2 or CH_4 at a measured surface temperature T, and A and B are empirically-derived constant coefficients.

Other model parameters were then selected using stepwise linear regressions relating a set of meteorological variables (Table 3.1) to the residuals of Eq. 2 for soils, CWD, and stems. Selected parameters included surface temperature, wind speed, photosynthetically active radiation, solar radiation, and a 7-day antecedent precipitation index (API) calculated as:

$$API = \sum_{i=1}^{7} \frac{P_i}{i} \tag{3}$$

where P_i is the precipitation (mm) i days before the date in question. As daily surface temperature measurements were not available, we fit linear functions relating manual measurements of soil, CWD, and stem surface temperature to a 7-day air temperature index (T_s) (r^2 = 0.85, 0.87, and 0.87 for soils, CWD, and stems respectively). T_s was calculated as:

$$T_s = \sum_{i=1}^{7} \frac{AT_i}{i} \tag{4}$$

where AT_i is the mean air temperature i days before the date in question. Fluxes of both gases from each categorical group were estimated for each day from May 1 to September 30, 2014 using models of the general form:

$$F_{gas} = Ae^{BT_s} + C_1x_1 + C_2x_2 \ldots \tag{5}$$

where F_{gas} is the estimated flux of CO_2 or CH_4, T_s is estimated surface temperature from Eq. 5, A and B are constants derived from Eq. 2, C_1 and C_2 are empirical constants for other model parameters x_1 and x_2. Table 1 gives a full list of parameters used in each model for soils, CWD, and stems, and the resulting r^2 values. Growing season mean fluxes were used as daily flux estimates for categorical groups that had insignificant model fits ($p > 0.05$; Table 3.1). For soil CH_4 fluxes, we used different daily mean flux estimates when surface temperature was above or below a threshold of 17 ^oC (see Results section), which was confirmed via breakpoint analysis. The means and 95% CI of daily flux estimates for each categorical group were multiplied by the estimated surface area of the corresponding category. The sum of the daily estimates yielded the estimated total growing season fluxes from soils, CWD, and stems per hectare. All modeling and statistical analyses were performed in R using the "base" and "segmented" packages (for break point identification) (R Core Team 2015, Muggeo 2008).

3.3 Results

Growing season conditions

Mean daily air temperature and daily precipitation ranged 8.3-27.4 ^oC and 0-36.8 mm with growing season means of 19.7 ^oC and 2.7 mm, respectively, and API ranged 0-18.8 with a growing season mean of 2.6 (Fig 3.1). Peak temperature and API occurred on 6/25/14 and 5/9/14, respectively.

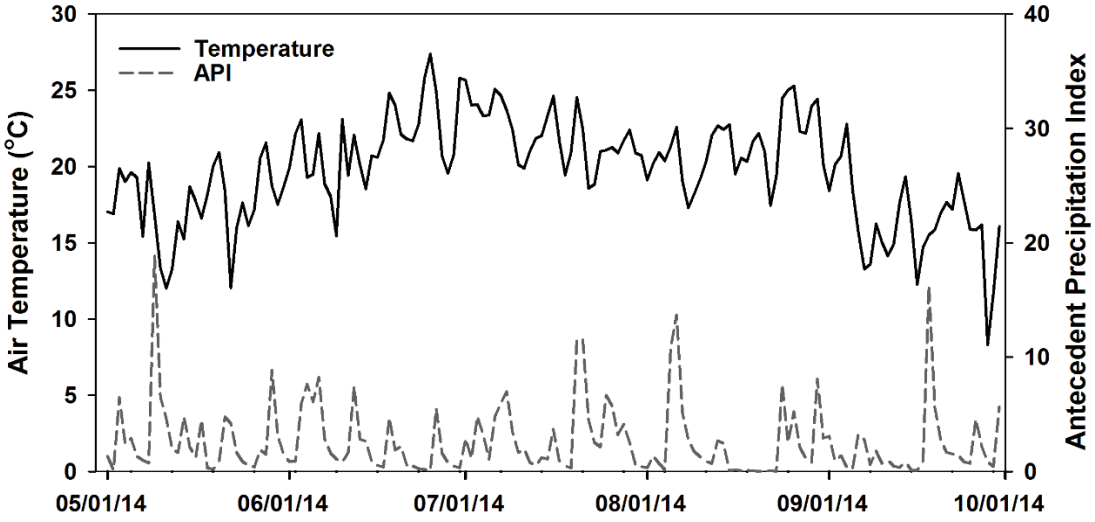

Figure 3.1 Temperature and Antecedent Precipitation Index (API) data over the course of the 2014 growing season considered in this study.

Seasonal flux variability between soils, CWD, and stems

CO_2 fluxes from all carbon pools showed a distinct seasonal trend (Fig 3.2), reaching a peak in midsummer. Soil CO_2 fluxes were generally 8% and 59% higher than CWD and stems, respectively, averaging 4.6 ± 0.59 µmol m^{-2} s^{-1} (± 95% CI; CV = 54%) in the growing season. CO_2 fluxes from CWD were more variable, averaging 4.2 ± 0.85 µmol m^{-2} s^{-1} (CV = 81%) over the growing season. Stem CO_2 fluxes, while variable, were generally small relative to soils and CWD, averaging 1.9 ± 0.39 µmol m^{-2} s^{-1} (CV = 84%) during the growing season. All CWD and stem fluxes per m^2 are reported based on CWD or stem surface area.

Only soils exhibited seasonal trends in CH_4 fluxes (Fig 3.2). Soils acted as strong net CH_4 sinks in summer relative to CWD and stems, averaging -2.2 ± 0.38 nmol m^{-2} s^{-1} (CV = 74%) during the growing season. Again, CWD CH_4 fluxes were more variable, with some sites acting as net sources and others as relatively weaker sinks, averaging -0.32 ± 0.26 nmol m^{-2} s^{-1} (CV = 385%). Stems acted as net CH_4 sources throughout the year and showed no clear temporal trends, averaging 0.11 ± 0.05 nmol m^{-2} s^{-1} (CV = 190%).

Categorical controlling factors on growing season mean fluxes

CO_2 fluxes from soil sites were unrelated to moisture, carbon, or nitrogen content. Across all soil sites, growing season mean CH_4 uptake was weakly positively related to C:N ($r^2 = 0.26$, $p < 0.1$). We also identified a weak negative correlation between VWC and growing season soil CH_4 uptake ($p < 0.01$, $r^2 = 0.2$).

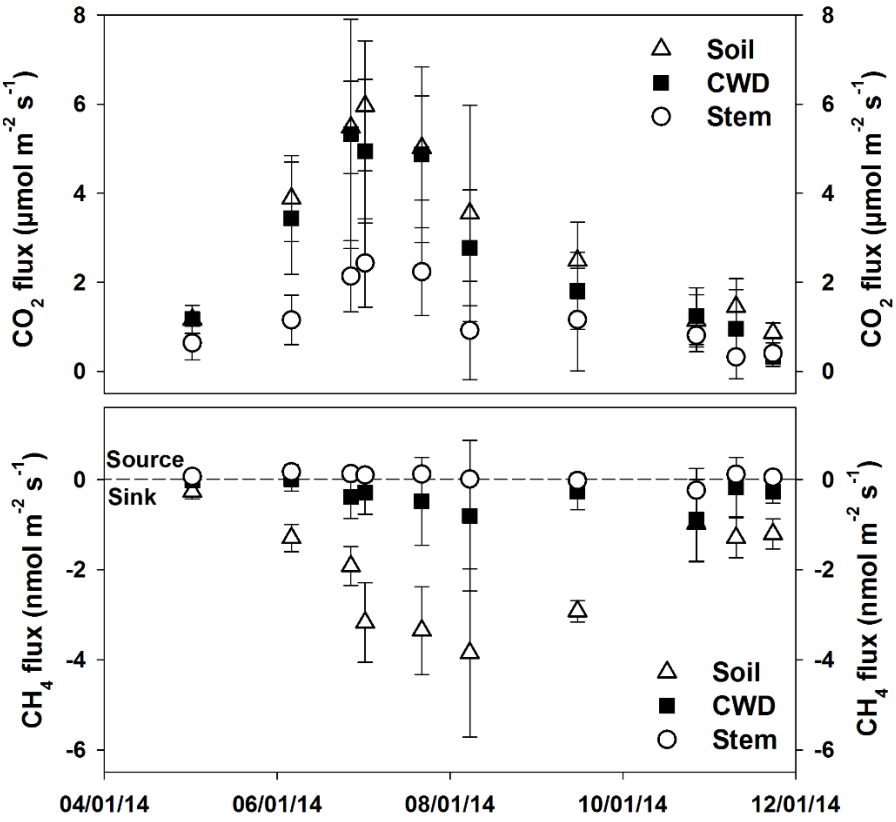

Figure 3.2 Seasonal variability in CO_2 (top) and CH_4 (bottom) fluxes throughout 2014. Soil fluxes presented as triangles, CWD as squares, and stems as circles. Error bars represent the 95% CI of all daily flux means from each carbon pool

CWD CO_2 fluxes were unrelated to decay status, wood density, or wood C and N content. Across all CWD sites, CH_4 fluxes were positively related to C:N ($r^2 = 0.28$, $p < 0.05$), and were significantly more variable in low-density wood (F-test, $p < 0.01$). Growing season mean CH_4 fluxes from "fresh" CWD were generally positive and significantly greater than those from "decayed" CWD ($p < 0.05$; Fig 3.3).

Growing season mean stem CO_2 and CH_4 fluxes were significantly different between species (K-W test, $p < 0.01$, $p < 0.05$, respectively). CO_2 fluxes were greatest from *L. tulipifera*, *A. rubrum*, and *Q. spp*. CH_4 fluxes were greatest from *N. sylvatica*, *L. tulipifera*, and *F. grandifolia*, while other species showed little to no emissions (Fig 3.3).

Tree species was the only significant controlling factor on stem CH_4 fluxes that we identified in this study. Fluxes of both gases were unrelated to DBH and height.

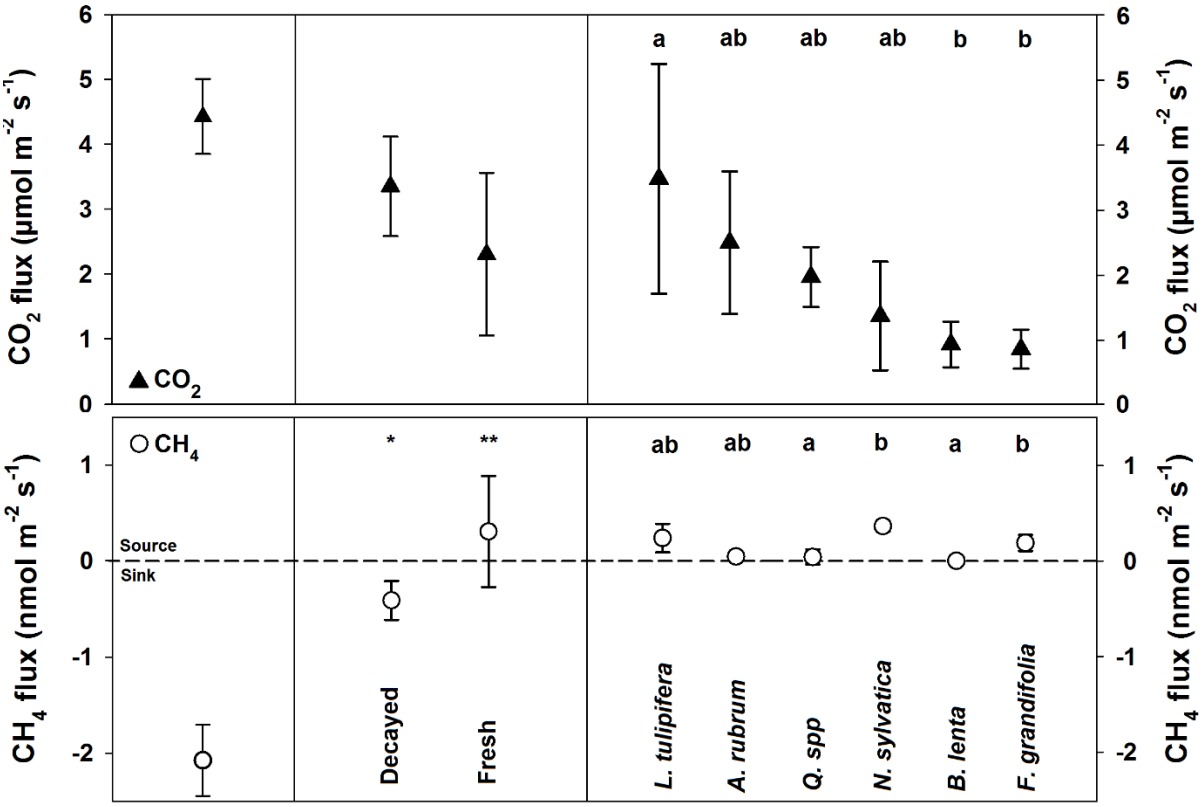

Figure 3.3 Growing season mean CO_2 (top) and CH_4 (bottom) fluxes from soils, CWD, and stems (left to right panels). CWD fluxes are grouped by decay status, and stem fluxes by species. Error bars represent 95% CI of growing season mean fluxes from each group.

Temperature dependence

Table 3.1 shows the r^2 values to all significant ($p < 0.05$) relationships between CO_2 flux and temperature in our study (see Eq. 2). Fresh CWD and *N. sylvatica* stems were the only two categorical groups where CO_2 fluxes were not related to temperature.

We applied same approach to examine the temperature sensitivity of soil CH_4 fluxes. However, Eq. 2 was only weakly, though significantly, related to soil CH_4 uptake ($r^2 = 0.14$, $p < 0.01$). Thus, instead of using an exponential relationship, we identified a

threshold at 17° C above which CH_4 uptake was significantly greater and more variable (t-test and F-test, $p < 0.01$) for the entire study site (Fig 3.4).

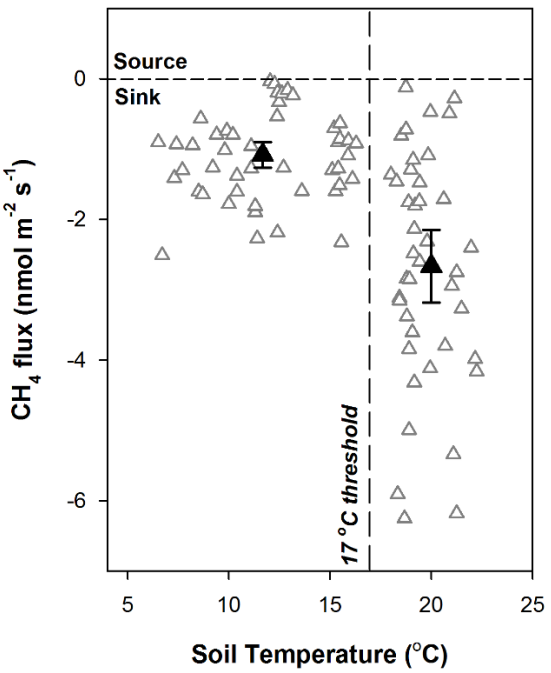

Figure 3.4 Relationship of soil CH_4 flux and temperature observed in this study. Vertical dashed line indicates the 17°C threshold. Black triangles and error bars represent the mean flux and 95% CI above and below this threshold.

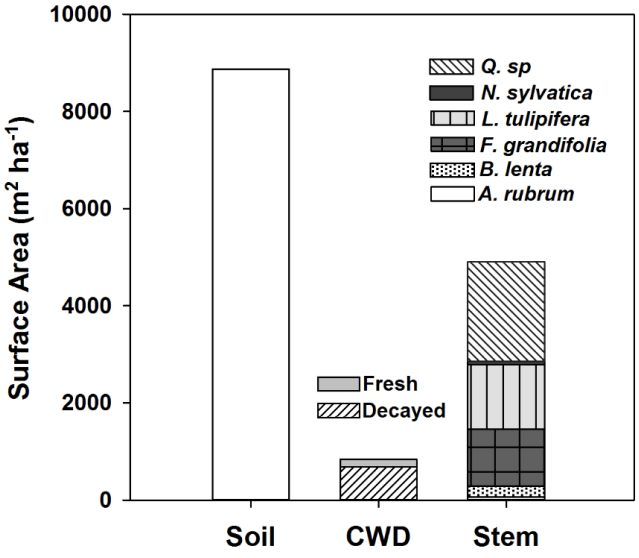

Figure 3.5 Comparison of surface area for each source (soil, CWD, and stem) and categorical group (decay status, species) within study forest.

This exponential approach for CH_4 fluxes was not suitable for examining the temperature dependence of CWD or stems, as their data were generally clustered around zero and variable above and below. Therefore, we did not find temperature to be an influential factor on CH_4 fluxes from CWD and stems.

Table 3.1 Summary of controlling factors used for upscaling flux observations. R^2 is reported for groups demonstrating significant fits to meteorological data used in upscaling. Numbers in parentheses are mean flux values for groups with no significant temporal controls, in which case group means were used for upscaling.

	CO_2			CH_4		
Source	**Soil**	**CWD**	**Stem**	**Soil**	**CWD**	**Stem**
Parameters	T_s, API, W, PAR	T_s, API, S_r	T_s, PAR	T_s (17°C threshold)	-	-
Adjusted R^2	0.64	Decayed: 0.64 Fresh: (3.3)	AR: 0.94 BL: 0.43 FG: 0.55 LT: 0.47 NS: (1.0) QS: 0.64	< 17°C: (-1.08) > 17°C: (-2.76)	Decayed: (-0.37) Fresh: (0.43)	AR: (0.03) BL: (0.00) FG: (0.16) LT: (0.16) NS: (0.28) QS: (0.05)

Parentheses indicate no significant temporal controls ($p > 0.05$), means used and reported instead of model fits in units of μmol m^{-2} s^{-1} for CO_2, nmol m^{-2} s^{-1} for CH_4

T_s = Surface Temperature	PAR = Photosynthetically	AR = A. rubrum	LT = L. tulipifera
API = Antecedent Precipitation Index	Active Radiation	BL = B. lenta	NS = N. sylvatica
W = Wind speed	S_r = Solar Radiation	FG = F. grandifolia	QS = Q. spp

Forest structure and flux upscaling

Based on the plot surveys mentioned previously, we estimated surface areas of 8870 ± 344 m^2 ha^{-1} for soils, 836 ± 181 m^2 ha^{-1} for CWD, and 4900 ± 1600 m^2 ha^{-1} for living stems (Fig 3.5). Roughly 82% of CWD surface area was classified as "Decayed". *A. rubrum*, *B. lenta*, *F. grandifolia*, *L. tulipifera*, *N. sylvatica*, and *Q. spp* accounted for 1, 5, 24, 27, 1, and 42% of living stem surface area, respectively (Fig 3.5).

We estimated cumulative growing season CO_2 fluxes of 18600 ± 4190 kg CO_2 ha^{-1} (± 95% CI), with corresponding net CH_4 fluxes of -4.11 ± 0.31 kg CH_4 ha^{-1} (Fig 3.6). In CO_2 equivalents, net CH_4 uptake offset a total of -282 ± 21.1 kg CO_2 eq. ha^{-1} (using a 100-year global warming potential of 25 mol CO_2 eq./mol CH_4 from Forster et al.

(2007)). Using 100-year sustained global warming/cooling potentials (SGWP/SGCP) (Neubauer and Megonigal 2015), the estimated strength of the net soil and CWD CH_4 sink increased to -833 ± 62.4 kg CO_2 eq. ha^{-1}, with a small 6.4 ± 1.4 kg CO_2 eq. ha^{-1} offset due to stem CH_4 emissions. Soils played the dominant role in both CO_2 and CH_4 fluxes (Fig 3.6). However, our estimates found stems and CWD to account for roughly 35% of total CO_2 emissions in (Fig 3.6). Net CH_4 uptake by CWD was negligible (~1%), while stem CH_4 emissions offset the soil CH_4 sink by roughly 3.5% (Fig 3.6).

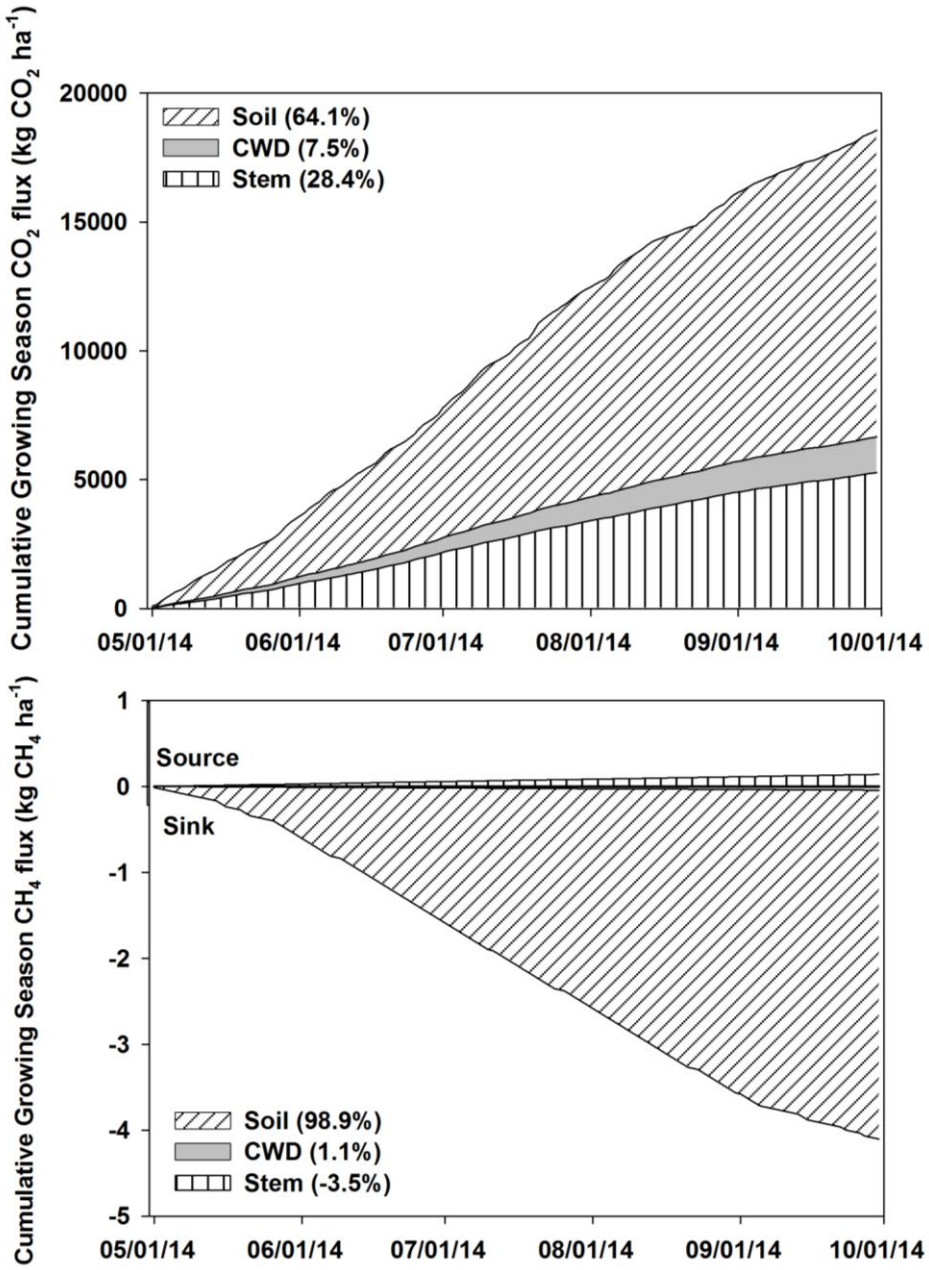

Figure 3.6 Cumulative estimated CO_2 (top) and CH_4 (bottom) fluxes (in mol C ha^{-1}). Uncertainty is reported in text. Parentheses indicate the relative contribution of each carbon pool to the total fluxes of each gas over the course of the 2014 growing season (total of 153 days)

3.4 Discussion

This study identified key differences in CO_2 and CH_4 fluxes and their controlling factors within soils, CWD, and living tree stems in a temperate upland forest. Below we discuss these fluxes, their environmental controlling factors, and their ecological significance.

Fluxes and their controlling factors

We found CO_2 fluxes to vary both between and within the soil, CWD, and stems components considered in this study. Mean soil CO_2 fluxes in our study were comparable to fluxes observed from similar topographic positions in other upland temperate forest studies (Hanson et al. 1993; Webster et al. 2008b; Atkins et al. 2014). We tried, but did not identify any dominant spatial controls (i.e. moisture, C and N content) on mean growing season CO_2 efflux from soils within our study area. However, moisture, C, and N content have all been identified as significant controlling factors for soil respiration in temperate forests at the catchment scale (Davidson et al. 1998; Ngao et al. 2012; Creed et al. 2013).

Our study estimated CWD CO_2 efflux in the growing season (880-1890 kg CO_2 ha^{-1} (95% CI); Fig 3.6) to be higher than estimates of CWD CO_2 efflux over an entire year made in a similar forest (440-1100 kg CO_2 ha^{-1}) (Gough et al. 2007). This discrepancy is likely due to differences in CWD abundance between the study sites; we measured roughly 3 times more CWD per unit area as a result of lack of CWD and wood fuel management at our forest.

We estimated a cumulative growing season flux of 3210-7350 kg CO_2 ha^{-1} (95% CI) from tree stems within our forest. This was comparable to ranges of cumulative annual stem CO_2 flux estimated from a similar temperate forest (5460-7480 kg CO_2 ha^{-1}) (Edwards

and Hanson 1996). We found significant differences in stem CO_2 fluxes between species (Fig 3.3), and our observations of CO_2 fluxes from *L. tulipifera* and *Q. spp* were more than double previously reported values (Edwards and Mclaughlin 1978). However, our *F. grandifolia* CO_2 fluxes were similar those reported for *F. sylvatica* in temperate European forests (Ceschia et al. 2002). These inconsistencies may be due to differences in the age and size of stems at our site. *L. tulipifera* and *Q. spp* had much larger diameters (and thus a much greater volume of woody tissue per unit stem surface area) than the stems in previous studies (54 cm median compared to 20-25 cm range) (Edwards and Mclaughlin 1978), while *F. grandifolia* were similar in size (8.4 cm mean compared to 7.2 cm mean) (Ceschia et al. 2002).

We identified a strong seasonal pattern for CO_2 efflux across soils, CWD and stems in this study (Fig 3.2), which reflects the influence of temperature on microbial and plant metabolisms as well as the influence of forest phenology. This finding is consistent with previous studies in similar temperate forests for soils, CWD, and stems (Hanson et al. 1993; Ceschia et al. 2002; Gough et al. 2007; Creed et al. 2013).

We observed a seasonal trend in net soil CH_4 uptake, with values ranging from -6.25 nmol m^{-2} s^{-1} in July to -0.04 nmol m^{-2} s^{-1} in late November (Fig 3.2). This range and seasonal variability is consistent with previous studies in temperate forests (Crill 1991; Smith et al. 2000). We identified a significant, albeit weak, negative correlation between VWC and net soil CH_4 uptake. This relationship is to be expected, as increasing VWC reduces diffusion of CH_4 and O_2 into the soil, limiting CH_4 oxidation and promoting methanogenesis (Ambus and Christensen 1995; Mosier et al. 1996; Del Grosso et al. 2000).

Compared to soils, little is known about CWD CH_4 fluxes, especially in upland temperate forests. This study provides some of the first *in situ* observations of CH_4 dynamics within this important forest compartment. We found CH_4 fluxes from CWD to be highly variable (CV = 385%), with some sites acting as net sources and others as net sinks. We found a positive relationship between CWD C:N and CH_4 fluxes, suggesting a shift from CWD CH_4 emission to CH_4 consumption as decay progresses and C:N decreases (Harmon et al. 2004). "Fresh" CWD was a weak CH_4 source in our study, but CH_4 fluxes from "decayed" CWD ranged widely (CV = 261%) (Fig 3.3). Some decayed logs acted similar to fresh logs, while others were net sinks with comparable net CH_4 uptake to our soil sites. Recent research has shown the potential for CH_4 production even under aerobic conditions by wood-decomposing fungi common to forest ecosystems (Mukhin and Voronin 2008; Lenhart et al. 2012). While this may explain the small net CH_4 efflux observed at some CWD sites, many sites acted as net CH_4 sinks. Differences in the specific microbial community colonization of the CWD may possibly drive its ecological function similar to findings of fungal assemblage effects on CWD decay rates by Fukami et al. (2010), but this remains to be explored. Noteworthy, we found that CH_4 fluxes from CWD have a very broad range (-3.5 to 3.5 nmol CH_4 m^2 s^{-1}) even within a relatively small spatial extent within a forest. This large variability may be a result of the relative higher abundance and diversity of CWD at our study site due to a lack of wood fuel removal practices.

Similar to CWD, little is known about the role of living tree stems in forest CH_4 dynamics. We found living stems to act as net sources of CH_4 throughout the year, with significant differences in CH_4 fluxes between species (Fig 3.2; Fig 3.3). Prior to this study, the vast majority of reported CH_4 fluxes from living stems have focused on wetland and

poorly drained systems (but see Wang and others 2016), where CH_4 is produced in anoxic soil layers and is routed through the roots and emitted to the atmosphere in the first few vertical meters of the stem (Pangala et al. 2013; Terazawa et al. 2015). In these systems, stem CH_4 fluxes may vary between species (Pangala et al. 2013), but are also dictated by hydrology, increasing and decreasing with rising and falling water table elevations (Terazawa et al. 2015). We found no influence of precipitation or soil moisture on the spatial and temporal variability of stem CH_4 fluxes, and our observed stem CH_4 fluxes were 1-2 orders of magnitude less than those reported in wetland systems (Terazawa et al. 2007; Pangala et al. 2013).

A second potential mechanism of CH_4 fluxes from stems may be lateral diffusion of microbially-derived CH_4 produced within the stem itself (Zeikus and Ward 1974; Mukhin and Voronin 2011; Covey et al. 2012; Wang et al. 2016). Previous studies have documented elevated CH_4 concentrations within upland stems (Covey et al. 2012; Wang et al. 2016) and microbial production of CH_4 within living stems (Zeikus and Ward 1974; Mukhin and Voronin 2011; Wang et al. 2016) even without obvious signs of infection on the bark surface. Species-specific differences in disease resistance and structural properties of the wood may possibly explain species differences in CH_4 fluxes. For example, both *F. grandifolia* and *L. tulipifera*, two species with consistent CH_4 emissions, are classified as "nonresistant" to disease, and are generally less resistant than *Q. spp*, which showed almost no CH_4 emission (Fig 3.3) (Scheffer 1966). However, decay resistance may vary substantially between or even within individuals of the same species (Scheffer 1966), and inspection of tree cores is necessary to fully assess this possibility. Noteworthy, we found no significant relationship between temperature and stem CH_4 efflux, though temperature-

driven increases of CH_4 efflux from stems and incubated living wood cores have been documented (Mukhin and Voronin 2011; Wang et al. 2016). We postulate that efflux of endogenic CH_4 from stems in our forest may not be production limited, but rather limited in its lateral transport pathways through woody tissues. This hypothesis is supported by Wang and others (2016), who measured upland stem CH_4 fluxes resulting from heartwood rot to be similar in magnitude to stem fluxes of soil-derived CH_4 in wetlands, and attributed this similarity to the limited lateral diffusion of CH_4 though woody tissues.

Significance of soils, CWD, and stems to forest fluxes

Our study identified soils as the dominant component of fluxes of both gases. However, CWD and stems contributed roughly 35% of measured CO_2 fluxes (Fig 3.6). We observed differences in fluxes between tree species and CWD decay status. Thus, forest species composition and CWD assemblages may be responsible for differences in fluxes within a forest. We did not investigate the vertical heterogeneity of gas fluxes along stems in this study. However, it is possible that our estimates of CO_2 efflux from stems are underestimates, as studies have identified increasing rates of stem respiration at higher positions (middle stem and higher) along stems (Ceschia et al. 2002; Tarvainen et al. 2014).

Within the forests, net CH_4 uptake offset below-canopy CO_2 emissions between 1.5 and 4.5% (depending on the global warming potentials used). Stem CH_4 emissions offset net soil and CWD CH_4 uptake by roughly 3.5% (Fig 3.6), assuming a homogenous flux for the entire height of the stems. However, if the stems in our site are releasing soil-derived CH_4 to the atmosphere along only the first few vertical meters (Pangala et al. 2013), applying our flux observations along the entire height of the stem may be an overestimation. Conversely, if the CH_4 originates within the tree, there may be vertical

heterogeneity in microbial colonization and oxygen availability (Eklund 2000; Covey et al. 2012), which further complicates accurately estimating CH_4 fluxes across stems in upland forests. Our measurements of stem CH_4 emissions were over ten times lower than other reported *in situ* measurements in an upland temperate forest (Wang et al. 2016). Because of this, we believe that our measurements are likely representative of the low-end of stem CH_4 emissions in upland forests. The large difference in CH_4 fluxes from stems between two upland temperate forests highlights the need for greater understanding of this newly considered CH_4 source from the local to the global scales.

We found CWD to play an overall negligible role in forest net CH_4 fluxes (~1% of the total sink) as fluxes were highly variable and consequently magnitudes cancelled out (Fig 3.6). However, we stress that while our net estimations of CWD CH_4 fluxes were very low, the individual measurements of these fluxes were highly variable (CV = 385%) and spanned a broad range between those from soils and stems (Fig 3.3). Given the diverse assemblage of CWD sampled in this study, it is not surprising that CWD CH_4 sources and sinks balanced each other out when considered at a per-hectare scale. In a system with a CWD assemblage of greater abundance and less diversity (e.g. similar age, species) due to natural or man-made disturbance, the relative contribution of CWD to total CH_4 flux may be larger as there would be less flux variability within the CWD assemblage. Thus, the role of this carbon pool in ecosystem CH_4 budgets warrants further investigation.

3.5 Conclusions

We measured CO_2 and CH_4 fluxes from soils, CWD, and tree stems in an upland temperate forest during the growing season, and found significant differences in both gas fluxes across all three sources, as well as across stem species and the level of CWD decay.

This study considered the relative importance of these ubiquitous forest carbon pools to below-canopy CO_2 and CH_4 fluxes in a way that larger-scale approaches (i.e. eddy covariance) cannot discern, and highlights the importance of considering multiple forest components and greenhouse gases when assessing the net global warming potential of forest ecosystems. Our findings imply that management strategies and environmental changes that alter CWD abundance and tree species composition may also alter CO_2 and CH_4 dynamics in upland temperate forests in unforeseen ways. Future research should address the mechanisms of CH_4 production and their resulting fluxes from CWD and stems to further assess how potential environmental changes may influence the roles of temperate forests in global CH_4 budgets. Studies utilizing high-frequency measurements or stable isotopes to identify carbon sources will be especially useful in identifying hot spots and hot moments of fluxes from CWD and stems.

Acknowledgements

This study was funded by the US Department of Agriculture (USDA-AFRI Grant 2013-02758). RV and KM acknowledge support from the Delaware Water Research Center. We thank Zulia Sanchez, Jillian Swank, the UD Soil Testing Facility, and the Delaware Environmental Observation System for field and laboratory support.

REFERENCES

Ambus P, Christensen S (1995) Spatial and Seasonal Nitrous Oxide and Methane Fluxes in Danish Forest-, Grassland-, and Agroecosystems. J. Environ. Qual. 24:993

Amthor JS (1984) The role of maintenance respiration in plant growth. Plant, Cell Environ 7:561–569. doi: 10.1111/j.1365-3040.1984.tb01856.x

Atkins JW, Epstein HE, Welsch DL (2014) Vegetation heterogeneity and landscape position exert strong controls on soil CO_2 efflux in a moist , Appalachian watershed. Biogeosciences 11:17631–17673. doi: 10.5194/bgd-11-17631-2014

Butenhoff CL, Khalil MAK (2007) Global methane emissions from terrestrial plants. Environ Sci Technol 41:4032–4037. doi: 10.1021/es062404i

Carmichael MJ, Bernhardt ES, Bräuer SL, Smith WK (2014) The role of vegetation in methane flux to the atmosphere: Should vegetation be included as a distinct category in the global methane budget? Biogeochemistry. doi: 10.1007/s10533-014-9974-1

Ceschia É, Damesin C, Lebaube S, et al (2002) Spatial and seasonal variations in stem respiration of beech trees (Fagus sylvatica). Ann For Sci 59:801–812. doi: DOI 10.1051/forest:2002078

Covey KR, Wood SA, Warren RJ, et al (2012) Elevated methane concentrations in trees of an upland forest. Geophys Res Lett. doi: 10.1029/2012GL052361

Creed IF, Webster KL, Braun GL, et al (2013) Topographically regulated traps of dissolved organic carbon create hotspots of soil carbon dioxide efflux in forests. Biogeochemistry. doi: 10.1007/s10533-012-9713-4

Crill PM (1991) Seasonal patterns of methane uptake and carbon dioxide release by a temperate woodland soil. Global Biogeochem Cycles 5:319–334. doi: 10.1029/91GB02466

Davidson EA, Belk E, Boone RD (1998) Soil water content and temperature as independent or confounded factors controlling soil respiration in a temperate mixed hardwood forest. Glob Chang Biol. doi: 10.1046/j.1365-2486.1998.00128.x

Del Grosso SJ, Parton WJ, Mosier AR, et al (2000) General CH_4 oxidation model and

comparisons of CH_4 oxidation in natural and managed systems. Global Biogeochem Cycles 14:999–1019

Dlugokencky EJ, Nisbet EG, Fisher R, Lowry D (2011) Global atmospheric methane: budget, changes and dangers. Philos Trans A Math Phys Eng Sci 369:2058–2072. doi: 10.1098/rsta.2010.0341

Edwards NT, Hanson PJ (1996) Stem respiration in a closed-canopy upland oak forest. Tree Physiol 16:433–439. doi: 10.1093/treephys/16.4.433

Edwards NT, Mclaughlin SB (1978) Temperature-Independent Diel Variations of Respiration Rates in Quercus alba and Liriodendron tulipifera. Oikos 31:200–206

Eklund L (2000) Internal oxygen levels decrease during the growing season and with increasing stem height. Trees 14:177–180. doi: 10.1007/PL00009761

Forster P, Ramaswamy V, Artaxo P, et al (2007) Changes in Atmospheric Constituents and in Radiative Forcing. In: Nakajima T, Ramanathan V (eds) Climate Change 2007: The Physical Science Basis. Contri- bution of Working Group I to the Fourth Assessment Report of the Intergovernmental Panel on Climate Change. Cambridge University Press, Cambridge, United Kingdom and New York, NY, USA, pp 129–234

Fukami T, Dickie IA, Paula Wilkie J, et al (2010) Assembly history dictates ecosystem functioning: Evidence from wood decomposer communities. Ecol Lett 13:675–684. doi: 10.1111/j.1461-0248.2010.01465.x

Gough CM, Vogel CS, Kazanski C, et al (2007) Coarse woody debris and the carbon balance of a north temperate forest. For Ecol Manage. doi: 10.1016/j.foreco.2007.03.039

Hanson PJ, Wullschleger SD, Bohlman SA, Todd DE (1993) Seasonal and topographic patterns of forest floor CO2 efflux from an upland oak forest. Tree Physiol. doi: 10.1093/treephys/13.1.1

Harmon ME, Bond-Lamberty B, Tang J, Vargas R (2011) Heterotrophic respiration in disturbed forests: A review with examples from North America. J Geophys Res Biogeosciences

116:1–17. doi: 10.1029/2010JG001495

Harmon ME, Franklin JF, Swanson FJ, et al (2004) Ecology of Coarse Woody Debris in Temperate Ecosystems. Adv Ecol Res 15:133–276. doi: 10.1016/S0065-2504(03)34002-4

Inamdar S, Finger N, Singh S, et al (2012) Dissolved organic matter (DOM) concentration and quality in a forested mid-Atlantic watershed, USA. Biogeochemistry. doi: 10.1007/s10533-011-9572-4

Keppler F, Hamilton JTG, McRoberts WC, et al (2008) Methoxyl groups of plant pectin as a precursor of atmospheric methane: Evidence from deuterium labelling studies. New Phytol. doi: 10.1111/j.1469-8137.2008.02411.x

Lenhart K, Bunge M, Ratering S, et al (2012) Evidence for methane production by saprotrophic fungi. Nat Commun 3:1046. doi: 10.1038/ncomms2049

Lloyd J, Taylor JA (1994) On the Temperature Dependence of Soil Respiration. Funct Ecol 8:315–323. doi: 10.2307/2389824

Mosier AR, Parton WJ, Valentine DW, Schimel DS (1996) CH_4 and N_2O fluxes in the Colorado shortgrass steppe : 1 . Impact of landscape and nitrogen addition. Global Biogeochem Cycles 10:387–399

Mukhin VA, Voronin PY (2011) Methane emission from living tree wood. Russ J Plant Physiol. doi: 10.1134/S1021443711020117

Mukhin VA, Voronin PY (2008) A new source of methane in boreal forests. Prikl Biokhim Mikrobiol 44:330–332. doi: 10.1134/S0003683808030125

Neubauer SC, Megonigal JP (2015) Moving Beyond Global Warming Potentials to Quantify the Climatic Role of Ecosystems. Ecosystems 18:1000–1013. doi: 10.1007/s10021-015-9879-4

Ngao J, Epron D, Delpierre N, et al (2012) Spatial variability of soil CO 2 efflux linked to soil parameters and ecosystem characteristics in a temperate beech forest. Agric For Meteorol. doi: 10.1016/j.agrformet.2011.11.003

Pachauri RK, Allen MR, Barros VR, et al (2014) IPCC Climate Change 2014: Synthesis Report

Pan Y, Birdsey RA, Fang J, et al (2011) A Large and Persistent Carbon Sink in the World's Forests. Science (80-). doi: 10.1126/science.1201609

Pangala SR, Moore S, Hornibrook ERC, Gauci V (2013) Trees are major conduits for methane egress from tropical forested wetlands. New Phytol 197:524–531. doi: 10.1111/nph.12031

Pearson AJ, Pizzuto JE, Vargas R (2016) Influence of run of river dams on floodplain sediments and carbon dynamics. Geoderma. doi: 10.1016/j.geoderma.2016.02.029

Pumpanen J, Kolari P, Ilvesniemi H, et al (2004) Comparison of different chamber techniques for measuring soil CO 2 efflux. Agric For Meteorol. doi: 10.1016/j.agrformet.2003.12.001

R Core Team (2015) R: A language and environment for statistical computing. R Foundation for Statistical Computing. Vienna, Austria

Raich JW, Potter CS (1995) Global patterns of carbon dioxide emissions from soils. Global Biogeochem Cycles 9:23–36

Rice AL, Butenhoff CL, Shearer MJ, et al (2010) Emissions of anaerobically produced methane by trees. Geophys Res Lett 37:1–6. doi: 10.1029/2009GL041565

Rodhe H (1990) A comparison of the contribution of various gases to the greenhouse effect. Science (80-) 248:1217–9. doi: 10.1126/science.248.4960.1217

Russell MB, Woodall CW, Fraver S, et al (2014) Residence Times and Decay Rates of Downed Woody Debris Biomass/Carbon in Eastern US Forests. Ecosystems 17:765–777. doi: 10.1007/s10021-014-9757-5

Ryan MG, Cavaleri MA, Almeida AC, et al (2009) Wood CO_2 efflux and foliar respiration for Eucalyptus in Hawaii and Brazil. Tree Physiol. doi: 10.1093/treephys/tpp059

Scheffer TC (1966) Natural Resistance of Wood to Microbial Deterioration. Annu Rev Phytopathol 4:147–168. doi: 10.1146/annurev.py.04.090166.001051

Smith KA, Dobbie KE, Ball BC, et al (2000) Oxidation of atmospheric methane in Northern European soils, comparison with other ecosystems, and uncertainties in the global terrestrial sink. Glob Chang Biol. doi: 10.1046/j.1365-2486.2000.00356.x

Steudler PA, Bowden RD, Melillo JM, Aber JD (1989) Influence of nitrogen fertilization on methane uptake in temperate forest soils. Nature 341:314–316. doi: 10.1038/341314a0

Tarvainen L, Räntfors M, Wallin G (2014) Vertical gradients and seasonal variation in stem CO_2 efflux within a Norway spruce stand. Tree Physiol 34:488–502. doi: 10.1093/treephys/tpu036

Terazawa K, Ishizuka S, Sakata T, et al (2007) Methane emissions from stems of Fraxinus mandshurica var. japonica trees in a floodplain forest. Soil Biol Biochem 39:2689–2692. doi: 10.1016/j.soilbio.2007.05.013

Terazawa K, Yamada K, Ohno Y, et al (2015) Spatial and temporal variability in methane emissions from tree stems of Fraxinus mandshurica in a cool-temperate floodplain forest. Biogeochemistry. doi: 10.1007/s10533-015-0070-y

Teskey RO, Saveyn A, Steppe K, McGuire MA (2008) Origin, fate and significance of CO_2 in tree stems. New Phytol 177:17–32. doi: 10.1111/j.1469-8137.2007.02286.x

Vigano I, van Weelden H, Holzinger R, et al (2008) Effect of UV radiation and temperature on the emission of methane from plant biomass and structural components. Biogeosciences 5:. doi: 10.5194/bgd-5-243-2008

Muggeo VMR (2008) segmented: an R Package to Fit Regression Models with Broken-Line Relationships. R News 8:1,20-25

Wang ZP, Gu Q, Deng FD, et al (2016) Methane emissions from the trunks of living trees on upland soils. New Phytol. doi: 10.1111/nph.13909

Webster KL, Creed IF, Bourbonnière RA, Beall FD (2008) Controls on the heterogeneity of soil respiration in a tolerant hardwood forest. J Geophys Res Biogeosciences. doi: 10.1029/2008JG000706

Zeikus JG, Ward JC (1974) Methane Formation in Living Trees: A Microbial Origin. Science (80-) 184:1181–1183. doi: 10.1177/0094582X07308119

Chapter 4

TRANSITIONAL SLOPES ACT AS HOTSPOTS OF BOTH SOIL CO_2 EMISSION AND CH_4 UPTAKE IN A TEMPERATE FOREST LANDSCAPE

As published in Biogeochemistry, 2018. DOI: 10.1007/s10533-018-0435-0

Daniel L. Warner[1], Rodrigo Vargas[1], Angelia Seyfferth[1], and Shreeram Inamdar[1*]

[1]Department of Plant and Soil Sciences, University of Delaware, Newark, Delaware, USA

Abstract

Forest soils are an important component of CO_2 and CH_4 fluxes at the global scale, but the magnitude of these fluxes varies greatly in space and time within a landscape. Understanding the spatial and temporal distributions of these fluxes across complex landscapes remains a major challenge for researchers and land managers alike. We investigated the spatiotemporal variability of soil-atmosphere CO_2 and CH_4 fluxes and the relationships of these fluxes to chemical and physical soil properties distributed across a topographically-heterogeneous landscape. Soil CO_2 and CH_4 fluxes were measured along with soil temperature, moisture, bulk density, texture, carbon, sorption capacity, and dissolved organic matter quality over two years along hillslope transects spanning valley bottom, transition zone, and upland landscape positions in a temperate forest watershed. Transition zone soil CO_2 efflux was 54 – 160% higher than low-lying valley bottoms, and 15-54% higher than uplands. Net seasonal CH_4 uptake was 58 –

150% higher in transition zone soils than in uplands, while valley bottoms were occasionally large net sources (up to 19 nmol CH_4 m^{-2} s^{-1}). Soil CO_2 efflux and net CH_4 uptake were both positively associated with seasonal temperature, and were highest in soils with relatively high carbon and clay content, and relatively low bulk density, moisture, and sorption capacity. We concluded that: 1) transition zone soils act as landscape hotspots for net CH_4 uptake in addition to CO_2 efflux, and 2) that this spatial distribution is more consistent across seasons for net CH_4 uptake than for CO_2 efflux.

Keywords: landscape, carbon dioxide, methane, flux, forest, soils

4.1 Introduction

At the global scale, forests are known to store large quantities of carbon and generally act as net sinks of atmospheric CO_2 (Pan et al. 2011). However, a large portion of the CO_2 taken up by forest canopies is offset by emissions from below-canopy carbon stored in soils and other carbon pools (Raich and Potter 1995; Gough et al. 2007; Warner et al. 2017). Although upland forest soils generally act as net sinks of CH_4, forested wetland soils may act as large net sources of CH_4 (Ambus and Christensen 1995; Boeckx et al. 1997; Smith et al. 2000). Temperate forest soils are estimated to store roughly 95 to 300 Mg C ha^{-1} (Dixon et al. 1994; Pregitzer and Euskirchen 2004), and relatively small disturbances to these soils may have major impacts on net ecosystem CO_2 and CH_4 fluxes (Harmon et al. 2011).

Soil CO_2 and CH_4 fluxes can vary widely across space and time due to spatial and temporal variability of soil properties and vegetation processes (Brumme and Borken 1999; Leon et al. 2014), which in turn vary with different land uses, dominant vegetation cover, and landscape positions (Ball 2013; Creed et al. 2013; Atkins et al. 2014; Gomez et al. 2017). Consequently, estimating soil CO_2 and CH_4 fluxes in heterogeneous landscapes remains a challenge for scientists and policy makers attempting to manage and account for local to global carbon budgets (King et al. 2015; Tonitto et al. 2016). Understanding the relationships between the spatial and temporal variability of soil properties and soil-atmosphere greenhouse gas fluxes may help researchers improve and evaluate these estimates.

Topography is a critical determinant of the spatial distributions of many soil properties, as it regulates the lateral transport and deposition of water, solutes, and soil particles across a landscape (Ceddia et al. 2009). If other soil forming factors are held relatively constant, that is, in localized areas with homogeneous bedrock, climate, and relatively evenly distributed vegetation, then topography should theoretically be a dominant control of spatially-distributed soil properties. Indeed, soil moisture content, carbon content, Fe and Al mineral content, bulk density, and clay content have been found to vary across landscape positions in different temperate ecosystem types around the world (Hishi et al. 2004; Yoo et al. 2006; Webster et al. 2008b; Wei et al. 2008; Creed et al. 2013; Yuan et al. 2013; Lecki and Creed 2016). Spatial variability of soil moisture is a known driver of spatial patterns of soil-atmosphere CO_2 and CH_4 fluxes across temperate forested landscapes. In non-water limited systems, poorly-drained forest soils often act as relatively small CO_2 sources and may be net sources of CH_4 due to the development of reducing conditions in the soil (Ambus and Christensen 1995; Davidson et al. 1998; Del Grosso et al. 2000; Le Mer and Roger 2001). Conversely, well-drained forest soils in these systems tend to act as relatively large sources of CO_2 and net sinks of CH_4 due to greater gaseous exchange between the soils and atmosphere, though both fluxes may approach zero in extremely dry conditions (Ambus and Christensen 1995; Davidson et al. 1998; Del Grosso et al. 2000). Soil texture and structure also influence spatial distributions of fluxes, since aerobic microbial processes such as aerobic respiration and methane oxidation may be limited by reduced gas exchange with the atmosphere in dense or clay-rich soils (Ball et al. 1997; Schjønning et al. 1999; Guckland

et al. 2009; Ball 2013; Shi et al. 2016). Spatial variability of the soil carbon content and potential sorption capacity (derived from Fe and Al-hydroxide content) have shown to have positive and negative relationships with soil CO_2 efflux, respectively (Lecki and Creed 2016). Furthermore, it has been suggested that accumulations of soil dissolved organic matter (DOM) create hotspots of CO_2 emission along transitional hillslopes between uplands and lowlands in forested landscapes (Creed et al. 2013). Comparatively little is known about spatial distributions of net soil CH_4 fluxes across hillslope gradients and the relationships of these fluxes to chemical and physical soil properties. Furthermore, although the quantity of organic matter has been positively linked to soil CO_2 efflux (Creed et al. 2013), there is a lack of research on how the chemical quality of organic matter relates to soil-atmosphere greenhouse gas fluxes, especially from *in situ* studies across topographic gradients.

Temperature, precipitation, and plant phenology (i.e., litterfall, root respiration) exhibit distinct seasonal patterns in temperate forests that may also influence seasonal patterns of soil-atmosphere CO_2 and CH_4 fluxes (Lloyd and Taylor 1994; Mosier et al. 1996; Vargas and Allen 2008; Kirschbaum 2013; Yvon-Durocher et al. 2014). Consequently, CO_2 and CH_4 fluxes vary across both landscape positions and seasons, and the strength of sources and sinks at different landscape positions may vary significantly in space due to seasonally-fluctuating temperature, moisture content, substrate availability, and vegetation activity (Mosier et al. 1996; Pacific et al. 2008; Kirschbaum 2013; Wang et al. 2013). However, measuring soil-atmosphere CO_2 and CH_4 fluxes in topographically-heterogeneous landscapes is logistically difficult (Gomez et al. 2017), and there is a scarcity of literature examining the spatial and seasonal relationships

between multiple greenhouse gas fluxes and soil properties across heterogeneous landscapes.

This study investigates the spatiotemporal variability of soil-atmosphere CO_2 and CH_4 fluxes and their relationships to various soil properties across landscape positions and seasons. We measured fluxes twice monthly for over two years at upland, transition zone, and valley bottom locations along hillslope transects. Spatial distributions of various soil properties were also measured along these transects. Our primary research questions were: (1) How do soil-atmosphere CO_2 and CH_4 fluxes vary across landscape positions? (2) How are soil-atmosphere CO_2 and CH_4 fluxes related to spatially and temporally-distributed soil properties across the landscape and seasons? (3) Does the spatial hierarchy of fluxes across the landscape (i.e. order of highest to lowest fluxes by landscape position) vary across seasons?

4.2 Methods

Study Site

This study was conducted in a 12 hectare forested headwater watershed in the Piedmont region of Cecil County, Maryland, USA (39° 42’ N, 75° 50’ W). The forest is primarily beech (*F. grandifolia*), poplar (*L. tulipifera*), and oak (*Q. spp*). This vegetation is evenly distributed across the landscape, with an estimated mean stem basal area (± 1 S.D.) of 52 ± 7 m^2 ha^{-1} based a series of plot surveys of valley bottom, transitional slope, and upland habitat structure (Warner and Dougherty, unpublished data). The understory is sparse, except in valley bottom areas where scattered growths of skunk cabbage (*S. foetidus)* are common during the growing season. The watershed is topographically heterogeneous, with slopes ranging from 0.1 to 25%, and mean a slope of 6.3%. Soils

within the study area are coarse-loamy, mixed, mesic Lithic Dystrucepts belonging to the Manor, Galla, and Glenelg series loams which overlay peltic gneiss and schist bedrock (Anderson and Matthews 1973), and have a slightly acidic pH between 5 and 6 (NRCS, 2018). Mean annual precipitation over the past 10 years is 1231 mm with little annual snowfall (DEOS 2017). Annual mean temperature is 12 ^{o}C, reaching a mean annual maximum of 25 ^{o}C in summer, and a mean annual minimum of -0.6 ^{o}C in winter (DEOS 2017).

Sampling locations across hillslope transects

To examine the effects of landscape position on gas fluxes and soil properties, we distributed 20 sampling locations between 4 hillslope transects. Locations were classified as upland (UL: flat or gentle slopes, high elevation), transition zone (TZ: steep slopes), or valley bottom (VB: flat or gentle slopes, low elevation) based on their slope angle and visual surveys of the study site (Fig 4.1). Specifically, the lowest and highest points on each transect were classified as valley bottom and upland, respectively. Moving upslope from the valley bottom, if a sampling location had greater than a 10% (1 S.D. above watershed mean) slope gradient, it was classified as transition zone. If the next location had less a 10% gradient, it was classified as upland. On one transect, two locations were classified as valley bottoms due to a minimal increase in elevation between them (Fig 4.1). The transect design allowed all locations to be sampled within a 4 hour mid-day window (11:00 to 15:00) on sampling dates. On each sampling date, a starting location was randomly chosen to avoid introducing systematic bias resulting from always sampling the same locations in the same order. Flux collars were placed at least 2 meters

away from the nearest tree stem with the hope of reducing potential confounding effects of proximity to dense root clusters.

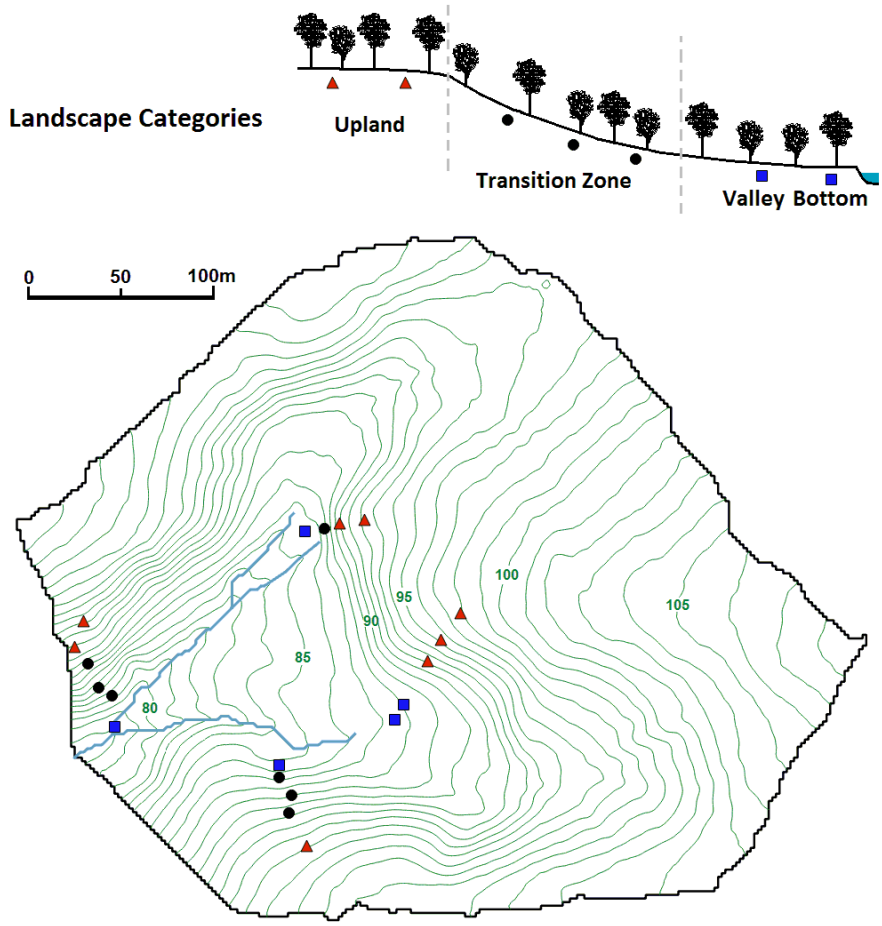

Figure 4.1 Map of study watershed in northeastern Maryland, USA. Sampling points are depicted along 4 hillslope transects, and are classified as valley bottom (VB, blue squares), transition zone (TZ, black dots), and upland (UL, red triangles) by color and shape.

Gas fluxes, soil moisture, and soil temperature

At each location, 2 mm thick PVC collars with a 10 cm internal diameter were inserted 5 cm into the soil, leaving the remaining 3 cm exposed. CO_2 and CH_4 concentrations were measured with an Ultra-Portable Greenhouse Gas Analyzer (Los Gatos Research, Mountain View, California, USA) connected to a 10 cm diameter closed-system chamber as described previously for the study site (Warner et al. 2017, see

Supplementary Materials). Quality assurance and quality controlled protocols to calculate CO_2 efflux and net CH_4 fluxes followed a standardize protocol for the study site (Warner et al. 2017, see Supplementary Materials).

Soil temperature and volumetric water content (VWC) were measured from 0 to 4 cm depth along with each flux measurement (WET Sensor, Delta-T Devices, Cambridge, UK). Gas flux, VWC, and temperature measurements were taken 1-2 times monthly from September 2014 to November 2016, with extra measurements taken immediately after large precipitation events or during drought conditions to capture a broad range of hydrologic conditions experienced by soils in the watershed. This ultimately yielded a dataset of 880 flux, temperature, and soil moisture measurements. These data were grouped by season as winter (Jan 1-Feb 28), spring (Mar 1-May 20), early summer (May 20-Jul 31), late summer (Aug 1-Sep 30), and fall (Oct 1-Dec 31) based on site-specific seasonal changes in temperature and precipitation. January and February are generally the coldest months in this area with gradually increasing temperatures from March to mid-May. The period from late May through July is typically hot (daily mean temperatures > 20 ^{o}C) and rainy, with patches of *S. foetidus* forming in the valley bottoms that persist until fall. Summer was divided in early and late portions due to droughts occurring in August and September during both measurement years, resulting in a decline of soil moisture, but not temperature, between the two seasons. From October through December is a period of gradual temperature decline and increasing precipitation, with most litterfall occurring in mid-November.

Soil porewater carbon and water-extractable carbon

To examine the influence of soil dissolved organic matter (DOM) quality on soil-atmosphere CO_2 and CH_4 fluxes, we installed and collected monthly samples from ceramic cup tension lysimeters (1900-series, Soilmoisture Equipment Corp., Santa Barbara, California, USA) buried 15 cm in the soil at all sampling locations. Porewater samples were collected every two months from October 2014 to June 2015, and monthly from August 2015 to November 2016, except during very dry periods when many upland and transition zone sites yielded no samples (see Supplementary Materials). In addition to DOM in soil porewater, we examined the quality of potentially mobilized soil DOM using water extractions. Soil cores for water-extractable DOM samples (DOM_{ex}) were collected from 0-15 cm in triplicate at each site (<1 m from flux ring). DOM from homogenized soil cores was extracted following the protocol provided in the Supplementary Materials. DOM_{ex} samples were collected during spring, summer, and fall from spring 2015 to fall 2016. All samples were filtered through 0.7 µm glass fiber filters and stored at 4 ^{o}C prior to analysis.

Optical DOM properties were analyzed on a HORIBA Aqualog® fluorescence spectrophotometer (Edison, New Jersey, USA). All samples for optical DOM characterization were diluted until absorbance at 254 nm was below 0.2 prior to analysis to reduce inner-filter effects (Ohno 2002). Absorbance spectra were measured from 240-550 nm, and fluorescence emission spectra were measured from 300-550 nm across an excitation range of 240-500 nm to produce excitation-emission matrices (EEMs) of fluorescence intensity across these wavelength ranges. Data processing and corrections were performed in MATLAB 2013b (MathWorks 2013) to produce a set of well-known

optical DOM quality metrics (Ohno 2002; Weishaar et al. 2003; Huguet et al. 2009; see Supplemental Materials). Additionally, DOM_{pw} and DOM_{ex} EEMs were used to generate a 7-component PARAFAC model following published protocols and validation techniques (Murphy and others 2013). The excitation-emission peaks for components identified in our PARAFAC model were compared to previously published models (Fellman et al. 2010) to qualitatively describe them (e.g. protein- or humic-like fluorescence; Supplemental Table 1). Overall DOM_{pw} and DOM_{ex} quality was estimated based on the first principal component of these optical metrics and fluorescent components, which significantly separated qualitative metrics and fluorescent components generally associated with high or low DOM bioavailability (Kalbitz et al. 2003; Fellman et al. 2009). Thus, this principal component served as an indicator of relative chemical DOM quality (from here on referred to as DOM_Q), with more positive values indicating characteristics of relatively bioavailable DOM (high protein-like fluorescence, low aromaticity and humification, referred to as "high quality"), and more negative values indicating characteristics of relatively less bioavailable DOM (high humic-like fluorescence, high aromaticity and humification indices, referred to as "low quality"). Due to the limited temporal frequency of DOM quality sample collection, DOM samples were grouped for winter and spring, early and late summer, and fall (3 seasonal means per year).

Bulk soil carbon

Bulk soil samples were analyzed for total carbon (TC). Samples were collected in triplicate from the A-horizon using a hand soil corer (for soils). All samples were dried at 60 ^{o}C until a stable mass was reached, sieved at 2 mm, and ground prior to analysis. TC

content was analyzed with a CN Elemental Analyzer (Carlo Erba, Lakewood, New Jersey, USA).

Soil texture, bulk density, and percent water-filled pore space

Soil texture was determined via a hydrometer method (Bouyoucos 1962) to identify the relative abundance of silt, sand, and clay soil particles (see Supplementary Materials). Bulk density (BD) was determined by the mean mass of three soil cores of known volume collected from the A-horizon at each site. Water-filled pore space of the A-horizon (WFPS) was calculated based on the VWC at 4 cm divided by the porosity as determined by A-horizon bulk density (BD) relative to that of solid quartz (2.65 g cm^{-3}; see Supplementary Materials).

Oxalate-extractable Al and Fe

The abundance of common carbon-stabilizing minerals, poorly-crystalline Al and Fe, was measured using ammonium oxalate extractions in the dark (McKeague and Day 1966). Extracts were analyzed for Fe and Al content using a Thermo Scientific Iris Intrepid II ICP-AES within 24 of extraction. Samples were carefully handled to avoid photodegradation during extraction and prior to analysis (see Supplementary Materials). Extracted Fe and Al were used to estimate potential sorption capacity (SC) of the soil (Creed et al. 2013). Molar concentrations of oxalate-extractable Fe and Al per gram of soil were multiplied by bulk density and divided by core depth, yielding an estimate of soil sorption capacity in units of moles Fe and Al per square meter.

Analytical approach

Principal components analysis was used to examine the associations of soil properties and fluxes across hillslopes and seasons. Comparisons of means were made using analyses of variance (ANOVA) and Kruskal-Wallis tests where assumptions of ANOVA were violated. All comparisons of means and regressions were considered significant if $p < 0.05$ unless otherwise noted, and full tables of p-values from post hoc pair-wise comparisons tests can be found in Supplementary Materials. All statistical analyses were performed in R (R Core Team 2017).

4.3 Results

Variability of soil temperature and moisture across seasons and hillslopes

Soil temperature varied significantly across seasons, but only varied significantly across hillslope transects during early summer, when the mean temperature of valley bottoms was approximately 1 ^{o}C lower than other positions (Fig 4.2a). Temperature did not vary significantly between early and late summer (21.0 ± 2.3 and 21.1 ± 2.0 ^{o}C, respectively) nor between spring and fall (12.6 ± 3.8 and 13.9 ± 3.1 ^{o}C, respectively), with the exception of valley bottoms which were slightly warmer in fall than in spring. Winter temperatures were lower than all other seasons, averaging 3.8 ± 2.0 ^{o}C, respectively (Fig 4.2a). In all seasons, WFPS was not significantly different between upland and transition zone sites, while WFPS in valley bottoms remained roughly 2-3 times higher than the other positions. WFPS was highest in winter and spring at all landscape positions. Uplands and transition zones had intermediate WFPS in early summer and fall and were significantly drier during late summer, while valley bottom WFPS did not vary significantly between early summer, late summer, and fall (Fig 4.2b).

Soil-atmosphere CO_2 and CH_4 fluxes

CO_2 emissions from transition zone soils were significantly higher than other landscape positions across all seasons except spring, when transition zone and upland CO_2 efflux was similar (Fig 4.2c). The highest seasonal mean mid-day CO_2 emissions occurred in transition zones during early summer, with a mean midday flux (± 1 S.D.) of 4.2 ± 1.7 µmol CO_2 m^{-2} s^{-1}, compared to 1.7 ± 1.1 and 3.5 ± 1.7 µmol CO_2 m^{-2} s^{-1} from valley bottom and upland sites in the same season, respectively. The lowest CO_2 efflux from uplands, transition zones, and valley bottoms occurred in winter, with a seasonal mean mid-day flux of 0.26 ± 0.09, 0.40 ± 0.15, and 0.26 ± 0.09 µmol CO_2 m^{-2} s^{-1}, respectively (Fig 4.2c).

The largest seasonal mean mid-day net CH_4 emissions occurred in valley bottoms in early summer, averaging 1.0 ± 3.6 (with a maximum of 19.0) nmol CH_4 m^{-2} s^{-1}, however net CH_4 fluxes remained near-zero during all other seasons in the valley bottoms (Fig 4.2d). Uplands and transition zone soils were net CH_4 sinks in all seasons. Net CH_4 uptake was relatively larger in transition zones than in uplands across almost all seasons (excluding early summer), reaching a maximum mid-day mean uptake of -2.0 ± 0.6 nmol CH_4 m^{-2} s^{-1} in late summer, compared to -1.1 ± 0.5 nmol CH_4 m^{-2} s^{-1} in upland sites (Fig 4.2d). Net CH_4 fluxes were smallest in winter and spring, with no significant differences between these seasons. Average winter CH_4 fluxes were -0.18 ± 0.06, -0.45 ± 0.14, and 0.02 ± 0.06 nmol CH_4 m^{-2} s^{-1} from upland, transition zone, and valley bottom soils, respectively.

Mean midday fluxes of CO_2 and CH_4 were negatively correlated across all seasons (Table 3), with the strongest such correlation in late summer ($p < 0.01$, $r = -0.67$) and weakest in winter ($p < 0.01$, $r = -0.59$). Patterns of the relative magnitudes of CO_2 efflux at different hillslope positions (which position had highest, medium, and lowest fluxes) were not consistent across all seasons, and a clear spatial hierarchy of significantly different CO_2 efflux from transition zones > uplands > valley bottoms was only observed in early and late summer (Fig 4.2c). Patterns of seasonal mean CH_4 fluxes across hillslope positions were more consistent, with net uptake in transition zones > uplands > valley bottoms in all seasons except early summer (Fig 4.2d).

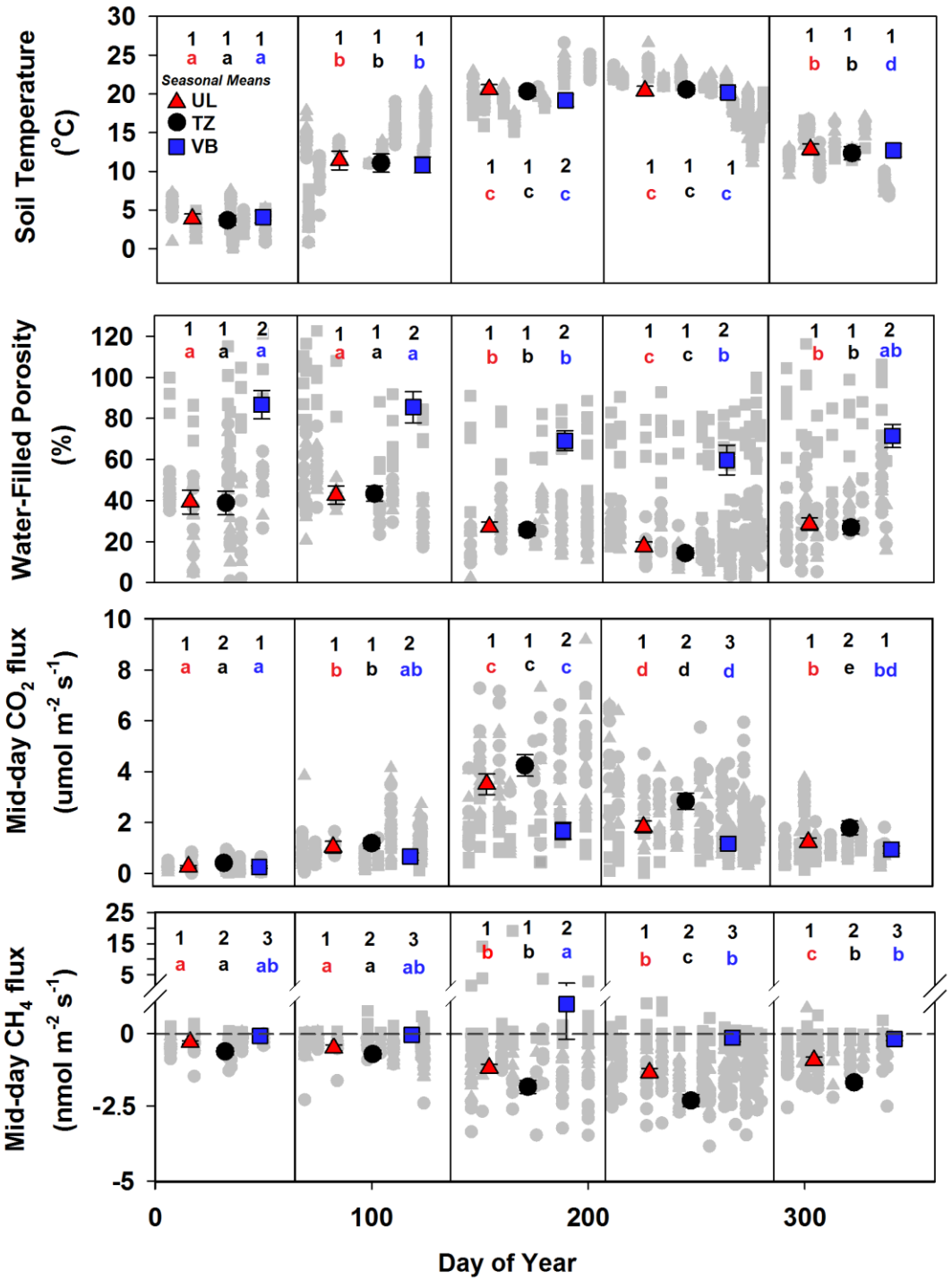

Figure 4.2 Annual and seasonal patterns of soil temperature (a), water-filled pore space (b), mid-day CO_2 efflux (c), and mid-day net CH_4 flux (d). Seasonal means for each landscape position overlay individual measurements, and are classified by color and shape (UL: upland (red triangles), TZ: transition zone (black dots), VB: valley bottom (blue squares)). Error bars represent the 95% confidence interval around the mean. Letters above seasonal means correspond to statistically significant seasonal variations within each position ($p < 0.05$), while numbers above seasonal means indicate statistically significant variations across landscape positions within each season.

Variability chemical and bulk soil properties hillslopes and seasons

Total carbon content (TC, % dry weight) was significantly greater in transition zones than in valley bottoms, while upland TC was intermediate (Table 4.1). Oxalate-extractable Fe, but not Al, was significantly greater in valley bottoms than in uplands. Furthermore, our estimate of soil sorption capacity was significantly higher in valley bottoms than in transition zones and uplands (Table 4.1).

Table 4.1 Summary of bulk soil properties across landscape positions. Mean (± 1 S.D.) values are reported, and superscript numbers indicate significant differences between landscape positions.

Landscape Position	Bulk Density ($g\ cm^{-3}$)	Total Carbon (% mass)	Sorption Capacity ($mol\ m^{-2}$)	Clay Content (% mass)
Uplands	0.76 ± 0.20 [1,2]	5.2 ± 2.8 [1,2]	12.4 ± 3.8 [1]	16.4 ± 6.4 [1]
Transition Zones	0.67 ± 0.18 [1]	7.5 ± 3.6 [1]	15.1 ± 5.1 [1]	25.3 ± 7.6 [2]
Valley Bottoms	0.99 ± 0.12 [2]	3.3 ± 0.9 [2]	21.5 ± 3.0 [2]	14.6 ± 3.7 [1]

Porewater and water-extractable DOM varied significantly in relative quality across and within landscape positions and seasons. Porewater DOM was significantly higher in quality (i.e., low aromaticity and exhibiting greater protein-like fluorescence) in valley bottoms than transition zones in spring and summer and uplands in summer. Though porewater DOM in transition zones and uplands was generally lower quality than valley bottoms, DOM quality at these positions increased in fall, and porewater DOM quality did not vary significantly between landscape positions during this season (Table 4.2). Water-extractable DOM quality only showed significant differences between positions in spring, when DOM quality was significantly higher in valley bottom soil extracts than in transition zone extracts. All positions had significantly higher quality extracted DOM in summer than in other seasons, and the lowest quality DOM was extracted in spring (Table 4.2).

Table 4.2 Summary of porewater and water-extractable DOM quality across landscape positions and seasons. Superscript numbers indicate significant differences ($p < 0.05$) between landscape positions for each season. Superscript letters indicate significant differences between seasons for each landscape position. *Values indicate mean (± 1 S.D.) loadings on primary principal component extracted from a set of DOM quality indices and metrics. Higher values correspond to lower aromaticity, molecular weight, and higher protein-like fluorescence. Lower values correspond to higher aromaticity, molecular weight, and humic-like fluorescence.

	Porewater DOM Quality*			**Water-extractable DOM Quality***		
Landscape Position	**Winter/ Spring**	**Summer**	**Fall**	**Winter/ Spring**	**Summer**	**Fall**
Uplands	-0.7 ± 0.5 $^{(1)a}$	-0.1 ± 1.2 $^{(1)ab}$	0.6 ± 1.4 $^{(1)b}$	-1.7 ± 1.4 $^{(1,2)a}$	1.6 ± 0.9 $^{(1)b}$	0.1 ± 0.9 $^{(1)ab}$
Transition Zones	-2.5 ± 1.0 $^{(2)a}$	-0.6 ± 0.7 $^{(1)b}$	0.4 ± 2.2 $^{(1)b}$	-2.3 ± 0.7 $^{(1)a}$	0.5 ± 1.4 $^{(1)b}$	0.0 ± 1.0 $^{(1)b}$
Valley Bottoms	1.0 ± 1.5 $^{(1)a}$	1.8 ± 1.3 $^{(2)a}$	1.3 ± 1.3 $^{(1)a}$	-0.3 ± 0.7 $^{(2)a}$	2.3 ± 1.1 $^{(1)b}$	1.0 ± 1.4 $^{(1)b}$

Transition zones had significantly higher clay content than both uplands and valley bottoms (26 ± 8 compared to 17 ± 6 and 15 ± 4%, respectively, Table 4.1), and lower A-horizon bulk density than valley bottoms (0.61 ± 0.13 compared to 0.99 ± 0.13 g cm^{-3}, respectively). Bulk density values from uplands fell within this range, and were not statistically different from the other two landscape positions (Table 4.1). Sand and silt content did not vary significantly across landscape positions.

Relationships of soil properties and soil fluxes across hillslopes and seasons

Table 4.3 indicates significant correlations between seasonal mean soil fluxes and soil properties at each sampling location. The first principal component (PC1) extracted from measured soil properties and fluxes explained 40.6% of total variability between sampling locations and seasons. In general, the static and more spatially-distributed soil properties loaded most strongly on PC1, as did seasonal mean net CH_4 uptake (Fig 4.3). Bulk density (BD), WFPS, and sorption capacity (SC) loaded negatively on PC1, while clay content, total carbon content (TC), and net CH_4 uptake loaded positively. Principal component 1 loadings varied significantly among landscape positions, with valley bottoms loading the lowest and transition zones loading significantly higher on PC1. Upland locations spanned the range in between the other two positions along PC1. There

was no significant seasonal variation in PC1 loadings across all landscape positions. Principle component 2 explained an additional 25.8% of the total variability between sampling locations and seasons. In general, the more temporally-distributed soil properties loaded strongest on this axis. Temperature and water-extractable DOM quality (DOM_{Qex}) loaded highest on PC2, while porewater DOM quality (DOM_{Qpw}) and seasonal mean CO_2 efflux loaded slightly higher onto PC2 than PC1 (Fig 4.3). Loadings on PC2 varied significantly across every season except early and late summer, but PC2 loadings only varied significantly between landscape positions in winter, when transition zones loaded significantly lower than valley bottoms.

Table 4.3 Correlation matrix (Pearson) of mean mid-day CO_2 and CH_4 fluxes and soil properties during winter, spring, early summer, late summer, and fall. Values indicate a significant correlation ($p < 0.05$), dashes indicate insignificant relationships.

	Winter		Spring		Early Summer		Late Summer		Fall	
	CO_2	CH_4	CO_2	CH_4	CO_2	CH_4	CO_2	CH_4	CO_2	CH_4
CH_4	-0.59	-	-0.62	-	-0.63	-	-0.67	-	-0.64	-
WFPS	-	0.66	-0.51	0.69	-0.74	0.88	-0.56	0.84	-0.60	0.77
TC	-	-0.56	-	-	-	-	0.74	-0.57	0.71	-0.65
BD	-0.48	0.64	-0.49	0.47	-0.56	0.53	-0.75	0.70	-0.71	0.70
% Clay	0.46	-0.61	-	-0.68	-	-0.52	-	-0.57	-	-0.61
DOM_{Qpw}	-	0.78	-	0.60	-0.52	0.57	-0.47	0.56	-	-
DOM_{Qex}	-	0.58	-0.59	0.45	-	-	-0.59	0.50	-0.50	0.52
SC	-0.52	0.49	-0.50	0.52	-0.64	0.56	-	0.61	-	0.58

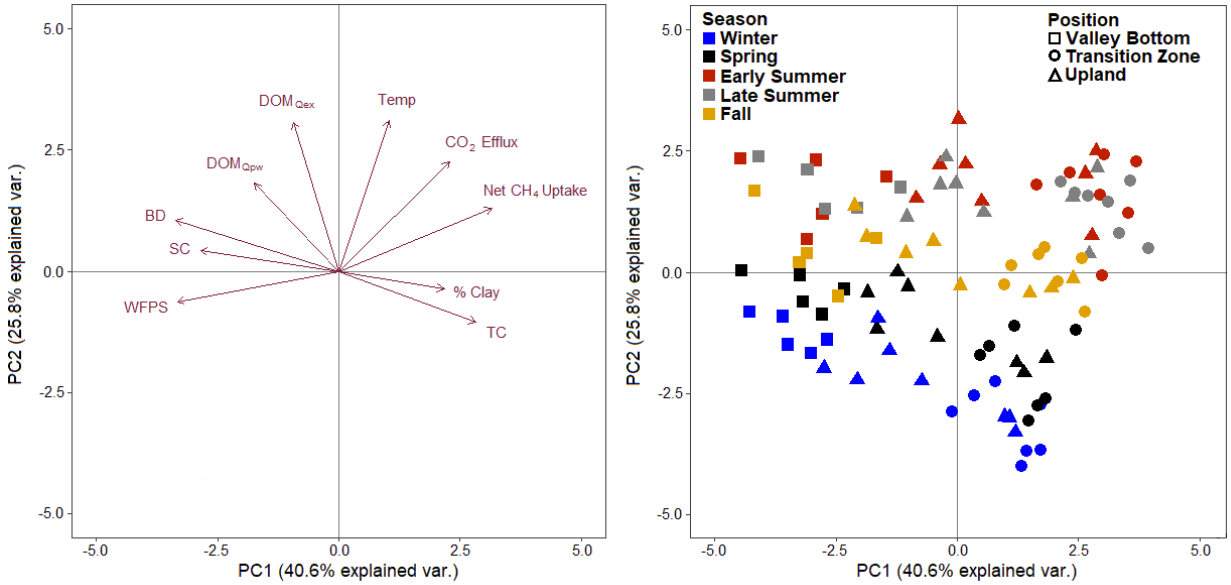

Figure 4.3 Variable rotations for principal components analysis performed on an array of soil properties found at the study sites each season (left), and loadings for each sample location in each season (right). Landscape positions are denoted by point shapes and seasons are denoted by colors. PCA plots were created using the "ggbiplot" package in R (Vu, V. 2012).

4.4 Discussion

Spatial variability of soil-atmosphere CO_2 and CH_4 fluxes

We found significant differences in the magnitudes of both CO_2 efflux and net CH_4 flux across different landscape positions in every season (Fig 4.2cd), though the ranges of fluxes across all sampling locations fell within ranges observed in other temperate forests (Crill 1991; Smith et al. 2000; Hibbard et al. 2005). Transition zone CO_2 efflux was significantly higher than that of valley bottoms in all seasons and was significantly higher than that of uplands in all seasons except spring and early summer. This observation is supported by previous research that has found soils along transitional slopes to act as landscape "hotspots" of CO_2 emission (Creed et al. 2013), with the highest effluxes occuring in summer (Webster et al. 2008). Transition zone and upland

soils both acted as net CH_4 sinks in all seasons, but transition zone soils had significantly higher net CH_4 uptake than uplands and all but one season. Valley bottoms had near-zero net CH_4 flux in all seasons except early summer, when brief periods of high CH_4 efflux were observed. It is known that wet, low-lying areas may have brief periods of high net CH_4 emissions (Pearson et al. 2016) while higher landscape positions remain net sinks (Wang et al. 2013), but the significantly higher net CH_4 uptake of sloping transition zones than that of uplands has not been widely observed or discussed in published literature. These observations suggest that sloping transition zones may function as landscape "hotspots" for net CH_4 uptake in addition to CO_2 emission in topographically-heterogeneous temperate forests.

Relationships between fluxes and soil properties

The position of CO_2 efflux in our principal components analysis suggested high rates of CO_2 efflux during warm seasons with relatively higher water-extractable DOM quality, with the highest effluxes occurring in soils with relatively high carbon and clay content and relatively low bulk density, sorption capacity, and soil moisture (Fig 4.3). The position of net CH_4 uptake on these components was similar to the position of CO_2 efflux, however net CH_4 uptake had a stronger positive association with the spatially-distributed soil properties on PC1 and a comparatively weak positive association with temperature and water-extractable DOM quality on PC2 (Fig 4.3). This positioning suggests high rates of net CH_4 uptake in soils with high rates of CO_2 efflux, but with a weaker association to seasonal temperature variability and DOM quality.

The spatial and temporal relationships of CO_2 efflux and other soil properties that we observed generally followed established patterns. It is well-established that soil CO_2 efflux is relatively low during cold seasons and in wet, dense soils (Davidson et al. 1998; Schjønning et al. 1999). Furthermore, disproportionately high CO_2 effluxes in transition zones relative to other landscape positions has been attributed to the tendency of these topographic features to accumulate organic carbon over time (Webster et al. 2008; Creed et al. 2013). Our sampling locations with high CO_2 efflux had low sorption capacity by Fe and Al minerals, but also a relatively larger clay size fraction in the soil. Although soil carbon may be stabilized by silicate clay minerals in this size fraction (Kleber et al. 2007), the low Fe and Al sorption capacity and correspondingly high CO_2 efflux of these soils is in agreement with previous observations in temperate forests (Lecki and Creed 2016).

The relationships between our DOM quality metrics and soil CO_2 fluxes were less clear. In laboratory incubations, the chemical quality of DOM has been demonstrated to have significant effects on mineralization rates by microorganisms, with more complex, aromatic, and humic-like organic matter having relatively low rates of mineralization (Kalbitz et al. 2003; Fellman et al. 2009). However, recent research has called into question the importance of chemical DOM structure relative to localized biogeochemical conditions, suggesting that organic matter stabilization, redox conditions, and microbial community composition may be more influential on organic carbon mineralization across heterogeneous soils than chemical characteristics (Kleber 2010; Schmidt et al. 2011). Although we observed a general increase in DOM quality, temperature, and soil CO_2 efflux from spring into summer, the spatial distribution of “high quality” DOM (low

aromaticity and high protein-like fluorescence) favored soils typical of valley bottoms, which are relatively wetter and denser with low total carbon content and high sorption capacity (Fig 4.3). These soils had comparatively low CO_2 efflux during warm seasons, suggesting that soils with high carbon, low moisture, and low sorption capacity may be associated with high CO_2 efflux regardless of spatial distributions of soil DOM quality across the landscape.

Soils that were wet and dense had little to no net CH_4 uptake and were net sources of CH_4 in some cases. High net CH_4 uptake was associated with the same soil properties as those with high CO_2 efflux, although net CH_4 uptake appeared to have a weaker association to seasonal temperature changes (Fig 4.3). This spatial distribution is expected, as several studies have found wet valley bottom and riparian soils to function as net CH_4 sources while higher hillslope soils function as net sinks (Ambus and Christensen 1995; Itoh et al. 2007; Semenov et al. 2010). However, net CH_4 uptake also varied significantly between upland and transition zone soils, though bulk density and water content, which are known to influence CH_4 uptake (Ball et al. 1997; Del Grosso et al. 2000), were not significantly different between the two positions. One key difference between the two positions was the higher clay size fraction in transition zones. High clay content has been shown to decrease CH_4 uptake in some soils, as it limits diffusion of O_2 and CH_4 from the atmosphere (Boeckx et al. 1997; Guckland et al. 2009). Conversely, elevated net CH_4 uptake has been observed in other soils that contain both fine clays and coarse particles, as the clays provide surface area for methanotroph colonization and the coarse particles support gas diffusion (Saari et al. 1997). It is possible that we observed a similar effect to the latter, since soils in our study watershed contained $\geq$ 38% sand at all

sampling locations, but transition zones had significantly higher clay content (26 ± 8%) than both uplands and valley bottoms (17 ± 6 and 15 ± 4%, respectively).

Comparatively little is known about the relationships between soil DOM quality and net CH_4 fluxes in well-drained forest soils. As with CO_2 efflux, we found that high net CH_4 uptake was associated with locations with lower quality DOM pools and high carbon content (Fig 4.3). Recent research has suggested that complex, aromatic soil organic matter (such as humic-like organic acids) may inhibit CH_4 production by acting as an alternative electron acceptor (Klüpfel et al. 2014; Miller et al. 2015), thus suppressing any potential methanogenesis and increasing the net rate of CH_4 oxidation. However, it remains unclear from our observations whether the relationship between elevated CH_4 uptake and soil DOM quality is functional or simply coincidental with other soil properties.

Consistency of spatial CO_2 and CH_4 flux distributions across seasons

We found that the spatial hierarchy of the magnitudes of fluxes across landscape positions (i.e. order of highest to lowest fluxes by landscape position) varied between seasons for CO_2 efflux, but was consistent for net CH_4 fluxes in almost every season. Seasonal mean upland CO_2 efflux fluctuated between seasons, having similar magnitudes to valley bottoms in winter and fall, but similar magnitudes to transition zones in spring and early summer. Significant differences of CO_2 efflux between all three landscape positions (transition zone > upland > valley bottom) were only observed during late summer, but this same order was observed for net CH_4 uptake in all but one season (Fig 4.2cd). In this study, not only did transition zones have elevated net CH_4 uptake relative

to other landscape positions, but this effect was more consistent on a seasonal basis than it was for CO_2.

We believe that this observation may be due to differences in the temperature sensitivity of the two gas fluxes, and perhaps seasonal changes in the autotrophic component of soil CO_2 efflux. Our principal components analysis found a strong positive association among CO_2 efflux and seasonally increasing temperature and soil DOM quality, while net CH_4 uptake was more strongly associated with more spatially-distributed soil properties. Rates of CO_2 efflux are very sensitive to temperature in moist, temperate ecosystems, and temperature variability across seasons greatly exceeded temperature variability across the landscape in this study (Fig 4.2a). Recent findings in a similar temperate forest suggested that there is a strong influence of spatially-distributed soil properties and vegetation cover on soil respiration during the warm growing season, but that this influence is obscured in colder months due to temperature limitations (Atkins et al. 2014). As net CH_4 fluxes are arguably less temperature sensitive than CO_2 fluxes (Crill 1991; Ueyama et al. 2015), spatially-distributed soil properties may have a stronger and more consistent relationship to spatial patterns of these fluxes across both warm and cold seasons. It should be noted that although vegetation is generally homogeneous across this landscape, we did not separate autotrophic and heterotrophic components of soil respiration. Seasonal changes in autotrophic respiration can be quite large (Hanson et al. 2000), and may have also had a role in shifting upland soil CO_2 efflux from resembling valley bottom efflux in winter and fall to resembling transition zone efflux in spring and early summer (Fig 4.2c). Net CH_4 fluxes are only the product of microbiological processes in the soil, and should theoretically be less affected by

seasonal variations in vegetation phenology, which may also explain the more consistent hierarchy of CH_4 fluxes across seasons.

A conceptual model of spatial distributions of fluxes and soil properties

We developed a conceptual model to provide a potential explanation for the observed relationships between soil-atmosphere CO_2 and CH_4 fluxes and the measured soil properties across the landscape (Fig 4.4). Valley bottom soils lie in the watershed floodplain, and are frequently flushed during storm events, resulting in depleted soil carbon pools and loss of fine clay sediments, which may yield a coarse, dense, and low-carbon soil environment. Indeed, end member mixing analysis of stream export from this watershed has suggested that valley bottom floodplains frequently export dissolved and particulate substances, but export from the higher landscape occurs only in response to relatively rare, large storm events (Inamdar et al. 2013, 2017). Transition zone soils lie above the floodplain, and receive lateral inputs of litter, clay particles, and organic matter from uplands over time, leading to a gradual accumulation of soil carbon, clays, and other materials. Though upland soils also lie above the floodplain, they occupy the terminal position on the hillslope and thus do not receive lateral inputs of organic matter and fine particles, yielding a soil environment that is dry and well-aerated, but less enriched in organic matter and clays than the transition zones found below (Fig 4.4). This spatially-heterogeneous distribution of soil properties may at least partially explain the differences in soil-atmosphere CO_2 and CH_4 fluxes across landscape positions we observed during every season (Fig 4.2cd).

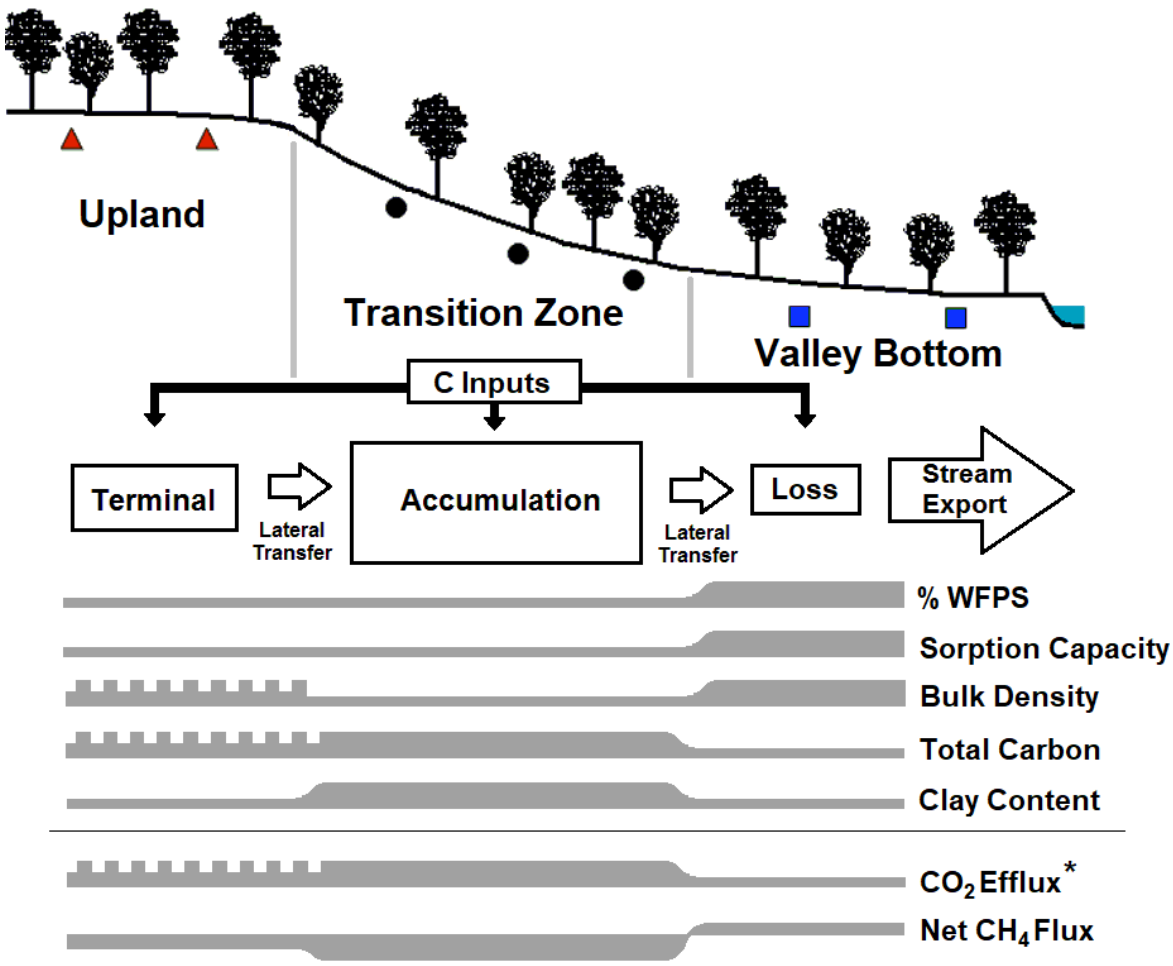

Figure 4.4 Illustration of topographic regulation of soil properties and resulting soil-atmosphere CO_2 and CH_4 fluxes. Vertical carbon inputs (litterfall and throughfall) are relatively homogeneous across landscape. Organic matter and clays are laterally transferred down the hillslope. Infrequently flushed transition zones gradually accumulate these substances, but frequently flushed valley bottoms experience a net loss. Relative thickness and direction of bands indicates relative rates of fluxes and quantities of measured soil properties. The checkered thick bands indicate a lack statistically significant differences between positions. For CO_2 efflux, the checkered thick band and * indicates the seasonal variation of CO_2 efflux from uplands, which was similar to efflux from valley bottoms in winter and fall, and similar to efflux from transition zones in spring and early summer, as described in the discussion.

4.5 Conclusions

Soil CO_2 and CH_4 fluxes varied significantly across landscape positions and seasons. Transition zone soils had the highest rates of CO_2 efflux and net CH_4 uptake across all seasons, highlighting their importance to CO_2 and CH_4 budgets at the watershed or landscape scale. High rates of CO_2 efflux and net CH_4 uptake were associated with warm temperatures in soils with relatively low water-filled pore space, bulk density, and sorption capacity and relatively high carbon and clay content. However, CO_2 efflux had a stronger association with seasonal temperatures while net CH_4 fluxes had a stronger association with spatially-distributed variables. This finding may help explain why net CH_4 fluxes appeared to have a more consistent spatial distribution across the three landscape positions in every season, while CO_2 efflux from uplands relative to the other two positions varied seasonally. Although DOM quality was investigated, its association with CO_2 and CH_4 fluxes across the landscape remains unclear. The findings of this study may facilitate the development of watershed-scale greenhouse gas flux models and strategies for managing sources and sinks of these gases in forest ecosystems.

Acknowledgements

This research was funded by the United States Department of Agriculture (USDA-AFRI Grant 2013-02758), and we would like to acknowledge the University of Delaware Soil Testing Facility, Shawn Del Percio, Catherine Winters, and Samuel Villarreal for their help in the field and laboratory.

REFERENCES

Ambus P, Christensen S (1995) Spatial and Seasonal Nitrous Oxide and Methane Fluxes in Danish Forest-, Grassland-, and Agroecosystems. J. Environ. Qual. 24:993

Anderson RH, Matthews ED (1973) Soil Survey of Cecil County, Maryland. United States Department of Agriculture Soil Conservation Service, Washington, D.C.

Atkins JW, Epstein HE, Welsch DL (2014) Vegetation heterogeneity and landscape position exert strong controls on soil CO_2 efflux in a moist, Appalachian watershed. Biogeosciences 11:17631–17673. doi: 10.5194/bgd-11-17631-2014

Ball BC (2013) Soil structure and greenhouse gas emissions: A synthesis of 20 years of experimentation. Eur J Soil Sci. doi: 10.1111/ejss.12013

Ball BC, Dobbie KE, Parker JP, Smith KA (1997) The influence of gas transport and porosity on methane oxidation in soils. J Geophys Res 102:23301. doi: 10.1029/97JD00870

Boeckx P, Cleemput O Van, Villaralvo I (1997) Methane oxidation in soils with different textures and land use. Nutr Cycl Agroecosystems 49:91–95. doi: 10.1023/A:1009706324386

Bouyoucos GJ (1962) Hydrometer Method Improved for Making Particle Size Analyses of Soils. Agron J 54:464–465. doi: 10.2134/agronj1962.00021962005400050028x

Brumme R, Borken W (1999) Site variation in methane oxidation as affected by atmospheric deposition and type of temperate forest ecosystem. Soil Sci 13:493–501

Ceddia MB, Vieira SR, Villela ALO, et al (2009) Topography and spatial variability of soil physical properties. Sci Agric 66:338–352. doi: 10.1590/S0103-90162009000300009

Creed IF, Webster KL, Braun GL, et al (2013) Topographically regulated traps of dissolved organic carbon create hotspots of soil carbon dioxide efflux in forests. Biogeochemistry. doi: 10.1007/s10533-012-9713-4

Crill PM (1991) Seasonal patterns of methane uptake and carbon dioxide release by a temperate woodland soil. Global Biogeochem Cycles 5:319–334. doi: 10.1029/91GB02466

Davidson EA, Belk E, Boone RD (1998) Soil water content and temperature as independent or

confounded factors controlling soil respiration in a temperate mixed hardwood forest. Glob Chang Biol. doi: 10.1046/j.1365-2486.1998.00128.x

Del Grosso SJ, Parton WJ, Mosier AR, et al (2000) General CH_4 oxidation model and comparisons of CH_4 oxidation in natural and managed systems. Global Biogeochem Cycles 14:999–1019

Delaware Environmental Observing System (DEOS) University of Delaware, Newark DE. Available online at: www.deos.udel.edu. Accessed: 1/31/2017

Dixon R, Solomon A, Brown S, et al (1994) Carbon pools and flux of global forest ecosystems. Science (80-) 263:185–90. doi: 10.1126/science.263.5144.185

Fellman JB, Hood E, D'Amore D V., et al (2009) Seasonal changes in the chemical quality and biodegradability of dissolved organic matter exported from soils to streams in coastal temperate rainforest watersheds. Biogeochemistry. doi: 10.1007/s10533-009-9336-6

Fellman JB, Hood E, Spencer RGM (2010) Fluorescence spectroscopy opens new windows into dissolved organic matter dynamics in freshwater ecosystems: A review. Limnol Oceanogr 55:2452–2462. doi: 10.4319/lo.2010.55.6.2452

Gomez J, Vidon P, Gross J, et al (2017) Spatial and Temporal Patterns of CO_2 , CH_4 , and N_2O Fluxes at the Soil-Atmosphere Interface in a Northern Temperate Forested Watershed. Sci Pages For Res 1:1–12

Gough CM, Vogel CS, Kazanski C, et al (2007) Coarse woody debris and the carbon balance of a north temperate forest. For Ecol Manage. doi: 10.1016/j.foreco.2007.03.039

Guckland A, Flessa H, Prenzel J (2009) Controls of temporal and spatial variability of methane uptake in soils of a temperate deciduous forest with different abundance of European beech (Fagus sylvatica L.). Soil Biol Biochem 41:1659–1667. doi: 10.1016/j.soilbio.2009.05.006

Hanson PJ, Edwards NT, Garten CT, Andrews JA (2000) Separating root and soil microbial contributions to soil respiration: A review of methods and observations. Biogeochemistry. doi: 10.1023/A:1006244819642

Harmon ME, Bond-Lamberty B, Tang J, Vargas R (2011) Heterotrophic respiration in disturbed forests: A review with examples from North America. J Geophys Res Biogeosciences 116:1–17. doi: 10.1029/2010JG001495

Hibbard KA, Law BE, Reichstein M, Sulzman J (2005) An Analysis of Soil Respiration across Northern Hemisphere Temperate Ecosystems. Source Biogeochem Soil Respir 73:29–70

Hishi T, Hirobe M, Tateno R, Takeda H (2004) Spatial and temporal patterns of water-extractable organic carbon (WEOC) of surface mineral soil in a cool temperate forest ecosystem. Soil Biol Biochem. doi: 10.1016/j.soilbio.2004.04.030

Huguet A, Vacher L, Relexans S, et al (2009) Properties of fluorescent dissolved organic matter in the Gironde Estuary. Org Geochem 40:706–719. doi: 10.1016/j.orggeochem.2009.03.002

Inamdar S, Dhillon G, Singh S, et al (2013) Temporal variation in end-member chemistry and its influence on runoff mixing patterns in a forested, Piedmont catchment. Water Resour Res. doi: 10.1002/wrcr.20158

Inamdar S, Johnson E, Rowland R, et al (2017) Freeze–thaw processes and intense rainfall: the one-two punch for high sediment and nutrient loads from mid-Atlantic watersheds. Biogeochemistry 1–17. doi: 10.1007/s10533-017-0417-7

Itoh M, Ohte N, Koba K, et al (2007) Hydrologic effects on methane dynamics in riparian wetlands in a temperate forest catchment. J Geophys Res Biogeosciences. doi: 10.1029/2006JG000240

Kalbitz K, Schmerwitz J, Schwesig D, Matzner E (2003) Biodegradation of soil-derived dissolved organic matter as related to its properties. Geoderma 113:273–291. doi: 10.1016/S0016-7061(02)00365-8

King AW, Andres RJ, Davis KJ, et al (2015) North America's net terrestrial CO_2 exchange with the atmosphere 1990-2009. Biogeosciences. doi: 10.5194/bg-12-399-2015

Kirschbaum MUF (2013) Seasonal variations in the availability of labile substrate confound the temperature dependence of organic matter decomposition. Soil Biol Biochem. doi:

10.1016/j.soilbio.2012.10.012

Kleber M (2010) What is recalcitrant soil organic matter? Environ Chem. doi: 10.1071/EN10006

Kleber M, Sollins P, Sutton R (2007) A conceptual model of organo-mineral interactions in soils: Self-assembly of organic molecular fragments into zonal structures on mineral surfaces. Biogeochemistry 85:9–24. doi: 10.1007/s10533-007-9103-5

Klüpfel L, Piepenbrock A, Kappler A, Sander M (2014) Humic substances as fully regenerable electron acceptors in recurrently anoxic environments. Nat Geosci 7:195–200. doi: 10.1038/NGEO2084

Le Mer J, Roger P (2001) Production, oxidation, emission and consumption of methane by soils: A review. Eur J Soil Biol. doi: 10.1016/S1164-5563(01)01067-6

Lecki NA, Creed IF (2016) Forest soil CO_2 efflux models improved by incorporating topographic controls on carbon content and sorption capacity of soils. Biogeochemistry 129:307–323. doi: 10.1007/s10533-016-0233-5

Leon E, Vargas R, Bullock S, et al (2014) Hot spots, hot moments, and spatio-temporal controls on soil CO_2 efflux in a water-limited ecosystem. Soil Biol Biochem. doi: 10.1016/j.soilbio.2014.05.029

Lloyd J, Taylor JA (1994) On the Temperature Dependence of Soil Respiration. Source Funct Ecol Funct Ecol 8:315–323

McKeague JA, Day JH (1966) Dithionite- and Oxalate-Extractable Fe and Al as Aids in Differentiating Various Classes Of Soils. Can J Soil Sci 46:13–22. doi: 10.4141/cjss66-003

Miller KE, Lai C-T, Friedman ES, et al (2015) Methane suppression by iron and humic acids in soils of the Arctic Coastal Plain. Soil Biol Biochem 83:176–183. doi: 10.1016/j.soilbio.2015.01.022

Mosier AR, Parton WJ, Valentine DW, Schimel DS (1996) CH_4 and N_2O fluxes in the Colorado shortgrass steppe : 1. Impact of landscape and nitrogen addition oxide. Global Biogeochem Cycles 10:387–399

Murphy KR, Stedmon CA, Graeber D, Bro R (2013) Fluorescence spectroscopy and multi-way techniques. PARAFAC. Anal Methods 5:6557. doi: 10.1039/c3ay41160e

National Resources Conservation Service. United States Department of Agriculture. Web Soil Survay. Available online at: websoilsurvey.sc.egov.usda.gov. Accessed: 1/29/2018

Ohno T (2002) Fluorescence inner-filtering correction for determining the humification index of dissolved organic matter. Environ Sci Technol 36:742–746. doi: 10.1021/es0155276

Pacific VJ, McGlynn BL, Riveros-Iregui DA, et al (2008) Variability in soil respiration across riparian-hillslope transitions. Biogeochemistry. doi: 10.1007/s10533-008-9258-8

Pan Y, Birdsey RA, Fang J, et al (2011) A Large and Persistent Carbon Sink in the World's Forests. Science (80-). doi: 10.1126/science.1201609

Pearson AJ, Pizzuto JE, Vargas R (2016) Influence of run of river dams on floodplain sediments and carbon dynamics. Geoderma. doi: 10.1016/j.geoderma.2016.02.029

Pregitzer KS, Euskirchen ES (2004) Carbon cycling and storage in world forests: Biome patterns related to forest age. Glob Chang Biol 10:2052–2077. doi: 10.1111/j.1365-2486.2004.00866.x

R Core Team (2017). R: A language and environment for statistical computing. R Foundation for Statistical Computing, Vienna, Austria. www.R-project.org

Raich JW, Potter CS (1995) Global patterns of carbon dioxide emissions from soils. Global Biogeochem Cycles 9:23–36

Saari A, Martikainen PJ, Ferm A, et al (1997) Methane oxidation in soil profiles of dutch and finnish coniferous forests with different soil texture and atmospheric nitrogen deposition. Soil. Biol. Biochem. 29:1625–1632

Schjønning P, Thomsen IK, Møberg JP, et al (1999) Turnover of organic matter in differently textured soils I. Physical characteristics of structurally disturbed and intact soils. Geoderma 89:177–198. doi: 10.1016/S0016-7061(98)00083-4

Schmidt MWI, Torn MS, Abiven S, et al (2011) Persistence of soil organic matter as an

ecosystem property. Nature. doi: 10.1038/nature10386

Semenov M V., Kravchenko IK, Semenov VM, et al (2010) Carbon dioxide, methane, and nitrous oxide fluxes in soil catena across the right bank of the Oka River (Moscow oblast). Eurasian Soil Sci. doi: 10.1134/S1064229310050078

Shi B, Gao W, Cai H, Jin G (2016) Spatial variation of soil respiration is linked to the forest structure and soil parameters in an old-growth mixed broadleaved-Korean pine forest in northeastern China. Plant Soil. doi: 10.1007/s11104-015-2730-z

Smith KA, Dobbie KE, Ball BC, et al (2000) Oxidation of atmospheric methane in Northern European soils, comparison with other ecosystems, and uncertainties in the global terrestrial sink. Glob Chang Biol. doi: 10.1046/j.1365-2486.2000.00356.x

Tonitto C, Gurwick NP, Woodbury PB, et al (2016) Quantifying Greenhouse Gas Emissions from Agricultural and Forest Landscapes for Policy Development and Verification. In: Advances in Agricultural Systems Modeling. pp 229–304

Ueyama M, Takeuchi R, Takahashi Y, et al (2015) Methane uptake in a temperate forest soil using continuous closed-chamber measurements. Agric For Meteorol. doi: 10.1016/j.agrformet.2015.05.004

Vargas R, Allen M (2008) Environmental controls and the influence of vegetation type, fine roots and rhizomorphs on diel and seasonal variation in soil respiration. New Phytol 179:460–471. doi: 10.1111/j.1469-8137.2008.02481

Wang JM, Murphy JG, Geddes JA, et al (2013) Methane fluxes measured by eddy covariance and static chamber techniques at a temperate forest in central Ontario, Canada. Biogeosciences. doi: 10.5194/bg-10-4371-2013

Warner DL, Villarreal S, McWilliams K, et al (2017) Carbon Dioxide and Methane Fluxes From Tree Stems, Coarse Woody Debris, and Soils in an Upland Temperate Forest. Ecosystems 1–12. doi: 10.1007/s10021-016-0106-8

Webster KL, Creed IF, Bourbonnière RA, Beall FD (2008) Controls on the heterogeneity of soil

respiration in a tolerant hardwood forest. J Geophys Res Biogeosciences. doi: 10.1029/2008JG000706

Wei JB, Xiao DN, Zeng H, Fu YK (2008) Spatial variability of soil properties in relation to land use and topography in a typical small watershed of the black soil region, northeastern China. Environ Geol 53:1663–1672. doi: 10.1007/s00254-007-0773-z

Weishaar J, Aiken G, Bergamaschi B, et al (2003) Evaluation of specific ultra-violet absorbance as an indicator of the chemical content of dissolved organic carbon. Environ Sci Technol 37:4702–4708. doi: 10.1021/es030360x

Yoo K, Amundson R, Heimsath AM, Dietrich WE (2006) Spatial patterns of soil organic carbon on hillslopes: Integrating geomorphic processes and the biological C cycle. Geoderma. doi: 10.1016/j.geoderma.2005.01.008

Yuan Z, Gazol A, Lin F, et al (2013) Soil organic carbon in an old-growth temperate forest: Spatial pattern, determinants and bias in its quantification. Geoderma. doi: 10.1016/j.geoderma.2012.11.008

Yvon-Durocher G, Allen AP, Bastviken D, et al (2014) Methane fluxes show consistent temperature dependence across microbial to ecosystem scales. Nature. doi: 10.1038/nature13164

Chapter 5

UPSCALING SOIL-ATMOSPHERE CO_2 AND CH_4 FLUXES ACROSS A TOPOGRAPHICALLY COMPLEX FORESTED LANDSCAPE

As submitted for publication in Agricultural and Forest Meteorology, 2018.

Authors:

Daniel L. Warner[1], Mario Guevara[1], Shreeram Inamdar[1], and Rodrigo Vargas[1]

Affiliations:

[1]University of Delaware Department of Plant and Soil Sciences, Newark, Delaware, USA

Abstract

Upscaling soil-atmosphere greenhouse gas fluxes across complex landscapes is a major challenge for environmental scientists and land managers alike. This study employs a quantile-based digital soil mapping approach for estimating the spatially continuous distributions (2 m pixel size) and uncertainties of seasonal mean mid-day soil CO_2 and CH_4 fluxes. This framework was parameterized using manual chamber measurements throughout two years within a temperate forested headwater watershed. Model accuracy was highest for early summer (r^2 = 0.61) and late summer (r^2 = 0.64) for CO_2 and CH_4 fluxes, respectively. Model uncertainty was generally lower for predicted CO_2 fluxes than CH_4 fluxes. Within the study area, predicted seasonal mean CO_2 fluxes ranged from 0.17 to 0.58 µmol m^{-2} s^{-1} in winter, and 1.4 to 5.1 µmol m^{-2} s^{-1} in early

summer. Predicted CH_4 fluxes across the study area ranged from 0.02 to -0.52 nmol m^{-2} s^{-1} in winter, and 0.61 to -2.1 nmol m^{-2} s^{-1} in early and late summer. The models estimated a watershed-scale net greenhouse gas potential ranging from 5.3 to 56.7 kg CO_2 eq. hr^{-1} in winter and early summer, with an estimated 1.5 to 0.4% of emissions offset by CH_4 uptake. Flux predictions fell within ranges reported in other temperate forest systems. Soil CO_2 fluxes were more sensitive to seasonal temperature changes than CH_4 fluxes, with significant temperature relationships for soil CO_2 emissions and CH_4 uptake along steep transitional slopes. In contrast, soil CH_4 fluxes from low-lying areas within the watershed were significantly correlated to seasonal precipitation. This study identifies some key challenges for modeling high resolution soil CO_2 and CH_4 fluxes, and suggests that modeling CH_4 fluxes may be more difficult due to their larger spatial heterogeneity and different underlying processes.

Keywords: carbon dioxide, methane, hot-moments, digital soil mapping, topography, forest

5.1 Introduction

The steady increase in atmospheric concentrations of greenhouse gases (GHG) such as CO_2 and CH_4 has major implications for the health of humans and ecological systems worldwide. Although human activities largely contribute to the increases in GHG concentrations, natural sources and sinks of both CO_2 and CH_4 account for large portions of their respective budgets from local to global scales (King et al. 2015; Saunois et al. 2016; Le Quéré et al. 2018). Soils are a major source of CO_2 and may act as both a major source or sink of CH_4. Soil CO_2 efflux represents the largest fraction of total terrestrial CO_2 emissions (Raich and Potter 1995). Wet, saturated soils such as those found in wetland environments are estimated to represent roughly 20-30% of global CH_4 emissions, while aerated upland soils account for roughly 5-10% of the CH_4 removed from the atmosphere annually (Dlugokencky et al. 2011).

Temperate forests are a major ecosystem type at the global scale, covering much of the eastern United States, Central and Eastern Europe, and East Asia. These ecosystems store large quantities of carbon (Post et al. 1982; Pan et al. 2011) and exchange large quantities of CO_2 and CH_4 from soils, coarse woody debris and tree stems with the atmosphere (Gough et al. 2007; Warner et al. 2017). Soil-atmosphere CO_2 and CH_4 fluxes in temperate forests are highly heterogeneous in space, varying across regional scales with climate, ecoregion, and land use types (Ambus and Christensen 1995; Raich and Tufekcioglu 2000; Smith et al. 2000); and at landscape scales with vegetation cover, hydrologic conditions, and topographic heterogeneity (Atkins et al., 2014; Gomez et al., 2017; Maier et al., 2017; Reyes et al., 2017; Warner et al., 2018). Fluxes also vary temporally with diel patterns in temperature and plant activity, and with

seasonally changing patterns in temperature, precipitation, and plant phenology (Crill 1991; Vargas and Allen 2008; Phillips et al. 2010; Wang et al. 2013). Thus, the spatiotemporal heterogeneity of soil-atmosphere CO_2 and CH_4 fluxes is especially large in topographically-heterogeneous landscapes that experience seasonal climates, and accurately quantifying CO_2 and CH_4 fluxes in these ecosystems is a major challenge for estimating and managing local to regional carbon budgets (King et al. 2015; Tonitto et al. 2016).

This scientific challenge has been approached in different ways. Top-down flux measurement techniques such as eddy covariance can measure fluxes at the ecosystem scale, but often are not well-suited for use in topographically-heterogeneous terrain (Baldocchi et al. 2000; Baldocchi 2003). Smaller scale techniques, such as flux chamber measurements employing portable gas analyzers, can better describe the heterogeneity of fluxes across different sources and sinks in an ecosystem (Gomez et al., 2017; Leon et al., 2014; Maier et al., 2017; Warner et al., 2017). However, estimating ecosystem-scale fluxes, and the relative importance of different sources and sinks within an ecosystem, is difficult using manual chamber flux measurements due to their small measurement footprint (Phillips et al. 2017). An alternative approach of landform classification and aggregation of mean fluxes from point measurements within each landform has been employed for estimating watershed-scale soil-atmosphere CO_2 (Webster et al. 2008a;

Riveros-Iregui and McGlynn 2009; Gomez et al. 2016) and CH_4 fluxes (Gomez et al. 2016) in temperate ecosystems. However, studies incorporating topographic variability into ecosystem-scale predictions of *in situ* chamber flux measurements of multiple GHGs are scarce. Furthermore, the aggregation of major landform elements, while useful, assumes spatial homogeneity of fluxes within each landform and does not reflect the spatially continuous nature of the land surface and soil processes.

Since the rapid acceleration of computer processing power, the field of digital soil mapping has expanded and found many novel applications for soil scientists attempting to model the continuous spatial distributions of soil properties (McBratney et al. 2003). Digital soil mapping utilizes high-resolution digital elevation models (DEMs), remote sensing data, legacy maps, and climate data to predict and map various soil properties across landscapes by relating field measurements of soil properties to spatial covariates derived from these publicly available data sources (McBratney et al. 2003; Hengl et al. 2004, 2017; Wiesmeier et al. 2011). As soil-atmosphere GHG fluxes are ultimately a product of soil biogeochemical processes that are influenced by soil properties, we postulated that digital soil mapping is an alternative, low-cost approach to predict the magnitude and variability of soil CO_2 and CH_4 fluxes at high spatial resolution across complex terrain.

Our overarching goal was to develop a framework for “upscaling” manual soil GHG chamber flux measurements to a continuous spatial distribution across complex terrain, and examine how this spatial distribution varied across seasons. In this study, we measured soil-atmosphere CO_2 and CH_4 fluxes for two years along hillslope transects in a forested headwater watershed in the Piedmont region of Maryland, USA. We then

applied digital soil mapping techniques to predict fluxes within the study watershed and across seasons, evaluated the uncertainty of these predictions, and investigated the functional relationships between seasonally changing soil-atmosphere CO_2 and CH_4 fluxes, temperature, and precipitation patterns. The goals of this study were to 1) evaluate data-model agreement between chamber CO_2 and CH_4 flux measurements and terrain attributes using a digital soil mapping approach and 2) assess the spatial relationships between predicted soil CO_2 and CH_4 fluxes and the relationships of each of these fluxes to seasonal changes in temperature and precipitation. We hypothesized that terrain attributes, including slope, aspect, and various terrain indices, could be reliable predictors of soil CO_2 and CH_4 fluxes, as vegetation and climate are relatively homogeneous within our spatial domain.

5.2 Methods

Study site and sampling design

This study was conducted in a 12-hectare forested headwater watershed at Fair Hill Natural Resources Management Area, Cecil County, Maryland, USA (39º 42’ N, 75º 50’ W). Forest vegetation is primarily composed of *Fagus grandifolia*, *Quercus spp.*, *Lirodendron tulipifera*, and *Acer spp*. Soils within the study area are coarse-loamy, mixed, mesic Lithic Dystrucepts belonging to the Manor and Glenelg series loams, which

overlay peltic gneiss and schist bedrock (Anderson and Matthews 1973). Annual precipitation is approximately 1200 mm. Annual mean temperature is 12 ^{o}C, reaching a mean annual maximum of 25 ^{o}C and mean annual minimum of -0.6 ^{o}C (DEOS 2017). We distributed 20 sampling locations across four hillslope transects with sampling points that spanned valley bottoms, transitional slopes, and upland areas (Warner et al. 2018).

Flux measurements

Soil-atmosphere CO_2 and CH_4 fluxes were measured from 10 cm diameter, 9 cm tall PVC collars inserted 5 cm into the soil at each sampling point along the transects. Fluxes were calculated based on the change of gas concentration within the chamber over the course of three minutes, which was measured with an ultraportable greenhouse gas analyzer (Los Gatos Research, Mountain View, California, USA) as described previously (Warner et al. 2017). Measurements were taken at mid-day (11:00 – 15:00) two times monthly from September 2014 to November 2016, with additional measurements following precipitation events and during drought periods, yielding a set of 880 total flux measurements. These measurements were classified by season based on annual patterns of soil temperature and moisture, which were measured simultaneously with fluxes. Seasons were defined as winter (cold-wet: Jan 1-Feb 28), spring (warm-wet: Mar 1-May 20), early summer (hot-wet: May 20-Jul 31), late summer (hot-dry: Aug 1-Sep 30), and fall (warm-dry: Oct 1-Dec 31). Seasonal groupings were determined based on site-specific temperature, precipitation, and phenological patterns (Warner et al. 2018).

Topographic analysis and processing

Topographic data was acquired from a LiDAR (Light Detecting and Ranging)-derived DEM with 2-meter spatial resolution (NOAA, 2005). The DEM was smoothed

and conditioned for further topographic and hydrologic analysis (Jenson and Domingue 1988). Flow direction was calculated as the maximum triangle slope (Tarboton 1997). Primary and secondary terrain attributes were derived from this DEM in SAGA GIS (Conrad et al. 2015), and a full list of these attributes is provided in Table 5.1. A GPS (Geographical Positioning System) survey was conducted to locate each chamber within 1-meter accuracy, allowing us to accurately identify the corresponding pixels on the terrain attribute grids.

Table 5.1 List of all primary and secondary terrain attributes used as potential predictors for seasonal CO_2 and CH_4 fluxes. Reference numbers are used for indicating selected predictors in Table 2. Asterisks indicate attributes that were ultimately selected as a predictor at least once, these are defined to the right.

No.	Attribute	Selected Definitions
1	Elevation	**Slope:** The angle of maximum rise over run at each pixel (percent).
2	Slope*	**Aspect:** The direction of a slope. In this case, aspect has been normalized such that maximum values are south-facing and minimum values are north facing (degrees).
3	Aspect*	
4	Local Curvature	
5	Upslope Curvature	**Downslope Curvature:** The mean local curvature of pixels along the downslope flow path running from a given pixel (radians m^{-1}).
6	Downslope Curvature*	
7	Cross Sectional Curvature	**Flowline Curvature:** The mean local curvature of pixels from a flow path running through a target pixel (radians m^{-1}).
8	Profile Curvature	
9	Tangential Curvature	**Channel Network Base Level:** The interpolated elevation of a stream channel network (m).
10	Minimal Curvature	
11	Maximal Curvature	**Vertical Distance to Channel Network:** The difference between surface elevation and Channel Network Base Level (m).
12	Flow Line Curvature*	
13	Channel Network Base Level*	**Upslope Accumulation Area:** The area of pixels that are routed through a given pixel by a flow direction calculation (m^2)
14	Vertical Distance to Channel Network*	
15	Upslope Accumulation Area*	**Catchment Slope:** The mean slope angle of pixels within an Upslope Accumulation Area (percent).
16	Catchment Slope*	
17	Topographic Wetness Index (SAGA)*	**Topographic Wetness Index (SAGA):** A SAGA modified version of the Topographic Wetness Index (Beven and Kirkby 1979b) that also accounts for vertical distance to the channel network.
18	Convexity	
19	Convergence Index	**Multiresolution Index of Valley Bottom Flatness:** A quantitative measure of valley bottom topographic characteristics based of slope angles of a pixel derived at multiple resolutions (Gallant and Dowling 2003).
20	Curvature Classification	
21	Analytical Hillshading	
22	Topographic Position Index	**Multiresolution Index of Ridge Top Flatness:** A quantitative measure of upland plateau topographic characteristics based of slope angles of a pixel derived at multiple resolutions (Gallant and Dowling 2003).
23	Multiresolution Index of Valley Bottom Flatness*	
24	Multiresolution Index of Ridge Top Flatness*	
25	Flow Accumulation	----------
26	Valley Depth	Definitions based on descriptions from Wilson and Gallant (2000) unless otherwise noted.
27	Slope Length and Steepness (LS) Factor	

Modeling fluxes and prediction uncertainty with quantile regression forests

Our digital soil mapping framework is summarized in Figure 5.1. Of the 27 topographic attributes considered, the attributes that were ultimately used in our predictions were selected for each season using the random forest-based variable selection method proposed by Genuer and others (2012). This method uses an automatic procedure to select the most informative variables for model interpretation and model prediction purposes. The variables are first ranked by importance and eliminated systematically to reduce model error, ultimately yielding a small set of highly important variables that are sufficient for making robust predictions (Table 5.2).

This study employed quantile regression forests (Meinshausen 2006), a variant of the random forests algorithm (Breiman 2001). Random forests creates an ensemble of regression trees based on bagging, a statistical subsetting technique applied to available data and available predictors. The final prediction is the average of all the regression trees which are evaluated by an out-of-bag cross-validation form. Alternatively, quantile regression forests estimates the variance of all the ensembled trees (not just the mean as with the original random forests algorithm), producing a full conditional distribution of the response variable (i.e., soil GHG flux) as a function of its predictors (i.e., terrain attributes). Therefore, quantile regression forests provide the means to judge the reliability of predictions, since prediction intervals can be extracted from the full conditional distribution of both predicted fluxes at each season for each pixel across the watershed. After variable selection, quantile regression forests model parameters *mtry* (the number of predictor variables randomly selected at each node in a tree) and *ntree* (the number of "trees" grown in the forest) were tested using leave-one-out cross

validation to minimize model error while maximizing explained variance. The *mtry* parameter was tested from 2 to n – 1 (n = number of predictors), and the *ntree* parameter was tested from 50 to 1000 at increments of 10. The result of the quantile regression forest was a set of conditional prediction distributions (*ntree* ranged 90 to 230 for CO_2 fluxes and 60 to 230 for CH_4 fluxes) of mean mid-day soil CO_2 and CH_4 fluxes at each pixel (total of 30134) within the study watershed during each season. As these prediction distributions often were not normally distributed, medians of the conditional prediction distributions at each pixel were used as final predictions, and the interquartile ranges of the conditional distributions were used as a spatially explicit measure of prediction uncertainty. This approach allowed us to predict spatially continuous distributions of seasonal mean mid-day soil-atmosphere CO_2 and CH_4 fluxes and the interquartile range of these predictions across the 12 ha watershed for each season.

Variable selection, parameter testing, and quantile regression forest predictions were performed in packages "VSURF" (Genuer et al. 2016), "e1071" (Meyer et al. 2015), "randomForest" (Liaw and Wiener 2002), and "quantregForest" (Meinshausen 2016) in the R software (R Core Team 2015). Model accuracy was evaluated for each soil GHG flux and each season based on root mean square error (RMSE) and the coefficient of determination (r^2). Whole watershed fluxes were estimated as the sum of the predicted fluxes at each 2-meter pixel multiplied by the true surface area (adjusted by slope) of each pixel.

In this study, model performance and soil GHG predictions were evaluated in two ways. First was "model accuracy" referred to the coefficient of determination (r^2) and root mean square error (RMSE) of our quantile regression forests model fit to our 20 observations of each GHG flux in each season. Second was "prediction uncertainty", which referred to the spread of the conditional prediction distribution (where n = the *ntree* parameter) generated by the quantile regression forests model at each pixel. Thus, "model accuracy" was used as an indicator of overall model fit, while "prediction uncertainty" was used as an indicator of the consistency of predictions made by individual trees grown within the quantile regression forests model. Prediction uncertainty was expressed both as a percentage (i.e., interquartile range of the conditional prediction distribution divided by the median) and as a unit (i.e., μmol m^{-2} s^{-1} or nmol m^{-2} s^{-1}) value equal to the interquartile range of the conditional prediction distribution.

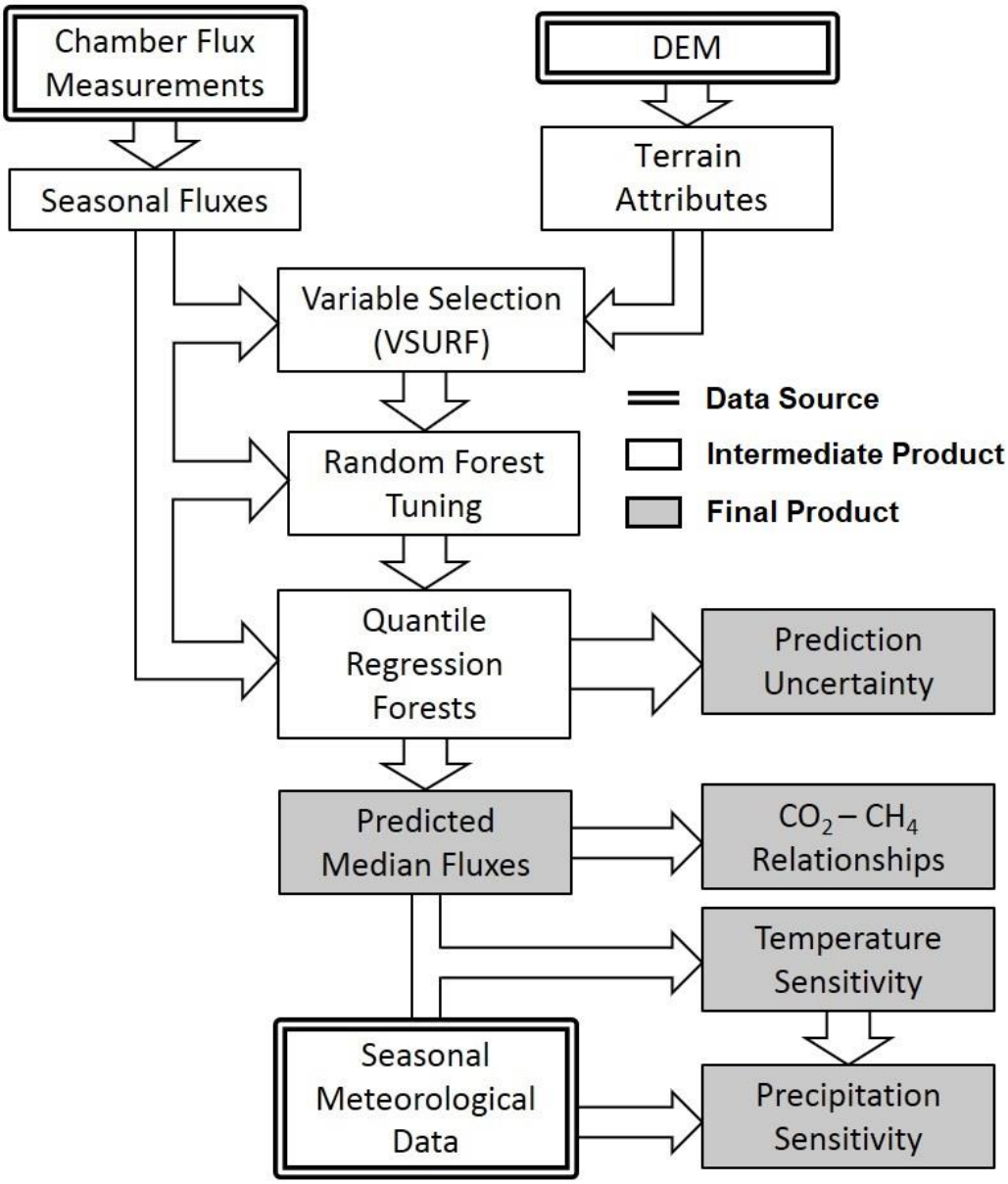

Figure 5.1 Flow diagram of modeling approach used in this study. Double outlines indicate primary data sources, while shaded boxes indicate final products presented in this paper.

Seasonal relationships of fluxes, temperature, and precipitation

Seasonal temperature and precipitation data were gathered from a nearby (~1 km) weather station operated by the Delaware Environmental Observation System (DEOS 2017). Temperature relationships to CO_2 and CH_4 fluxes were assessed by fitting pixel-wise linear

models of mean seasonal temperature to mean seasonal GHG fluxes and extracting the slope for each pixel, yielding a seasonal temperature relationship in units of μmol CO_2 m^{-2} s^{-1} or nmol CH_4 m^{-2} s^{-1} per degree Celsius. We also examined the potential influence of seasonal precipitation patterns on fluxes. In pixels where temperature-flux relationships were significant, the residuals of these relationships were related to mean weekly precipitation for each season. In pixels where temperature-flux relationships were not significant, original predicted flux values were related to mean weekly precipitation in each season instead of residuals from the temperature-flux relationships. Pixel-wise linear models were also used to examine relationships between CO_2 and CH_4 fluxes across seasons.

5.3 Results

Selected variables for each season and gas flux

A total of 10 prediction grids were made (one for each season and each flux), and the selected predictor variables were different between seasons and between CO_2 and CH_4 fluxes. Table 2 lists which variables were selected for each model. A topographic wetness index was selected as a predictor of CH_4 fluxes across all seasons, and as a predictor for CO_2 from early summer to fall. Flowline curvature was selected as a predictor for CO_2 fluxes in all seasons, but never for CH_4 fluxes. Slope angle, upslope

accumulation area, and the Multiresolution index of Valley Bottom Flatness (MRVBF) were also commonly selected as predictors of CH_4 fluxes, while upslope accumulation area and the interpolated channel network base elevation were selected in three seasons for CO_2 fluxes. Other variables, such as aspect, were selected only once for a specific season and flux (Table 5.2).

Table 5.2 Selected predictor variables for predicting seasonal mean CO_2 and CH_4 fluxes using quantile regression forests. Predictor numbers correspond to reference numbers in Table 1.

Season	**CO_2 predictors**	**CH_4 predictors**
Winter	12, 13, 16, 6, 3	17, 23, 15
Spring	12, 24, 14	17, 23, 15, 2
Early Summer	12, 17, 15, 13	2, 15
Late Summer	12, 17, 2, 13	17, 23, 2
Fall	12, 17, 15	17, 23

Predicted fluxes and model accuracy

Model predictions of mean mid-day fluxes were close to our observed mean fluxes across sampling locations in each season (Fig 5.2). A detailed description of observed fluxes can be found in Warner et al. (2018). Model accuracy was lowest in spring for both CO_2 and CH_4 with r^2 of 0.1 and 0.35, and RMSE of 0.39 µmol CO_2 m^{-2} s^{-1} and 0.25 nmol CH_4 m^{-2} s^{-1}, respectively. Model accuracy was highest in early summer for CO_2 (r^2 = 0.61, RMSE = 0.90 µmol m^{-2} s^{-1}) and in late summer for CH_4 (r^2 = 0.64, RMSE = 0.47 nmol m^{-2} s^{-1}). A list of model r^2 and RMSE is provided in Table 5.3.

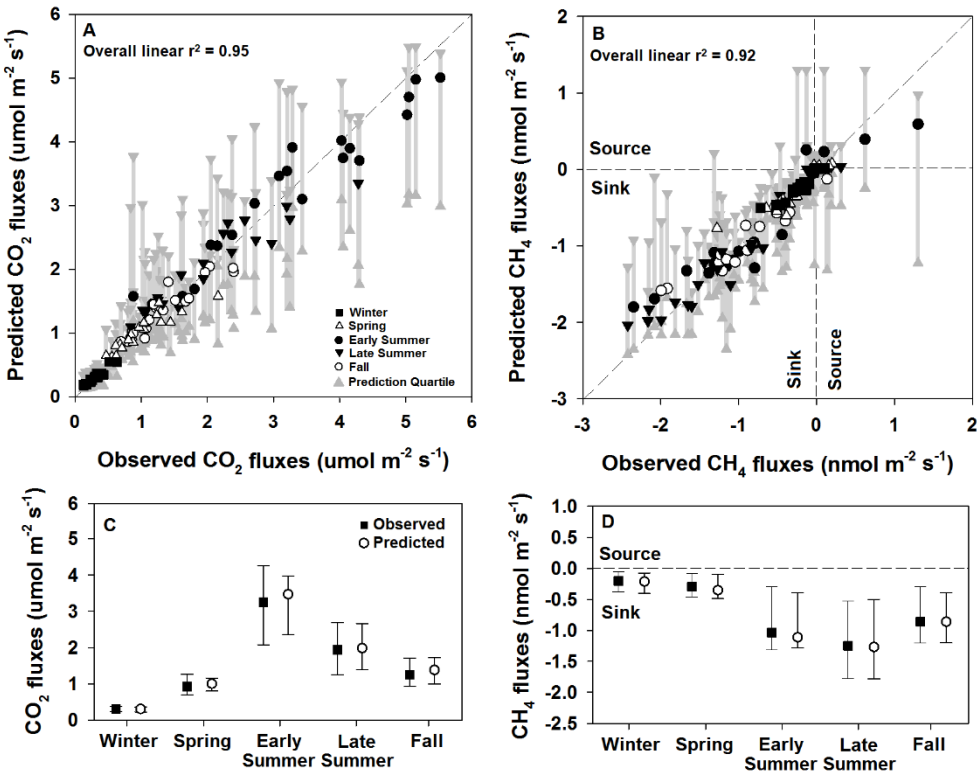

Figure 5.2 Comparisons of observed CO_2 and CH_4 fluxes and predicted fluxes from the medians of conditional prediction distributions generated by quantile regression forests. In panels A and B, seasons are denoted by shapes, and error bars indicate the upper and lower quartiles of the conditional prediction distributions. Panels C and D present seasonal means (and upper and lower quartiles) of observed (full square) and predicted (empty circle) fluxes from all 20 sampling locations used in this study.

Table 5.3 R-squared and Root Mean Square Error values for assessing model accuracy of quantile regression forests models.

	CO_2 fluxes		CH_4 fluxes	
Season	**R^2**	**RMSE (μmol m^{-2} s^{-1})**	**R^2**	**RMSE (nmol m^{-2} s^{-1})**
Winter	0.42	0.09	0.57	0.13
Spring	0.10	0.39	0.35	0.25
Early Summer	0.61	0.90	0.50	0.60
Late Summer	0.40	0.70	0.64	0.47
Fall	0.40	0.39	0.39	0.46

Like the observed GHG fluxes, predicted seasonal mean fluxes varied across the landscape and across seasons (Fig 5.3). Predicted CO_2 efflux was generally low in winter (range 0.15 to 0.55 μmol m^{-2} s^{-1}), with the highest fluxes along the steep south-facing

slopes near the watershed outlet, and lowest in floodplain areas along the stream network and in the upper reaches of the watershed. Winter predictions of net CH_4 uptake were highest along convergent hillslopes (maximum -0.52 nmol m^{-2} s^{-1}), with neutral to slightly positive net CH_4 fluxes predicted in low lying areas (Fig 5.3). In spring, predicted CO_2 efflux was highest along steep hillslopes and in high elevation upland areas (range 0.60 to 1.6 µmol m^{-2} s^{-1}), while predicted CH_4 uptake was highest on the steepest sections of hillslopes (maximum -0.81 nmol m^{-2} s^{-1}), again with neutral to slightly positive soil CH_4 fluxes predicted in low lying valley bottom areas (Fig 5.3). Early summer predicted mean CO_2 efflux was the highest of any season (maximum of 5.2 µmol m^{-2} s^{-1}) along the steep slopes near the watershed outlet, but low CO_2 efflux (minimum of 1.4 µmol m^{-2} s^{-1}) was predicted in flat valley bottom areas. Early summer also had the highest predicted soil CH_4 emissions (maximum of 0.6 nmol m^{-2} s^{-1}), which corresponded to areas of very low predicted CO_2 efflux. Low soil CH_4 uptake (~ -0.2 nmol m^{-2} s^{-1}) was predicted for most of the watershed except along hillslopes, where predicted soil CH_4 uptake was relatively high (maximum of -1.9 nmol m^{-2} s^{-1}) (Fig 5.3). In late summer, predicted CO_2 efflux was again highest on hillslopes, but relatively small across the rest of the watershed (range 1.1 to 3.4 µmol m^{-2} s^{-1}). Predicted net CH_4 uptake was highest during this season, with the highly negative values concentrated along convergent hillslopes (maximum of -2.1 nmol m^{-2} s^{-1}) and neutral to slightly positive soil CH_4 fluxes predicted in valley bottom areas. Predicted CO_2 efflux and CH_4 uptake was slightly lower across the watershed in fall than in late summer, but the spatial patterns of the highest and highest predicted fluxes were similar between the two seasons (Fig 5.3).

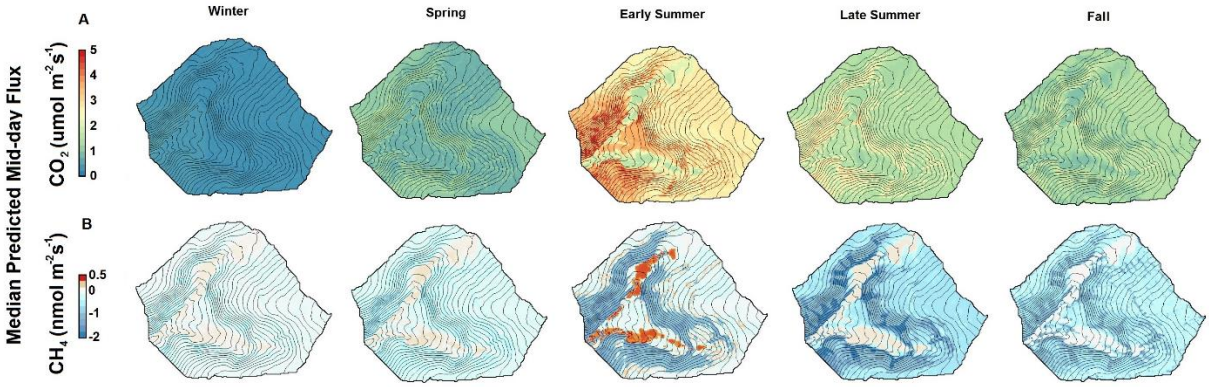

Figure 5.3 Predicted seasonal mean mid-day CO_2 (top) and CH_4 (bottom) fluxes at each pixel in our study watershed during each season. Predicted values represent the median of the conditional prediction distribution of seasonal mean fluxes generated for each pixel.

Prediction uncertainty

Percent prediction uncertainty (the interquartile range of the prediction distribution at each pixel as a percentage of the median of the prediction distribution) of predicted CO_2 efflux was relatively low compared to predicted CH_4 fluxes (Fig 5.4), generally staying below 100% across all seasons. For CO_2 efflux, spatial distributions of areas with relatively high percent prediction uncertainty varied between seasons. Areas of high percent prediction uncertainty were focused in upland areas (winter and spring), steep stream banks (early summer), flat valley bottoms and uplands (late summer), but were scattered across the watershed in fall (Fig 5.4). Predicted CH_4 fluxes had very large ranges in percent prediction uncertainty, but the spatial patterns of this uncertainty were more consistent than for CO_2 predictions. Percent uncertainty for each prediction was relatively low (< 100%) across the steep hillslopes in the watershed during all seasons, but extremely high percent uncertainty (> 1000%) was observed for CH_4 fluxes in some areas with near-zero predicted net fluxes (Fig 5.4; 5.5). In general, percent prediction uncertainty was highest in pixels where predicted fluxes were nearest to zero,

although these low predicted fluxes were often associated with similarly low interquartile ranges in their prediction distributions (Fig 5.5). In exception, soil CH_4 flux predictions were highly uncertain in upland areas during early summer, and the interquartile range of predicted distributions from many of these pixels ranged from moderate sinks to moderate sources of CH_4 (Fig 5.4; 5.5).

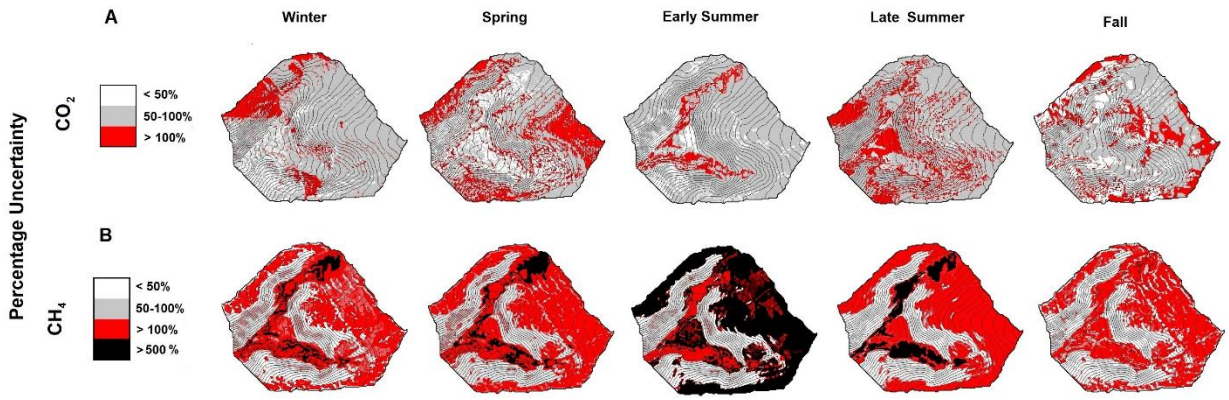

Figure 5.4 Percent prediction uncertainty for CO_2 (top) and CH_4 (bottom) fluxes at each pixel in our study watershed during each season. Percent uncertainty was calculated as the interquartile range divided by the median of the conditional prediction distribution generated for each pixel.

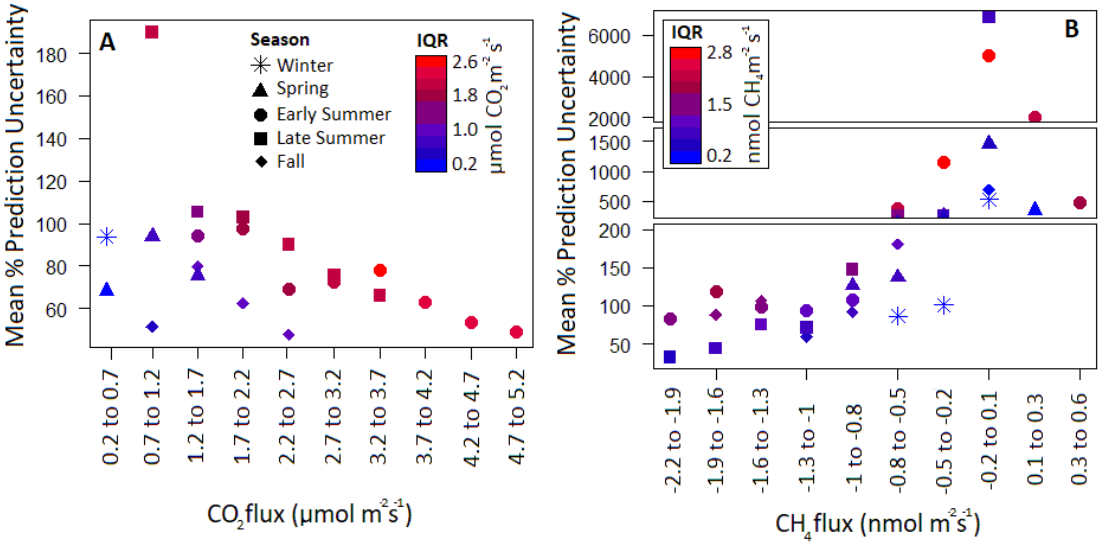

Figure 5.5 Comparison of binned flux predictions (10 equal bins) during each season to average percent prediction uncertainty within each bin. Shapes denote different seasons, colors indicate the mean width of the interquartile ranges of the conditional prediction distributions for each binned flux value. This figure aims to clarify interpretations of prediction uncertainty when expressed both in units of flux (i.e. interquartile range) and as a percentage of the median predicted flux value.

Watershed-scale flux predictions

We predicted the mean mid-day watershed-scale flux of both gases as the sum of predicted fluxes at each pixel. Watershed-scale CO_2 emissions were greatest in early summer, with predicted mean mid-day efflux (sum of lower and upper quartiles of prediction distribution) of 1290 (877 to 1800) mol CO_2 hr^{-1} for the whole watershed. Early summer predicted CH_4 fluxes had the greatest uncertainties, leading to predicted mean mid-day net flux of -205 (-646 to 261) mmol CH_4 hr^{-1}. Predicted watershed-scale net CH_4 flux was greatest in late summer and fall, with fluxes of -354 (-621 to -75) and -264 (-497 to -77) mmol CH_4 hr^{-1}, respectively. Fluxes were lowest during winter months, with estimated watershed-scale mid-day fluxes of 120 (67 to 178) mol CO_2 hr^{-1} and -70.9 (-136 to -7.1) mmol CH_4 hr^{-1} (Fig 5.6). When comparing CO_2 equivalents using a 100-year global warming potential of 25 for CH_4, we estimated that soil CH_4 fluxes could offset the global warming potential of CO_2 efflux by 1.5% (2.8 - 0.5%) in winter, 0.4% (1.3 - +0.5%) in early summer, and 1.2% (2.1 - 0.3%) in late summer.

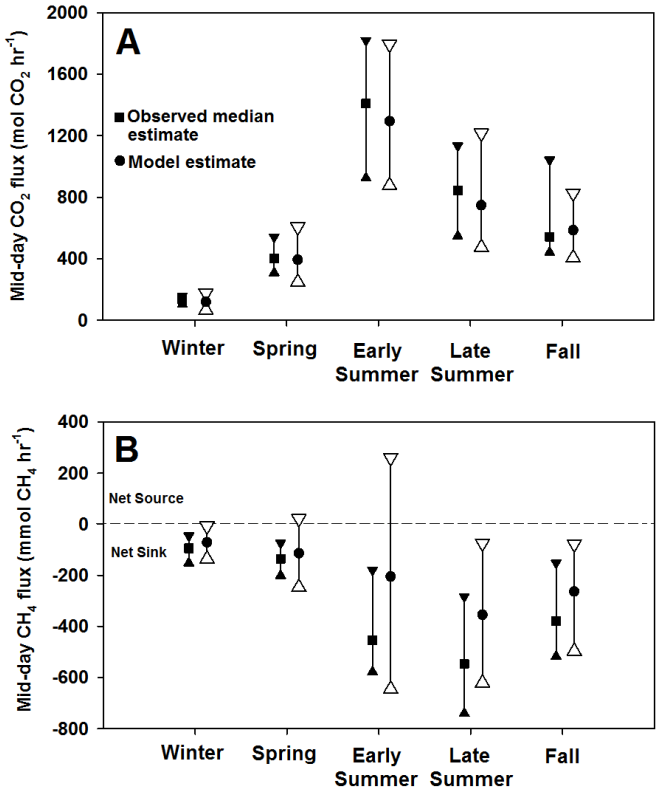

Figure 5.6 Comparisons of whole-catchment seasonal mid-day flux estimates made by multiplying the median of all observed fluxes for each season by catchment area (observed median estimate, squares) and by the summation of model flux predictions at each pixel in the watershed (model estimate, circles). Error bars indicate the upper and lower quartiles of observed fluxes at all 20 locations (filled) and the summation of model prediction quartiles at each pixel (empty).

Estimates of watershed-scale GHG fluxes from our models (referred to as model estimate; Fig 5.6) were compared to estimates made by simply scaling the seasonal median flux across all sampling locations to the watershed area (referred to as observed estimate; Fig 5.6).

Watershed-scale CO_2 fluxes were similar between these two estimates (Fig 5.6a), while observed estimates of CH_4 fluxes tended to indicate a larger soil CH_4 sink than our model estimates in the summer and fall (Fig 5.6b). This was particularly evident in early summer, when CH_4 flux estimates ranged from a relatively large net sink to a moderate net source at the watershed scale (Fig 5.6b).

Seasonal relationships between fluxes, temperature, and precipitation

Linear models relating seasonal mean temperature (explanatory variable) with predicted seasonal mean CO_2 efflux (response variable) were significant ($p < 0.05$) at every pixel in the watershed. The slopes of these relationships ranged from 0.2 to 0.6 µmol CO_2 m^{-2} s^{-1} $^oC^{-1}$ with lower values found in flat valley bottom areas and higher values found along steep transitional slopes (Fig 5.7a). Linear models relating seasonal mean soil CH_4 fluxes and temperature were significant along steep transitional slopes and in a few scattered pixels in the low slope valley bottom areas, but were not significant for large portions of the lowland and upland areas of the watershed. Where significant, slopes of temperature relationships ranged from -0.23 to -0.02 (nmol CH_4 m^{-2} s^{-1} $^oC^{-1}$), with the greatest relationship for soil CH_4 uptake across sloped convergent zones and along the base of slopes (Fig 5.7b).

There were not significant relationships ($p < 0.05$) between precipitation and the residuals of the CO_2-temperature relationships in any pixel, nor were there any such relationships with CH_4-temperature residuals in the pixels where these relationships were significant. However, mean weekly precipitation was significantly positively correlated to soil CH_4 fluxes (higher net CH_4 emissions in wet seasons) in low lying valley bottom areas (~ 0.07 nmol CH_4 m^{-2} s^{-1} mm^{-1}), and negatively correlated in some pixels adjacent to these areas (~ -0.07 nmol CH_4 m^{-2} s^{-1} mm^{-1}), (Fig 5.7c).

Seasonal CO_2 and CH_4 fluxes were significantly correlated to each other for a small portion of the watershed that was primarily made up of steep transitional slopes (Fig 5.7d). This correlation was generally negative where it was significant, indicating a seasonal increase in soil CH_4 uptake with increasing CO_2 efflux.

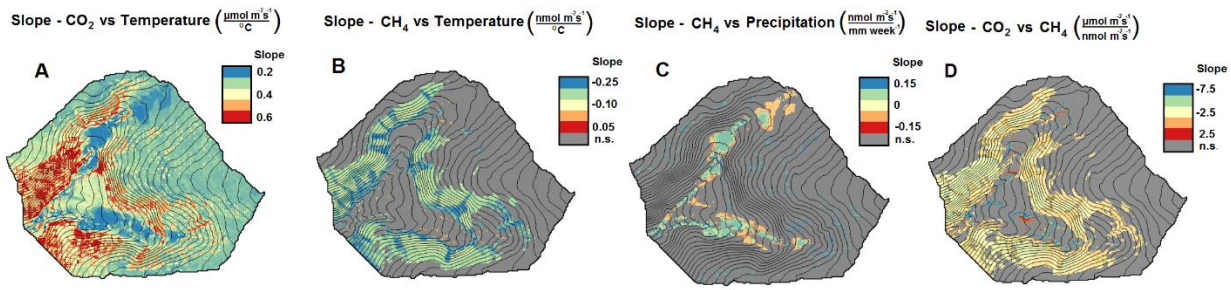

Figure 5.7 Pixel-wise slopes derived from linear models of seasonal (B) CO_2 and seasonal mean temperature, (C) CH_4 fluxes and seasonal mean temperature, (C) seasonal CH_4 fluxes and seasonal mean weekly precipitation, (D) seasonal mean CO_2 fluxes and CH_4 fluxes. Gray areas indicate pixels with non-significant ($n = 5$, $p > 0.1$) relationships.

5.4 Discussion

Continuously distributed flux predictions

This study demonstrates that a digital soil mapping framework is applicable to predict soil-atmosphere CO_2 and CH_4 fluxes across a forested watershed. Predicted mean fluxes from quantile regression forests closely represented our observations in all seasons (Fig 5.2), suggesting that soil surface GHG flux measurements and DEM-derived terrain attributes may be used in tandem to estimate soil-atmosphere fluxes across topographically heterogeneous ecosystems. Unlike approaches that rely on classification and aggregation of fluxes from major landforms (Webster et al. 2008a; Gomez et al. 2016), this approach allowed us to estimate the continuous spatial distributions of these

fluxes. Though both approaches can discern differences in fluxes between major landscape features (i.e., hillslopes, upland and valley bottom flats), our approach also provided a detailed estimate of flux variability *within* major landscape features that cannot be achieved through landform classification.

The ranges of our flux predictions were comparable to fluxes reported in other temperate forests. Our CO_2 efflux predictions fell within the ranges reported in another temperate forest, which ranged from a median of 0.7 µmol CO_2 m^{-2} s^{-1} in winter/spring to 4.1 µmol CO_2 m^{-2} s^{-1} in summer, with higher fluxes on transitional slopes than in valley bottom wetland areas (Webster et al. 2008b; Creed et al. 2013). Our predictions of net CH_4 fluxes were also comparable to observations in a similar temperate forest, that found mean late summer net CH_4 fluxes of -2.0 nmol CH_4 m^{-2} s^{-1} in transitional slopes and uplands, but high emissions of CH_4 (some instantaneous measurements as high as 100 nmol CH_4 m^{-2} s^{-1}) only during early summer in low lying areas of the watershed (Wang et al. 2013). While our predicted mean CH_4 efflux only reached a maximum of 0.6 nmol CH_4 m^{-2} s^{-1}, we too observed brief "hot moments" of emissions in early summer (as high as 19 nmol CH_4 m^{-2} s^{-1}) in low lying valley bottom areas, which had near-zero net fluxes during the rest of the year (Warner et al. 2018).

Whole watershed-scale flux predictions and uncertainty

Estimates of watershed-scale CO_2 efflux based on our predicted values and scaled observed medians were similar across all seasons despite the wide ranges in magnitudes of predicted fluxes across the watershed. These results suggest that the sampling sites in this study were representative of the relative contributions of different landscape features to whole watershed CO_2 fluxes (Fig 5.6a). However, simply scaling median observed

fluxes tended to suggest a stronger net watershed-scale CH_4 sink, especially in early summer. Model estimates of watershed-scale CH_4 flux in this season ranged from a moderate net source to a moderate net sink, while the scaled observations method suggested a relatively high net CH_4 (Fig 6b). We attribute this discrepancy to the large prediction uncertainties of CH_4 fluxes in some areas of the watershed. In some cases (such as in low-lying areas during late summer), the high percent CH_4 prediction uncertainty was a product of a prediction distribution with a median near zero and an interquartile range that, while small in units of flux, was much larger than the median prediction (for example, a median and interquartile range of 0.001 and 0.1 nmol m^{-2} s^{-1} would have a percent prediction uncertainty of 10000%; Fig 5.5). In early summer however, high percent prediction uncertainty was a product of highly variable conditional prediction distributions in some areas of the watershed (Fig 5.4; 5.5, early summer predictions), which led to a highly uncertain estimate of whole-watershed soil CH_4 flux in early summer (Fig 5.6b).

As ecosystem models continue to provide increasingly detailed insights into biogeochemical processes, communicating their uncertainty, and the underlying implications of this uncertainty, becomes increasingly important. In the former case described above, percent prediction uncertainty may be high, but the degree of this uncertainty in units of flux may be too small to be ecologically relevant. In the latter case, the high level of prediction uncertainty in the uplands has major implications for interpreting the net CH_4 source or sink status of the landscape. Beyond communicating the uncertainty of model estimates, understanding the causes for this uncertainty may highlight certain aspects of the processes that we are trying to model.

The high uncertainty of early summer CH_4 fluxes at the watershed scale may stem from the large variability of CH_4 fluxes within landscape features that have similar topographic characteristics (e.g., valley bottom flats, upland plateaus) in hot, wet environmental conditions. We observed large CH_4 emissions in a few valley bottom sampling locations while other, similarly flat valley bottom and upland areas had no net flux, or were weak net sinks of CH_4. Studies in other temperate forests have observed brief early summer "hot moments" of CH_4 emissions from small areas of low-lying soils that may entirely offset or exceed CH_4 uptake occurring across most of the watershed (Itoh et al. 2007; Wang et al. 2013). Furthermore, it is known that anaerobic biogeochemical processes, such as methane production, can vary significantly in space due to subtle variations in surface microtopography (Frei et al. 2012), which may help explain why CH_4 flux observations from different small-footprint chambers may vary significantly even within areas with similar DEM-derived terrain attributes. Our variable selection process selected only terrain attributes of slope and upslope accumulation area as predictors of CH_4 fluxes in early summer (Table 5.2). Slope was similarly low in both flat valley bottom areas and upland plateaus, while upslope accumulation area was variable in flat valley bottoms and low in upland plateaus. Thus, in some cases our quantile regression forests model made predictions based on attributes of topographically similar pixels with distinctly different CH_4 fluxes, which led to highly variable conditional prediction distributions of CH_4 fluxes in flat upland areas and flat valley bottoms. As flat upland areas occupy a large portion of this study watershed, the high prediction uncertainty of these pixels was compounded in watershed-scale flux estimates. These findings highlight the difficulties

that “hot spots” and “hot moments” of CH_4 fluxes introduce to large-scale modeling efforts (Savage et al. 2014).

While high variability of fluxes from topographically similar pixels can cause large prediction uncertainty, the same problem may arise when similar fluxes are observed from topographically distinct pixels. This effect may be responsible for the much lower model accuracy for spring CO_2 efflux ($r^2 = 0.1$; Table 5.3) than for any other season or flux. We observed similar CO_2 efflux in slopes and flat upland areas of the watershed during spring, but CO_2 efflux from sloping soils significantly exceeded upland areas in other seasons (Warner et al. 2018). For spring CO_2 efflux, our variable selection process selected flowline curvature, multiresolution index of ridge top flatness, and vertical distance to channel network as predictors. Transitional sloping areas have high, low, and intermediate values of these attributes, while upland plateaus have low, high, and high values, respectively. Thus, when two landforms with major differences in selected terrain attributes had similar fluxes, the model did a poor job relating fluxes to surficial terrain attributes.

Relationships of seasonal CO_2 and CH_4 fluxes, temperature, and precipitation

Temporal relationships between seasonal meteorological patterns and fluxes were different for each gas. The highest temperature-CO_2 efflux relationship corresponded to soils along steep transitional hillslopes near the catchment outlet, and relatively lower temperature-CO_2 efflux relationships were found in valley bottoms and flat upland soils (Fig 5.7a). The higher temperature-CO_2 efflux relationship from these areas indicates the potential importance of these sloping features to landscape-scale CO_2 budgets in a warmer future climate. The residuals of the temperature-CO_2 efflux relationship were not correlated to mean weekly precipitation in any pixel, suggesting that the temperature is the dominant regulator of the seasonal variability of soil CO_2 efflux across this watershed. However, it should be noted that this watershed rarely experiences prolonged drought conditions, and that precipitation variability is a well-known major driver of the seasonal variability of soil CO_2 efflux in many ecosystem types (Takahashi et al. 2011; Riveros-Iregui et al. 2012; Stielstra et al. 2015).

Conversely, sloping landscape features (strong net CH_4 sinks) were the only portions of the watershed where significant linear relationships between seasonal temperature and CH_4 fluxes were observed (Fig 5.7b). Sloping areas, specifically convergent zones along and at the base of slopes, showed increasing negative CH_4 fluxes (i.e., CH_4 sinks) in warmer seasons. Areas that were consistently net CH_4 sources (i.e., valley bottoms), or areas that with near-zero net CH_4 fluxes in most seasons (i.e., flat lowlands and uplands), were not significantly related to seasonal temperature (Fig 5.7b). However, we found significant relationships between mean seasonal CH_4 fluxes and weekly precipitation in low-lying valley bottom areas along the stream networks.

Notably, the central valley bottom areas showed a positive relationship between seasonal mean precipitation and CH_4 flux (i.e. more CH_4 emission in wetter seasons), but opposite relationships were observed in the adjacent perimeter areas (Fig 5.7c). Similar patterns have been observed during rainy periods in temperate forests (Itoh et al. 2007), which has been explained by a frequent lateral influx of oxygen-rich water to valley bottom perimeter soils that is rapidly depleted before it reaches more central soils. This results in sustained saturation and significantly increased CH_4 production in the central areas, but also suppressed CH_4 production in the adjacent perimeter soils (Itoh et al. 2007).

In addition to the relationships between GHG fluxes and seasonal meteorological patterns, we also examined the potential seasonal correlations between the GHG fluxes themselves. There has recently been increasing interest in the relationships between soil CO_2 and CH_4 fluxes across landscapes, which may provide insights into the shared functional controls of heterogeneous soil types, vegetation, and microbial community structure on multiple soil greenhouse gas fluxes within an ecosystem (Maier et al. 2017). In general, soils with high CO_2 efflux tend to have high CH_4 uptake, while soils with low CO_2 efflux may have near-zero CH_4 fluxes or act as net sources of CH_4 (Maier et al. 2017; Warner et al. 2018). We found significant correlations between predicted seasonal CO_2 and CH_4 fluxes almost exclusively along sloping transitional landscape features (Fig 5.7d), the same areas where we found significant correlations between predicted CH_4 uptake and temperature. These sloped soils are generally well-aerated and well-drained,

which consistently provides conditions conducive for aerobic heterotrophic activity and methane oxidation even in periods of frequent rain. Flatter and lower elevation areas of the watershed may be less well-drained, creating a soil environment that may be more conducive to CH_4 production, or may have a closer balance between methanogenic and methanotrophic processes. As rates of both methanogenesis and methanotrophy increase with temperature (Semenov et al. 2004; Yvon-Durocher et al. 2014), areas containing soils that support both microbial processes may have no relationship between temperature and the net CH_4 flux at the soil surface.

Thus, these findings suggest that warmer mean seasonal temperatures may cause transitional hillslopes in forested ecosystems to act as relatively greater CO_2 sources, but also relatively greater net CH_4 sinks. However, changes in precipitation patterns may have a greater impact on CH_4 fluxes in flatter valley bottom and upland areas than changes in seasonal temperatures, making the combined (and confounding) effects of climate variability in temperature and precipitation on soil-atmosphere CH_4 exchange difficult to predict across topographically-complex landscapes.

5.5 Conclusions

This study demonstrates the application of digital soil mapping for making estimates of seasonal soil-atmosphere CO_2 and CH_4 fluxes across a topographically-heterogeneous watershed based on manual soil flux measurements and publicly available topographic data. This approach appears to work better for predicting CO_2 efflux in most seasons, while predictions of CH_4 fluxes became more uncertain during hot, wet periods when hotspots of CH_4 efflux developed in some areas in the watershed. We found soils along transitional slopes to have high relationship between temperature and CO_2 efflux

and net CH_4 uptake, indicating the potential importance of soils on these landscape features to GHG budgets under future climate regimes. The well-drained soils of these slopes likely support aerobic soil processes across all seasons, resulting in a significant spatial correlation between CO_2 efflux and net CH_4 that was not observed in other areas of the watershed. The application of this digital soil mapping framework could provide insights about the spatial variability of soil GHG fluxes, the spatial variability of factors controlling them, and could aid the development of GHG budgets in complex terrain. We hope that this work encourages modeling efforts at larger spatial scales, which will need to incorporate publicly available data on vegetation, land use, and climate surfaces in addition to terrain attributes.

Acknowledgements

This study was funded by the US Department of Agriculture (USDA-AFRI Grant 2013-02758), and State of Delaware's Federal Research and Development Matching Grant Program. We thank Samuel Villarreal and Shawn Del Percio for support during the field measurements.

REFERENCES

Ambus P, Christensen S (1995) Spatial and Seasonal Nitrous Oxide and Methane Fluxes in Danish Forest-, Grassland-, and Agroecosystems. J. Environ. Qual. 24:993

Anderson RH, Matthews ED (1973) Soil Survey of Cecil County, Maryland. United States Department of Agriculture Soil Conservation Service, Washington, D.C.

Atkins JW, Epstein HE, Welsch DL (2014) Vegetation heterogeneity and landscape position exert strong controls on soil CO2 efflux in a moist , Appalachian watershed. Biogeosciences 11:17631–17673. doi: 10.5194/bgd-11-17631-2014

Baldocchi D (2003) Assessing the eddy covariance technique for evaluating carbon dioxide exchange rates of ecosystems: past, present and future. Glob Chang Biol 9:479–492. doi: 10.1046/j.1365-2486.2003.00629.x

Baldocchi DD, Finnigan J, Wilson KB, et al (2000) On measuring net ecosystem carbon exchange over tall vegetation on complex terrain. Boundary-Layer Meteorol 96:257–291. doi: 10.1023/A:1002497616547

Beven KJ, Kirkby MJ (1979) A physically based, variable contributing area model of basin hydrology. Hydrol Sci Bull. doi: 10.1080/02626667909491834

Breiman L (2001) Random forests. Mach Learn 45:5–32. doi: 10.1023/A:1010933404324

Conrad O, Bechtel B, Bock M, et al (2015) System for Automated Geoscientific Analyses (SAGA) v. 2.1.4. Geosci Model Dev. doi: 10.5194/gmd-8-1991-2015

Creed IF, Webster KL, Braun GL, et al (2013) Topographically regulated traps of dissolved organic carbon create hotspots of soil carbon dioxide efflux in forests. Biogeochemistry. doi: 10.1007/s10533-012-9713-4

Crill PM (1991) Seasonal patterns of methane uptake and carbon dioxide release by a temperate woodland soil. Global Biogeochem Cycles 5:319–334. doi: 10.1029/91GB02466

Delaware Environmental Observing System (DEOS) University of Delaware, Newark DE. Available online at: www.deos.udel.edu. Accessed: 1/31/2017

Dlugokencky EJ, Nisbet EG, Fisher R, Lowry D (2011) Global atmospheric methane: budget, changes and dangers. Philos Trans A Math Phys Eng Sci 369:2058–2072. doi: 10.1098/rsta.2010.0341

Frei S, Knorr KH, Peiffer S, Fleckenstein JH (2012) Surface micro-topography causes hot spots of biogeochemical activity in wetland systems: A virtual modeling experiment. J Geophys Res Biogeosciences. doi: 10.1029/2012JG002012

Gallant JC, Dowling TI (2003) A multiresolution index of valley bottom flatness for mapping depositional areas. Water Resour Res 39:. doi: 10.1029/2002WR001426

Genuer R, Poggi J, Tuleau-malot C (2012) Variable selection using Random Forests. Pattern Recognit Lett 31:2225–2236

Genuer R, Poggi JM, Tuleau-Malot C (2016) VSURF: Variable selection using random forests. R package version 1.0.3

Gomez J, Vidon P, Gross J, et al (2017) Spatial and Temporal Patterns of CO_2, CH_4, and N_2O Fluxes at the Soil-Atmosphere Interface in a Northern Temperate Forested Watershed. Sci Pages For Res 1:1–12

Gomez J, Vidon P, Gross J, et al (2016) Estimating greenhouse gas emissions at the soil–atmosphere interface in forested watersheds of the US Northeast. Environ Monit Assess 188:295. doi: 10.1007/s10661-016-5297-0

Gough CM, Vogel CS, Kazanski C, et al (2007) Coarse woody debris and the carbon balance of a north temperate forest. For Ecol Manage. doi: 10.1016/j.foreco.2007.03.039

Hengl T, Heuvelink GBM, Stein A (2004) A generic framework for spatial prediction of soil variables based on regression-kriging. Geoderma 120:75–93. doi: 10.1016/j.geoderma.2003.08.018

Hengl T, Mendes de Jesus J, Heuvelink GBM, et al (2017) SoilGrids250m: Global gridded soil information based on machine learning

Itoh M, Ohte N, Koba K, et al (2007) Hydrologic effects on methane dynamics in riparian

wetlands in a temperate forest catchment. J Geophys Res Biogeosciences. doi: 10.1029/2006JG000240

Jenson SK, Domingue JO (1988) Extracting Topographic Structure from Digital Elevation Data for Geographic Information System Analysis. Photogramm Eng Remote Sensing 8825:

King AW, Andres RJ, Davis KJ, et al (2015) North America's net terrestrial CO2 exchange with the atmosphere 1990-2009. Biogeosciences. doi: 10.5194/bg-12-399-2015

Le Quéré C, Andrew RM, Friedlingstein P, et al (2018) Global Carbon Budget 2017. Earth Syst Sci Data 10:405–448. doi: 10.5194/essd-10-405-2018

Leon E, Vargas R, Bullock S, et al (2014) Hot spots, hot moments, and spatio-temporal controls on soil CO_2 efflux in a water-limited ecosystem. Soil Biol Biochem. doi: 10.1016/j.soilbio.2014.05.029

Liaw A, Weiner M (2002) Classification and regression by randomForest. R News 2(3): 18-22

Maier M, Paulus S, Nicolai C, et al (2017) Drivers of Plot-Scale Variability of CH_4 Consumption in a Well-Aerated Pine Forest Soil. Forests 8:193. doi: 10.3390/f8060193

McBratney AB, Mendonça Santos ML, Minasny B (2003) On digital soil mapping

Meinshausen N (2006) Quantile Regression Forests. J Mach Learn Res 7:983–999. doi: 10.1111/j.1541-0420.2010.01521.x

Meinshausen N (2016) quantregForest: Quantile regression forests. R package version 1.3

Meyer D, Dimitriadou E, Hornik K, Weingessel A, Leisch F (2015) e1071: Misc functions for the department of statistics, probability theory group. R package version 1.6-7

National Oceanic and Atmospheric Administration (NOAA) (2005) Coastal LiDAR Survey. Silver Spring, MD, USA.

Pan Y, Birdsey RA, Fang J, et al (2011) A Large and Persistent Carbon Sink in the World's Forests. Science (80-). doi: 10.1126/science.1201609

Phillips CL, Bond-Lamberty B, Desai AR, et al (2017) The value of soil respiration measurements for interpreting and modeling terrestrial carbon cycling. Plant Soil 413:1–25.

doi: 10.1007/s11104-016-3084-x

Phillips SC, Varner RK, Frolking S, et al (2010) Interannual, seasonal, and diel variation in soil respiration relative to ecosystem respiration at a wetland to upland slope at Harvard Forest. J Geophys Res 115:1–18. doi: 10.1029/2008JG000858

Post WM, Emanuel WR, Zinke PJ, Stangenberger AG (1982) Soil carbon pools and world life zones. Nature. doi: 10.1038/298156a0

R Core Team (2017). R: A language and environment for statistical computing. R Foundation for Statistical Computing, Vienna, Austria. www.R-project.org

Raich JW, Potter CS (1995) Global patterns of carbon dioxide emissions from soils. Global Biogeochem Cycles 9:23–36

Raich JW, Tufekcioglu A (2000) Vegetation and soil respiration: Correlations and controls. Biogeochemistry 48:71–90

Reyes WM, Epstein HE, Li X, et al (2017) Complex terrain influences ecosystem carbon responses to temperature and precipitation. Global Biogeochem Cycles 31:1306–1317. doi: 10.1002/2017GB005658

Riveros-Iregui DA, McGlynn BL (2009) Landscape structure control on soil CO_2 efflux variability in complex terrain: Scaling from point observations to watershed scale fluxes. J Geophys Res Biogeosciences. doi: 10.1029/2008JG000885

Riveros-Iregui DA, Mcglynn BL, Emanuel RE, Epstein HE (2012) Complex terrain leads to bidirectional responses of soil respiration to inter-annual water availability. Glob Chang Biol. doi: 10.1111/j.1365-2486.2011.02556.x

Saunois M, Bousquet P, Poulter B, et al (2016) The global methane budget 2000-2012. Earth Syst Sci Data 8:697–751. doi: 10.5194/essd-8-697-2016

Savage K, Phillips R, Davidson E (2014) High temporal frequency measurements of greenhouse gas emissions from soils. Biogeosciences. doi: 10.5194/bg-11-2709-2014

Semenov VM, Kravchenko IK, Kuznetsova T V., et al (2004) Seasonal Dynamics of

Atmospheric Methane Oxidation in Gray Forest Soils. Microbiology 73:356–362. doi: 10.1023/B:MICI.0000032249.72956.9f

Smith KA, Dobbie KE, Ball BC, et al (2000) Oxidation of atmospheric methane in Northern European soils, comparison with other ecosystems, and uncertainties in the global terrestrial sink. Glob Chang Biol. doi: 10.1046/j.1365-2486.2000.00356.x

Stielstra CM, Lohse KA, Chorover J, et al (2015) Climatic and landscape influences on soil moisture are primary determinants of soil carbon fluxes in seasonally snow-covered forest ecosystems. Biogeochemistry. doi: 10.1007/s10533-015-0078-3

Takahashi M, Hirai K, Limtong P, et al (2011) Topographic variation in heterotrophic and autotrophic soil respiration in a tropical seasonal forest in Thailand. Soil Sci Plant Nutr. doi: 10.1080/00380768.2011.589363

Tarboton DG (1997) A new method for the determination of flow directions and upslope areas in grid digital elevation models. Water Resour Res 33:309–319. doi: 10.1029/96WR03137

Tonitto C, Gurwick NP, Woodbury PB, et al (2016) Quantifying Greenhouse Gas Emissions from Agricultural and Forest Landscapes for Policy Development and Verification. In: Advances in Agricultural Systems Modeling. pp 229–304

Vargas R, Allen M (2008) Environmental controls and the influence of vegetation type, fine roots and rhizomorphs on diel and seasonal variation in soil respiration. New Phytol 179:460–471. doi: 10.1111/j.1469-8137.2008.02481

Wang JM, Murphy JG, Geddes JA, et al (2013) Methane fluxes measured by eddy covariance and static chamber techniques at a temperate forest in central Ontario, Canada. Biogeosciences. doi: 10.5194/bg-10-4371-2013

Warner DL, Vargas R, Seyfferth A, Inamdar S (2018) Transitional slopes act as hotspots of both soil CO_2 emission and CH_4 uptake in a temperate forest landscape. Biogeochemistry 2:. doi: 10.1007/s10533-018-0435-0

Warner DL, Villarreal S, McWilliams K, et al (2017) Carbon Dioxide and Methane Fluxes From

Tree Stems, Coarse Woody Debris, and Soils in an Upland Temperate Forest. Ecosystems 1–12. doi: 10.1007/s10021-016-0106-8

Webster KL, Creed IF, Beall FD, Bourbonnière RA (2008a) Sensitivity of catchment-aggregated estimates of soil carbon dioxide efflux to topography under different climatic conditions. J Geophys Res Biogeosciences. doi: 10.1029/2008JG000707

Webster KL, Creed IF, Bourbonnière RA, Beall FD (2008b) Controls on the heterogeneity of soil respiration in a tolerant hardwood forest. J Geophys Res Biogeosciences. doi: 10.1029/2008JG000706

Wiesmeier M, Barthold F, Blank B, Kögel-Knabner I (2011) Digital mapping of soil organic matter stocks using Random Forest modeling in a semi-arid steppe ecosystem. Plant Soil 340:7–24. doi: 10.1007/s11104-010-0425-z

Wilson J, Gallant J (2000) Terrain Analysis: Principles and Applications. John Wiley and Sons, New York, NY, USA.

Yvon-Durocher G, Allen AP, Bastviken D, et al (2014) Methane fluxes show consistent temperature dependence across microbial to ecosystem scales. Nature. doi: 10.1038/nature13164

Chapter 6

CONCLUSIONS

This research spans across several levels of ecological organization, from the exchange of CO_2 and CH_4 between the atmosphere and a single tree, log, or patch of soil, to the relative contributions of these exchanges within a small plot, to the seasonal variation of soil gas fluxes across an entire watershed.

6.1 Key conclusions

The key conclusions from this research are summarized below:

- Within a temperate forest, CO_2 and CH_4 fluxes are the product of distinct sources (i.e., soils, stems, CWD), that in turn vary based on distinctly different environmental factors. This is an important consideration with regards to land management decisions such as CWD removal and selective tree harvest, as well as potential climate change feedbacks, as shifts in forest species composition, disease and insect outbreaks, and windthrow events are expected.
- Of the ecosystem components of soils, stems, and CWD, soils are the dominant component of plot scale CO_2 and CH_4 fluxes. However, both stems and CWD contribute a substantial fraction of total CO_2 efflux, and stem CH_4 emissions may offset some of the soil CH_4 sink.

- Soil CO_2 and CH_4 fluxes in temperate forests vary predictably across topographic gradients along with soil biogeochemical properties. This effect is consistent across seasons for CH_4 fluxes, but less so for CO_2 fluxes. This finding suggests a relatively stronger relationship between soil CH_4 processes and spatially distributed soil properties (e.g., clay content, water content) than for CO_2.
- Soil environments that are conducive for high CO_2 efflux are also conducive for high CH_4 uptake. Such soils are generally loose and well-drained, with large amounts of carbon and a mixture of both coarse and fine particle fractions. In our study watershed, these soils occupied the steep transitional hillslopes in the landscape.
- Soil CO_2 and CH_4 fluxes can be upscaled from chamber measurements across complex terrain using tools from the digital soil mapping community. This approach allows landscape scale flux estimates to be made based on spatially continuous distributions of fluxes. Using this approach across multiple seasons can demonstrate the shifting strength of sources and sinks across the landscape over time, potentially identifying areas of vulnerability to climate change.

6.2 Future directions

These findings have helped fill several key knowledge gaps regarding CO_2 and CH_4 fluxes in complex forest ecosystems. However, questions inevitably remain after these knowledge gaps are addressed, and this section will help guide current and future

researchers in their investigations to greenhouse gas dynamics, climate change feedbacks, and ecological modeling.

The variability of CH_4 fluxes from CWD and living tree stems is an important area of research; these sources of CH_4 are highly heterogeneous and their importance to large scale CH_4 budgets is currently highly uncertain. Future studies should examine the variability of fluxes along stems, the physiological drivers of differences in fluxes between species, and the potential sources (soil or internal) of stem CH_4 emissions. The transition of CWD from a CH_4 source to sink as it decays should also be examined, and how CWD species may influence this process.

Soils along transitional slopes acted as a strong source of CO_2 and sink of CH_4 at the landscape scale, but will this behavior change under future climate scenarios? Increasingly extreme drought and storm cycles may alter the erosion and deposition patterns that we suggested are responsible for the high CO_2 emission and CH_4 uptake along this portion of the hillslope. Simulated drought and rewetting experiments in these areas could provide important insights into the future function of these soils.

The methods for upscaling chamber measurements based on spatial covariates presented in this research is promising for ecological forecasting. There is enormous potential in the increasing affordability and portability of instrumentation for measuring multiple greenhouse gas fluxes from different components of heterogeneous ecosystems. This, coupled with increasingly available high-resolution data on land use, topography, and vegetation phenology, will allow researchers to make large scale estimates of greenhouse gas exchange that preserves the inherent variability of fluxes within these large areas. Measurements and models from mixed land uses will be especially useful in

identifying the impacts of human development on soil CO_2 and CH_4 fluxes at the landscape scale.

6.3 Final thoughts

The core message of this work is that although large scale exchanges of CO_2 and CH_4 are critical considerations for future climate, agricultural, and economic forecasts, the immense heterogeneity of CO_2 and CH_4 fluxes from multiple sources in the environment are a critical consideration as well. It is likely that the responses of fluxes to climate and environmental changes will not be consistent across, or even within, different sources (i.e., soils, living stems, dead wood). Findings from this and other research that enhance the mechanistic understanding of fluxes and their spatiotemporal variability will help refine ecological forecasts, and will facilitate the development of targeted mitigation strategies.

Appendix A

TRANSITIONAL SLOPES ACT AS HOTSPOTS OF BOTH SOIL CO_2 EMISSION AND CH_4 UPTAKE IN A TEMPERATE FOREST LANDSCAPE – SUPPLEMENTAL MATERIALS

Gas fluxes, soil moisture, and soil temperature

At each sampling point, 2 mm thick PVC collars with a 10 cm internal diameter were inserted 5 cm into the soil, leaving the remaining 3 cm exposed. CO_2 and CH_4 concentrations were measured with an Ultra-Portable Greenhouse Gas Analyzer (Los Gatos Research, Mountain View, California, USA) connected to a 10 cm diameter PVC chamber that sealed tightly over the collars. Prior to each measurement, the chamber and instrument were allowed to equilibrate with ambient air. Once sealed, gas was accumulated in the chamber for 3 minutes while being circulated through the instrument via an internal vacuum pump. Gas concentrations were measured at 1 Hz frequency, with a range and error of 1 to 20,000 ± 0.3 ppm and 0.01 to 100 ± 0.002 ppm for CO_2 and CH_4, respectively (Pearson et al. 2016). Thus, a total of 180 concentration measurements were taken over the 3 minute accumulation period, and fluxes were calculated by fitting the following equation (Pumpanen et al. 2004):

$$F = \left(\frac{dC}{dt}\right)\left(\frac{V_c}{A_c}\right)\frac{P}{(R*(T+273.15))} \quad (1)$$

where F is the flux of a gas, dC/dt is the change in concentration over time as measured by the instrument (ppm s^{-1}), V_c is the closed system volume (0.00119 m^3), A_c is the chamber area (0.0081 m^2), P is the atmospheric pressure (101.325 kg m^{-1} s^{-2}), R is the

ideal gas law constant (0.00831447 kg m^2 μmol^{-1} K^{-1} s^{-2}), *T* is measured soil temperature (^oC), and 273.15 is the Celsius to Kelvin conversion factor. Slopes (i.e. *dC/dt* in Eq. 1) with a p-value greater than 0.1 were determined to be insignificant and were set to zero. Slopes that showed non-linear trends due to poor seals or disturbances to the chamber or surrounding soils during measurement were removed from our dataset entirely.

Soil temperature and volumetric water content (VWC) were measured from 0 to 4 cm depth along with each flux measurement (WET Sensor, Delta-T Devices, Cambridge, UK). Gas flux, VWC, and temperature measurements were taken 1-2 times monthly from September 2014 to November 2016, with extra measurements taken immediately after large precipitation events or during drought conditions to capture a broad range of conditions experienced by soils in the catchment. Soil flux, moisture, and temperature data was grouped by season as winter (Jan 1-Feb 28), spring (Mar 1-May 20), early summer (May 20-Jul 31), late summer (Aug 1-Sep 30), and fall (Oct 1-Dec 31) based on seasonal changes in temperature and moisture in the watershed (Fig 2a, 2b). Summer was divided into early and late sections due to a catchment-wide decline in soil moisture toward the end of the hot growing season.

Soil porewater carbon and water-extractable carbon

To examine the influence of the character of soil dissolved organic matter (DOM) on soil-atmosphere CO_2 efflux and CH_4 fluxes, we installed and drew monthly samples from ceramic cup tension lysimeters (1900-series, Soilmoisture Equipment Corp., Santa Barbara, California, USA) buried 15 cm in the soil at all sampling points. Prior to installation, lysimeters were cleaned with 10% HCl, and thoroughly rinsed in reagent-grade water ($\geq$ 18.2 MΩ cm^{-1}), to remove any organic carbon residue. Holes were bored

with a hand auger and filled with a silica flour slurry to ensure hydrologic connectivity between the porous ceramic cup and surrounding soil matrix. To avoid the disturbance of installation, lysimeters settled for over one month before any samples were drawn.

Lysimeters were emptied of liquid and evacuated to a vacuum of 60 centibars 48 hours before sample collection. Samples were drawn using a syringe and small tubing, filtered through 0.7 µm glass fiber filters into amber glass vials, and refrigerated until further analysis. Sampling equipment was thoroughly rinsed in reagent water between each sample. If necessary, aliquots for optical analysis were diluted until absorbance at 254 nm was below 0.2 prior to analysis to reduce inner-filter effects (Ohno 2002). Samples were collected every two months from October 2014 to June 2015, and monthly from August 2015 to November 2016, except during very dry periods when many upland and transition zone sites yielded no samples.

In addition to porewater DOM, we also examined the quality of potentially mobilized soil DOM using water extractions. Soil cores for water-extractable DOM samples (DOM_{ex}) were collected from 0-15 cm in triplicate at each site (<1 m from ring) using a 2 cm hand auger. The O-horizon was carefully scraped away prior to coring. Samples were homogenized in the laboratory while still moist, and 2.5 g subsamples (rocks and roots excluded) of the homogenized soils were added to 40 mL amber vials to protect the DOM from photodegradation. Vials were treated with 35 mL reagent water and allowed to soak for 24 hours at 4 ^{o}C. After soaking, samples were agitated at 100 rpm for 1 hour, and particles were allowed to settle out for another 24 hours at 4 ^{o}C. Supernatants were filtered to 0.22 µm to remove any biota and light-scattering particles that may be present, and the filtrates were stored at 4 ^{o}C in amber glass vials until further

analysis. DOM_{ex} samples were collected during spring, summer, and fall from spring 2015 to fall 2016.

Optical DOM characterization

Optical DOM properties were analyzed on a HORIBA Aqualog® fluorescence spectrophotometer (Edison, New Jersey, USA). Absorbance spectra were measured from 240-550 nm at 4 nm intervals and 5 nm slit widths. Fluorescence emission spectra were measured from 300-550 nm at 4 nm intervals across an excitation range of 240-500 nm through 5 nm slit widths to produce excitation-emission matrices (EEMs) of fluorescence intensity across these wavelength ranges. Data processing and corrections were performed in MATLAB 2013b (MathWorks 2013), and the DOM quality indices of specific UV absorbance ($SUVA_{254}$, indicating aromaticity of DOM) (Weishaar et al. 2003), humification index (HIX, higher values indicate more humified DOM) (Ohno 2002), and biological index (BIX, higher values indicate fresher, labile DOM) (Huguet et al. 2009) were calculated. Additionally, DOM_{pw} and DOM_{ex} EEMs were used to generate a 7-component PARAFAC model following published protocols and validation techniques in Matlab 2013b using the drEEM toolbox (MathWorks 2013, Murphy and others 2013). The excitation-emission peaks for components of our PARAFAC model were compared to previously published PARAFAC models (Fellman et al. 2010) to qualitatively assess them (i.e. protein- or humic-like fluorescence; Supplementary Table 1). Overall DOM_{pw} and DOM_{ex} quality was estimated based on principle components analysis of $SUVA_{254}$, HIX, BIX, total % humic-like fluorescence (HLF, relative abundance of components 1,3,4, and 5), and total % protein-like fluorescence (PLF, relative abundance of components 6 and 7). The first principle component explained

61.6% and 59.5% of the variance of this data for DOM_{pw} and DOM_{ex} samples, respectively. For both DOM_{pw} and DOM_{ex}, $SUVA_{254}$, HIX, and HLF (indicators of chemically recalcitrant DOM (Kalbitz et al. 2003)) loaded negatively on the first component while BIX and PLF (indicators of labile DOM (Cory and Kaplan 2012)) loaded positively on the first component. Thus, this component served as an indicator of relative DOM quality (from here on referred to as DOM_Q), with more positive values indicating relatively more labile DOM, and more negative values indicating relatively more recalcitrant DOM. Due to the limited temporal frequency of DOM quality sample collection, DOM samples were pooled for winter and spring, early and late summer, and fall (3 seasonal means per year).

Soil texture, bulk density, and % water-filled pore space

Soil texture was determined via a hydrometer method (Bouyoucos 1962). Briefly, 50 g of dried, sieved (<2 mm), homogenized soil was added to a suspension column with 1 L of water, and allowed to soak for 15 minutes. The mixture was treated with 5 mL of 1N sodium hexametaphosphate, and thoroughly mixed with an electric blender. A hydrometer reading was taken after 40 seconds and 2 hours to calculate the percent sand, silt, and clay fraction of the soil.

Bulk density was determined by the mean mass of three soil cores collected from the A-horizon at each site. Cores had a known width of 2 cm and were measured in length to calculate cylinder volume. Cores were then dried and weighed, to yield bulk density in g cm^{-3}. Water-filled porespace of the A-horizon (WFPS) was calculated based on the VWC at 4 cm and A-horizon bulk density (BD) relative to that of solid quartz (2.65 g cm^{-3}) using the following formula:

$$WFPS = \frac{VWC}{(1-\frac{BD}{2.65})} \quad (2)$$

Oxalate-extractable Al and Fe

Poorly-crystalline Al and Fe content was measured using ammonium oxalate extractions in the dark (McKeague and Day 1966). Briefly, dried soil cores used for bulk density analysis were homogenized and sieved to 0.125 mm. 0.5 g of this soil was agitated with 30 mL ammonium oxalate (0.2 M) and oxalic acid solution (0.1 M) at pH 3 for 2 hours. This solution was centrifuged, and the supernatant was then filtered to 0.22 µm and refrigerated in dark vials before being analyzed for Fe and Al content using a Thermo Scientific Iris Intrepid II ICP-AES within 24 of extraction. Samples were carefully handled to avoid photodegradation during extraction and prior to analysis. To better interpret the implications of oxalate-extractable Al and Fe content for soil carbon availability, we ultimately examined the molar sorption capacity of the soil, which was calculated based on the total mols of oxalate-extractable Fe and Al normalized to bulk density.

Table 1 Supplementary. Description of fluorescent components identified by PARAFAC analysis of EEMs from porewater and water-extracted DOM. Descriptions are based on previously published values compiled in Fellman and others (2010).

Component	Ex/Em Wavelength	Description
1	254/464	Humic-like, high molecular weight
2	334/395	Unknown
3	262/446	Humic-like, high molecular weight
4	270/520	Humic-like, high molecular weight
5	302/427	Humic-like, low molecular weight
6	280/340	Protein-like (tryptophan)
7	270/300	Protein-like (tyrosine)

Table 2 Supplementary. P-values from pair-wise (Tukey's HSD) comparisons of seasonal mean temperature, water-filled pore space, and CO_2 efflux and CH_4 fluxes across landscape positions within each season.

	Temperature	WFPS	Mean CO_2 efflux	Mean CH_4 flux
Winter				
VB – TZ	0.67	< 0.01	< 0.01	< 0.01
VB – UL	0.64	< 0.01	0.97	< 0.01
TZ – UL	0.99	0.66	< 0.01	< 0.01
Spring				
VB – TZ	0.90	< 0.01	< 0.01	< 0.01
VB – UL	0.63	< 0.01	0.04	< 0.01
TZ – UL	0.86	0.18	0.51	< 0.01
Early Summer				
VB – TZ	0.04	< 0.01	< 0.01	< 0.01
VB – UL	< 0.01	< 0.01	< 0.01	< 0.01
TZ – UL	0.81	0.81	0.71	0.17
Late Summer				
VB – TZ	0.34	< 0.01	< 0.01	< 0.01
VB – UL	0.31	< 0.01	< 0.01	< 0.01
TZ – UL	0.99	0.89	< 0.01	< 0.01
Fall				
VB – TZ	0.83	< 0.01	< 0.01	< 0.01
VB – UL	0.97	< 0.01	0.10	< 0.01
TZ – UL	0.65	0.75	< 0.01	< 0.01

ANOVA – Tukey HSD

Table 3 Supplementary. P-values from pair-wise (Tukey's HSD) comparisons of mean temperature at each landscape position across different seasons.

	Upland	**Transition Zone**	**Valley Bottom**
Winter – Spring	< 0.01	< 0.01	< 0.01
Winter – Early Summer	< 0.01	< 0.01	< 0.01
Winter – Late Summer	< 0.01	< 0.01	< 0.01
Winter – Fall	< 0.01	< 0.01	< 0.01
Spring – Early Summer	< 0.01	< 0.01	< 0.01
Spring – Late Summer	< 0.01	< 0.01	< 0.01
Spring – Fall	0.07	0.16	0.01
Early Summer – Late Summer	0.99	0.99	0.73
Early Summer – Fall	< 0.01	< 0.01	< 0.01
Late Summer – Fall	< 0.01	< 0.01	< 0.01

ANOVA – Tukey HSD

Table 4 Supplementary. P-values from pair-wise (Tukey's HSD) comparisons of mean water-filled pore space at each landscape position across different seasons.

	Upland	**Transition Zone**	**Valley Bottom**
Winter – Spring	0.26	0.13	0.99
Winter – Early Summer	< 0.01	< 0.01	0.04
Winter – Late Summer	< 0.01	< 0.01	< 0.01
Winter – Fall	< 0.01	< 0.01	0.06
Spring – Early Summer	< 0.01	< 0.01	0.02
Spring – Late Summer	< 0.01	< 0.01	< 0.01
Spring – Fall	< 0.01	< 0.01	0.07
Early Summer – Late Summer	< 0.01	< 0.01	0.35
Early Summer – Fall	0.96	0.93	0.99
Late Summer – Fall	< 0.01	< 0.01	0.09

ANOVA – Tukey HSD

Table 5 Supplementary. P-values from pair-wise (Tukey's HSD) comparisons of mean CO_2 efflux at each landscape position across different seasons.

	Upland	**Transition Zone**	**Valley Bottom**
Winter – Spring	< 0.01	0.01	0.08
Winter – Early Summer	< 0.01	< 0.01	< 0.01
Winter – Late Summer	< 0.01	< 0.01	< 0.01
Winter – Fall	< 0.01	< 0.01	< 0.01
Spring – Early Summer	< 0.01	< 0.01	< 0.01
Spring – Late Summer	< 0.01	< 0.01	< 0.01
Spring – Fall	0.78	0.04	0.24
Early Summer – Late Summer	< 0.01	< 0.01	< 0.01
Early Summer – Fall	< 0.01	< 0.01	< 0.01
Late Summer – Fall	< 0.01	< 0.01	0.42

ANOVA – Tukey HSD

Table 6 Supplementary. P-values from pair-wise (Tukey's HSD) comparisons of mean CH_4 fluxes at each landscape position across different seasons.

	Upland	**Transition Zone**	**Valley Bottom**
Winter – Spring	0.31	0.97	0.99
Winter – Early Summer	< 0.01	< 0.01	0.11
Winter – Late Summer	< 0.01	< 0.01	0.99
Winter – Fall	< 0.01	< 0.01	0.99
Spring – Early Summer	< 0.01	< 0.01	0.08
Spring – Late Summer	< 0.01	< 0.01	0.99
Spring – Fall	< 0.01	< 0.01	0.99
Early Summer – Late Summer	0.30	< 0.01	0.04
Early Summer – Fall	< 0.01	0.72	0.01
Late Summer – Fall	< 0.01	< 0.01	0.99

ANOVA – Tukey HSD

Appendix B

REPRINT PERMISSION LETTERS

ECOSYSTEMS

SPRINGER NATURE LICENSE TERMS AND CONDITIONS

Jun 13, 2018

This Agreement between Daniel Warner ("You") and Springer Nature ("Springer Nature") consists of your license details and the terms and conditions provided by Springer Nature and Copyright Clearance Center.

License Number	4367170738017
License date	Jun 13, 2018
Licensed Content Publisher	Springer Nature
Licensed Content Publication	Ecosystems
Licensed Content Title	Carbon Dioxide and Methane Fluxes From Tree Stems, Coarse Woody Debris, and Soils in an Upland Temperate Forest
Licensed Content Author	Daniel L. Warner, Samuel Villarreal, Kelsey McWilliams et al
Licensed Content Date	Jan 1, 2017
Licensed Content Volume	20
Licensed Content Issue	6
Type of Use	Thesis/Dissertation
Requestor type	academic/university or research institute
Format	electronic
Portion	full article/chapter
Will you be translating?	no
Circulation/distribution	<501
Author of this Springer Nature content	yes
Title	Biogeochemical controls and spatial modelling of CO2 and CH4 fluxes in a complex forest landscape

Instructor name	Dr. Shreeram Inamdar
Institution name	University of Delaware
Expected presentation date	Jul 2018
Requestor Location	Daniel Warner 1109 Blair Ct NEWARK, DE 19711 United States Attn: Daniel Warner
Billing Type	Invoice
Billing Address	Daniel Warner 1109 Blair Ct NEWARK, DE 19711 United States Attn: Daniel Warner
Total	0.00 USD

Terms and Conditions

Springer Nature Terms and Conditions for RightsLink Permissions Springer Customer Service Centre GmbH (the Licensor) hereby grants you a nonexclusive, world-wide licence to reproduce the material and for the purpose and requirements specified in the attached copy of your order form, and for no other use, subject to the conditions below:

1. The Licensor warrants that it has, to the best of its knowledge, the rights to license reuse of this material. However, you should ensure that the material you are requesting is original to the Licensor and does not carry the copyright of another entity (as credited in the published version).

   If the credit line on any part of the material you have requested indicates that it was reprinted or adapted with permission from another source, then you should also seek permission from that source to reuse the material.

2. Where print only permission has been granted for a fee, separate permission must be obtained for any additional electronic re-use.

3. Permission granted free of charge for material in print is also usually granted for any electronic version of that work, provided that the material is incidental to your work as a whole and that the electronic version is essentially equivalent to, or substitutes for, the print version.

4. A licence for 'post on a website' is valid for 12 months from the licence date. This licence does not cover use of full text articles on websites.

5. Where 'reuse in a dissertation/thesis' has been selected the following terms apply: Print rights for up to 100 copies, electronic rights for use only on a personal website or institutional repository as defined by the Sherpa guideline (www.sherpa.ac.uk/romeo/).

6. Permission granted for books and journals is granted for the lifetime of the first edition and does not apply to second and subsequent editions (except where the first edition permission was granted free of charge or for signatories to the STM Permissions Guidelines http://www.stm-assoc.org/copyright-legal-affairs/permissions/permissions-guidelines/), and does not apply for editions in other languages unless additional translation rights have been granted separately in the licence.

7. Rights for additional components such as custom editions and derivatives require additional permission and may be subject to an additional fee. Please apply to Journalpermissions@springernature.com/bookpermissions@springernature.com for these rights.

8. The Licensor's permission must be acknowledged next to the licensed material in print. In electronic form, this acknowledgement must be visible at the same time as the figures/tables/illustrations or abstract, and must be hyperlinked to the journal/book's homepage. Our required acknowledgement format is in the Appendix below.

9. Use of the material for incidental promotional use, minor editing privileges (this does not include cropping, adapting, omitting material or any other changes that affect the meaning, intention or moral rights of the author) and copies for the disabled are permitted under this licence.

10. Minor adaptations of single figures (changes of format, colour and style) do not require the Licensor's approval. However, the adaptation should be credited as shown in Appendix below.

Appendix — Acknowledgements:

For Journal Content:
Reprinted by permission from [the Licensor]: [Journal Publisher (e.g. Nature/Springer/Palgrave)] [JOURNAL NAME] [REFERENCE CITATION (Article name, Author(s) Name), [COPYRIGHT] (year of publication)

For Advance Online Publication papers:
Reprinted by permission from [the Licensor]: [Journal Publisher (e.g. Nature/Springer/Palgrave)] [JOURNAL NAME] [REFERENCE CITATION (Article name, Author(s) Name), [COPYRIGHT] (year of publication), advance online publication, day month year (doi: 10.1038/sj.[JOURNAL ACRONYM].)

For Adaptations/Translations:
Adapted/Translated by permission from [the Licensor]: [Journal Publisher (e.g. Nature/Springer/Palgrave)] [JOURNAL NAME] [REFERENCE CITATION (Article name, Author(s) Name), [COPYRIGHT] (year of publication)

Note: For any republication from the British Journal of Cancer, the following credit line style applies:

Reprinted/adapted/translated by permission from [the Licensor]: on behalf of Cancer
Research UK: : [Journal Publisher (e.g. Nature/Springer/Palgrave)] [JOURNAL NAME] [REFERENCE CITATION (Article name, Author(s) Name), [COPYRIGHT] (year of publication)

For Advance Online Publication papers:
Reprinted by permission from The [the Licensor]: on behalf of Cancer Research UK:
[Journal Publisher (e.g. Nature/Springer/Palgrave)] [JOURNAL NAME] [REFERENCE CITATION (Article name, Author(s) Name), [COPYRIGHT] (year of publication), advance online publication, day month year (doi: 10.1038/sj. [JOURNAL ACRONYM])

For Book content:
Reprinted/adapted by permission from [the Licensor]: [Book Publisher (e.g. Palgrave Macmillan, Springer etc) [Book Title] by [Book author(s)] [COPYRIGHT] (year of publication)

Other Conditions:

Version 1.0

Questions? customercare@copyright.com or +1-855-239-3415 (toll free in the US) or +1-978-646-2777.

BIOGEOCHEMISTRY

SPRINGER NATURE LICENSE TERMS AND CONDITIONS

Jun 13, 2018

This Agreement between Daniel Warner ("You") and Springer Nature ("Springer Nature") consists of your license details and the terms and conditions provided by Springer Nature and Copyright Clearance Center.

License Number	4367170395042
License date	Jun 13, 2018
Licensed Content Publisher	Springer Nature
Licensed Content Publication	Biogeochemistry
Licensed Content Title	Transitional slopes act as hotspots of both soil CO2 emission and CH4 uptake in a temperate forest landscape
Licensed Content Author	Daniel L. Warner, Rodrigo Vargas, Angelia Seyfferth et al
Licensed Content Date	Jan 1, 2018
Licensed Content Volume	138
Licensed Content Issue	2
Type of Use	Thesis/Dissertation
Requestor type	academic/university or research institute
Format	electronic
Portion	full article/chapter
Will you be translating?	no
Circulation/distribution	<501
Author of this Springer Nature content	yes
Title	Biogeochemical controls and spatial modelling of CO2 and CH4 fluxes in a complex forest landscape
Instructor name	Dr. Shreeram Inamdar
Institution name	University of Delaware
Expected presentation date	Jul 2018

Requestor Location	Daniel Warner 1109 Blair Ct NEWARK, DE 19711 United States Attn: Daniel Warner
Billing Type	Invoice
Billing Address	Daniel Warner 1109 Blair Ct NEWARK, DE 19711 United States Attn: Daniel Warner
Total	0.00 USD

Terms and Conditions

Springer Nature Terms and Conditions for RightsLink Permissions Springer Customer Service Centre GmbH (the Licensor) hereby grants you a nonexclusive, world-wide licence to reproduce the material and for the purpose and requirements specified in the attached copy of your order form, and for no other use, subject to the conditions below:

1. The Licensor warrants that it has, to the best of its knowledge, the rights to license reuse of this material. However, you should ensure that the material you are requesting is original to the Licensor and does not carry the copyright of another entity (as credited in the published version).

   If the credit line on any part of the material you have requested indicates that it was reprinted or adapted with permission from another source, then you should also seek permission from that source to reuse the material.

2. Where print only permission has been granted for a fee, separate permission must be obtained for any additional electronic re-use.

3. Permission granted free of charge for material in print is also usually granted for any electronic version of that work, provided that the material is incidental to your work as a whole and that the electronic version is essentially equivalent to, or substitutes for, the print version.

4. A licence for 'post on a website' is valid for 12 months from the licence date. This licence does not cover use of full text articles on websites.

5. Where 'reuse in a dissertation/thesis' has been selected the following terms apply: Print rights for up to 100 copies, electronic rights for use only on a personal website or institutional repository as defined by the Sherpa guideline (www.sherpa.ac.uk/romeo/).

6. Permission granted for books and journals is granted for the lifetime of the first edition and does not apply to second and subsequent editions (except where the first edition permission was granted free of charge or for signatories to the STM Permissions Guidelines http://www.stm-assoc.org/copyright-legal-affairs/permissions/permissions-guidelines/), and does not apply for editions in other languages unless additional translation rights have been granted separately in the licence.

7. Rights for additional components such as custom editions and derivatives require additional permission and may be subject to an additional fee. Please apply to Journalpermissions@springernature.com/bookpermissions@springernature.com for these rights.

8. The Licensor's permission must be acknowledged next to the licensed material in print. In electronic form, this acknowledgement must be visible at the same time as the figures/tables/illustrations or abstract, and must be hyperlinked to the journal/book's homepage. Our required acknowledgement format is in the Appendix below.

9. Use of the material for incidental promotional use, minor editing privileges (this does not include cropping, adapting, omitting material or any other changes that affect the meaning, intention or moral rights of the author) and copies for the disabled are permitted under this licence.

10. Minor adaptations of single figures (changes of format, colour and style) do not require the Licensor's approval. However, the adaptation should be credited as shown in Appendix below.

Appendix — Acknowledgements:

For Journal Content:
Reprinted by permission from [the Licensor]: [Journal Publisher (e.g. Nature/Springer/Palgrave)] [JOURNAL NAME] [REFERENCE CITATION (Article name, Author(s) Name), [COPYRIGHT] (year of publication)

For Advance Online Publication papers:
Reprinted by permission from [the Licensor]: [Journal Publisher (e.g. Nature/Springer/Palgrave)] [JOURNAL NAME] [REFERENCE CITATION (Article name, Author(s) Name), [COPYRIGHT] (year of publication), advance online publication, day month year (doi: 10.1038/sj.[JOURNAL ACRONYM].)

For Adaptations/Translations:
Adapted/Translated by permission from [the Licensor]: [Journal Publisher (e.g.

Nature/Springer/Palgrave)] [JOURNAL NAME] [REFERENCE CITATION (Article name, Author(s) Name), [COPYRIGHT] (year of publication)

Note: For any republication from the British Journal of Cancer, the following credit line style applies:

Reprinted/adapted/translated by permission from [the Licensor]: on behalf of Cancer
Research UK: : [Journal Publisher (e.g. Nature/Springer/Palgrave)] [JOURNAL NAME] [REFERENCE CITATION (Article name, Author(s) Name), [COPYRIGHT] (year of publication)

For Advance Online Publication papers:
Reprinted by permission from The [the Licensor]: on behalf of Cancer Research UK:
[Journal Publisher (e.g. Nature/Springer/Palgrave)] [JOURNAL NAME] [REFERENCE CITATION (Article name, Author(s) Name), [COPYRIGHT] (year of publication), advance online publication, day month year (doi: 10.1038/sj. [JOURNAL ACRONYM])

For Book content:
Reprinted/adapted by permission from [the Licensor]: [Book Publisher (e.g. Palgrave Macmillan, Springer etc) [Book Title] by [Book author(s)] [COPYRIGHT] (year of publication)

Other Conditions:

Version 1.0

Questions? customercare@copyright.com or +1-855-239-3415 (toll free in the US) or +1-978-646-2777.